Blood-Brain Barrier Dysfunction and Repair after Blast-Induced Traumatic Brain Injury

Christopher Donald Hue

Submitted in partial fulfillment of the
requirements for the degree of
Doctor of Philosophy
in the Graduate School of Arts and Sciences

COLUMBIA UNIVERSITY

2015

ABSTRACT

Blood-Brain Barrier Dysfunction and Repair after Blast-Induced Traumatic Brain Injury

Christopher Donald Hue

Traumatic brain injury (TBI) is the signature injury of modern military conflicts due to widespread use of improvised explosive devices (IEDs) and modern body armor. However, the exact biophysical mechanisms of blast-induced traumatic brain injury (bTBI) and its pathological effects on the blood-brain barrier (BBB) – a structure essential for maintaining brain homeostasis – remain poorly understood. The specific aims of this thesis are to: 1) determine a threshold for primary blast-induced BBB dysfunction *in vitro*; 2) determine the effect of repeated blast on BBB integrity *in vitro*; 3) improve BBB recovery *in vitro* as a potential therapeutic strategy for mitigating effects of blast; and 4) quantify the time course and pore-size of BBB opening *in vivo*.

In this work we utilized a shock tube driven by compressed gas to generate operationally relevant, ideal pressure profiles consistent with IEDs. By multiple measures, the barrier function of an *in vitro* BBB model was disrupted after exposure to a range of blast-loading conditions. Trans-endothelial electrical resistance (TEER) decreased acutely in a dose-dependent manner that was most strongly correlated with impulse, as opposed to peak overpressure or duration. Significantly increased hydraulic conductivity and solute permeability post-injury further confirmed acute alterations in barrier function. Compromised ZO-1 immunostaining identified a structural basis for BBB breakdown. These results are the first to demonstrate acute disruption of an *in vitro* BBB model after primary blast exposure; defined tolerance criteria may be important for development of novel helmet designs to help mitigate effects of blast on the BBB.

After determining that exposure to a single primary blast caused BBB disruption, we hypothesized that exposure to two consecutive blast injuries would result in exacerbated damage to the BBB *in vitro*. However, contrary to our hypothesis, repeated mild or moderate primary blast delivered within 24 or 72 hours did not significantly exacerbate reductions in TEER across a brain endothelial monolayer compared to sister cultures receiving a single exposure. Single blast exposure significantly reduced immunostaining of ZO-1 and claudin-5 tight junction proteins, but subsequent exposure did not cause additional damage to tight junctions. The second injury delayed recovery of TEER and hydraulic conductivity in BBB cultures. Extending the inter-injury interval to 72 hours, the effects of repeated injury on the BBB were independent given sufficient recovery time between consecutive exposures. Investigation of repeated blast on the BBB will help identify a temporal window of vulnerability to repeated exposure.

Restoration of the BBB after blast injury has emerged as a promising therapeutic target. We hypothesized that treatment with dexamethasone (DEX) after primary blast would potentiate recovery of an *in vitro* BBB model. DEX treatment resulted in complete recovery of TEER and hydraulic conductivity 1 day after injury, compared with 3 days for vehicle-treated injured cultures. Administration of RU486 (mifepristone) inhibited effects of DEX, confirming that barrier restoration was mediated by glucocorticoid receptor signaling. Potentiated recovery with DEX treatment was accompanied by stronger ZO-1 tight junction immunostaining and expression, suggesting that increased ZO-1 expression was a structural correlate to BBB recovery. This is the first study to provide a mechanistic basis for potentiated functional recovery of an *in vitro* BBB model due to glucocorticoid treatment after blast injury.

Using an *in vivo* bTBI model, systemic administration of sodium fluorescein (NaFl; 376 Da), Evans blue (EB; 69 kDa when bound to serum albumin) and dextrans (3 – 500 kDa) was

used to estimate the pore-size of BBB opening and time required for recovery. Exposure to blast resulted in significant acute extravasation of NaFl, 3 kDa dextran, and EB. However, there was no significant acute extravasation of 70 kDa or 500 kDa dextrans, and minimal to no extravasation of NaFl, dextrans, or EB 1 day after exposure. This work is the first to quantify the time course and size of BBB opening after bTBI, suggesting that the BBB recovered 1 day post-injury. This study supports our hypothesis that transient opening of the BBB may permit serum-components to infiltrate the brain parenchyma and contribute to pathological secondary cascades.

This research has shown that BBB damage, demonstrated *in vitro* and *in vivo*, is a major mechanism contributing to vascular and neuronal pathology of bTBI at exposure levels above a critical threshold. Compared with published studies on blast-induced damage to the BBB, we have developed primary blast injury tolerance criteria by precisely controlling the biomechanical initiators of injury and measuring resulting alterations to the structure and function of an *in vitro* BBB model by methods not possible *in vivo*. We have also developed a potential glucocorticoid treatment to rapidly restore the BBB after injury, which may lead to more promising therapeutic strategies to treat TBI-related pathologies. This work will also guide the development of novel armor designs to protect service members and civilians in order to more effectively address the burden to society of bTBI.

Table of Contents

List of Figures

List of Tables

List of Abbreviations

Abbreviation	Full Name
BBB	blood-brain barrier
bTBI	blast-induced traumatic brain injury
CNS	central nervous system
CTE	chronic traumatic encephalopathy
DEX	dexamethasone
DMEM	Dulbecco's Modified Eagle's Medium
EB	Evans blue
ENT	entorhinal cortex
JTTR	Joint Theater Trauma Registry
mTBI	mild traumatic brain injury
MO	motor cortex
NaFl	sodium fluorescein
OEF	Operation Enduring Freedom
OIF	Operation Iraqi Freedom
PERI	perirhinal cortex
PIR	piriform cortex
SS	somatosensory cortex
TBI	traumatic brain injury
TEER	transendothelial electrical resistance
ZO	zonula occludens

1 Introduction

Blast injury has risen to a new level of importance and is recognized as a major cause of injuries to the brain for civilians and military populations (Warden 2006, Owens et al. 2008, Long et al. 2009). Between 2000 and 2014, there have been over 300,000 medical diagnoses of traumatic brain injury (TBI) among U.S. Armed Forces alone due to recent conflicts in Iraq and Afghanistan, the majority of which have been attributed to blast exposure (Magnuson et al. 2012, Chen et al. 2013). Head injuries and blasts have been the cause of two-thirds of Army war zone evacuations and 88% of injuries seen in second echelon treatment sites; reducing their incidence and mitigating their effects are a major concern for the U.S. Military (Owens et al. 2008, Long et al. 2009). In addition, a 2004 survey assessment of surgeon preparedness for the management of domestic terrorism and mass casualty incidents conducted by the Eastern Association for the Surgery of Trauma reported that only 73% of leading US trauma surgeons claimed to understand the medical management of blast physiology (Ciraulo et al. 2004). The emergence of blast-induced TBI (bTBI) is largely due to the development of improved personal protective armor, which has led to increased survival of modern warfighters who sustain injuries from blast (Taylor and Ford 2009, Magnuson et al. 2012).

Understanding the physics of the injury is central to mitigating the threat. High explosive detonation results from a nearly instantaneous conversion of a solid or a liquid into a gas. These gasses expand rapidly, causing compression in the surrounding air, forming a pulse of pressure that moves through the air faster than the speed of sound – the shock front (Taber et al. 2006). There are four types of traumatic injuries caused by explosive blast: 1) primary injury caused directly by the pressure wave, which can travel through tissue at velocities close to that of sound

in water (Suneson et al. 1990); 2) secondary injury caused by objects put in motion by the blast; 3) tertiary injury caused by an individual being put in motion by the blast and hitting another object (Warden 2006); and 4) quaternary injury caused by burns, explosion-related injuries, illnesses and diseases not attributed to the other three blast trauma injury types (DePalma et al. 2005). Compared to non-blast TBI, primary blast injury is a biomechanically distinct phase of bTBI that consists of pressure wave transmission through brain tissue, and remains the least understood phase of blast injury (Nakagawa et al. 2011). There is ongoing controversy over the physical mechanisms by which the primary wave causes damage at the tissue and cellular level. This knowledge-gap stymies the advancement of helmet and armor designs to the detriment of the warfighter.

Despite the high incidence of bTBI, there are currently no injury tolerance criteria specific for the blood-brain barrier (BBB) or brain parenchyma exposed to primary blast-loading (Chafi et al. 2010), nor are there any effective drug therapies for mitigating the injurious effects of blast. The BBB is a heterogeneous and multicellular unit consisting primarily of brain endothelial cells expressing tight junctions that are essential for maintaining the barrier's integrity and low permeability (Risau and Wolburg 1990, Wolburg and Lippoldt 2002, Abbott et al. 2006, Simon et al. 2010). Intercellular tight junctions are made up of claudins, occludin, and the zonula occludens (ZO) accessory proteins, which together establish the restrictive paracellular diffusion barrier characterized by high electrical resistance (Kniesel and Wolburg 2000, Simon et al. 2010). Because the BBB plays a central role in preventing the transport of potentially neurotoxic blood-borne molecules into the brain parenchyma, damage to the barrier has been known to exacerbate several central nervous system (CNS) pathologies such as multiple sclerosis and stroke, and may be a crucial mediator in bTBI (Huber et al. 2001, Hicks et al. 2010,

Readnower et al. 2010, Svetlov et al. 2010, Chen and Huang 2011, Garman et al. 2011). However, further investigation is warranted to understand the physical mechanism responsible for BBB breakdown resulting from militarily-relevant levels of blast exposure, and to develop improved strategies for mitigating its damaging consequences.

1.1 Structure and function of the blood-brain barrier

The BBB is a specialized cerebrovascular structure that helps to maintain the brain's microenvironment, protect neural function, and tightly regulate molecular transport to and from the CNS (Abbott et al. 2010, Abbott and Friedman 2012). The BBB is a heterogeneous unit, consisting of multiple cellular associations and interactions. Brain endothelial cells are a principal component of the BBB and express intercellular tight junctions that form the highly restrictive paracellular diffusional pathway across the BBB (Abbott et al. 2010). Endothelial cells are embedded in basal lamina and enveloped by pericytes, basement membrane, and foot processes from astrocytes along the length of the capillary (Abbott et al. 2006, Abbott et al. 2010) (Figure 1.1). Axonal projections from surrounding neurons may be metabolically coupled to, and dynamically interact with, brain capillaries (Hawkins and Davis 2005, Abbott et al. 2006, Shlosberg et al. 2010). Close cellular associations among these different cell types together form a "neurovascular unit" and functional barrier that separates the systemic circulatory system from the brain parenchyma.

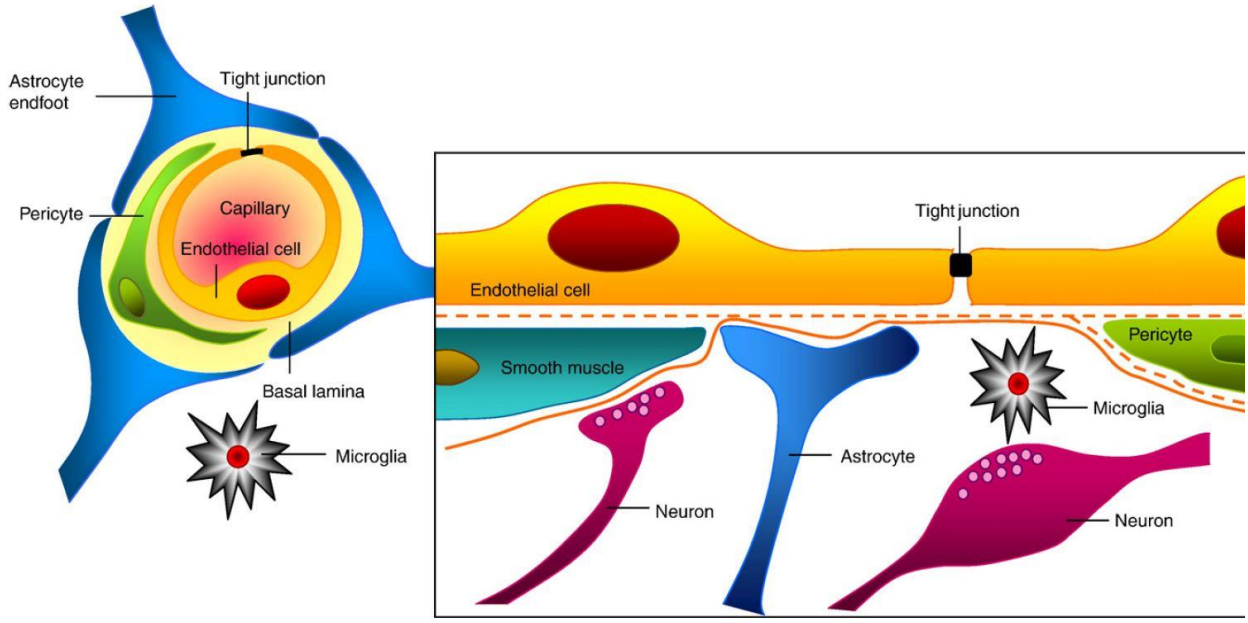

Figure 1.1 A schematic representation of the blood-brain barrier (BBB) with its heterogeneous cellular structure and associations. Reproduced, with permission, from (Abbott et al. 2010)[1] © (2010) Elsevier (doi: 10.1016/j.nbd.2009.07.03010.1016/j.nbd.2009.07.030) and from (Abbott et al. 2006)[2] © (2006) Nature Publishing Group (doi:10.1038/nrn1824).

Complex tight junctions expressed between neighboring brain endothelial cells are a key feature of the BBB that restrict the passage of blood-borne solutes, macromolecules, and other substances from entering the brain (Abbott et al. 2010). Tight junctions are an elaborate complex of intercellular cleft proteins, occludin and claudin-1, -3, -5, which are linked to cytoplasmic scaffolding proteins including cingulin, ZO-1, -2, and -3 (all anchored to the cytoskeleton) (Huber et al. 2001, Wolburg and Lippoldt 2002, Hawkins and Davis 2005, Abbott et al. 2010) (Figure 1.2). Complex tight junctions are primarily responsible for BBB function and account for the high electrical resistance of the barrier (approximately 2,000 Ω*cm^2) *in vivo*

[1] Reprinted from Neurobiology of Disease, 37(1), Abbott, N. J., Patabendige, A. A., Dolman, D. E., Yusof, S. R. and Begley, D. J., "Structure and function of the blood-brain barrier," 13-25, 2010, with permission from Elsevier.
[2] Adapted by permission from Macmillan Publishers Ltd: [Nature Reviews Neuroscience] (Abbott, N. J., Rönnbäck, L. and Hansson, E. (2006). "Astrocyte–endothelial interactions at the blood–brain barrier." Nat Rev Neurosci **7**(1): 41-53), copyright (2006)

(Hamm et al. 2004, Abbott et al. 2010). Damage to one or a number of the components of the BBB due to traumatic insult or disease can impair its ability to form a functional barrier, ultimately compromising the health and function of the CNS (Hawkins and Davis 2005, Shlosberg et al. 2010, Shetty et al. 2014).

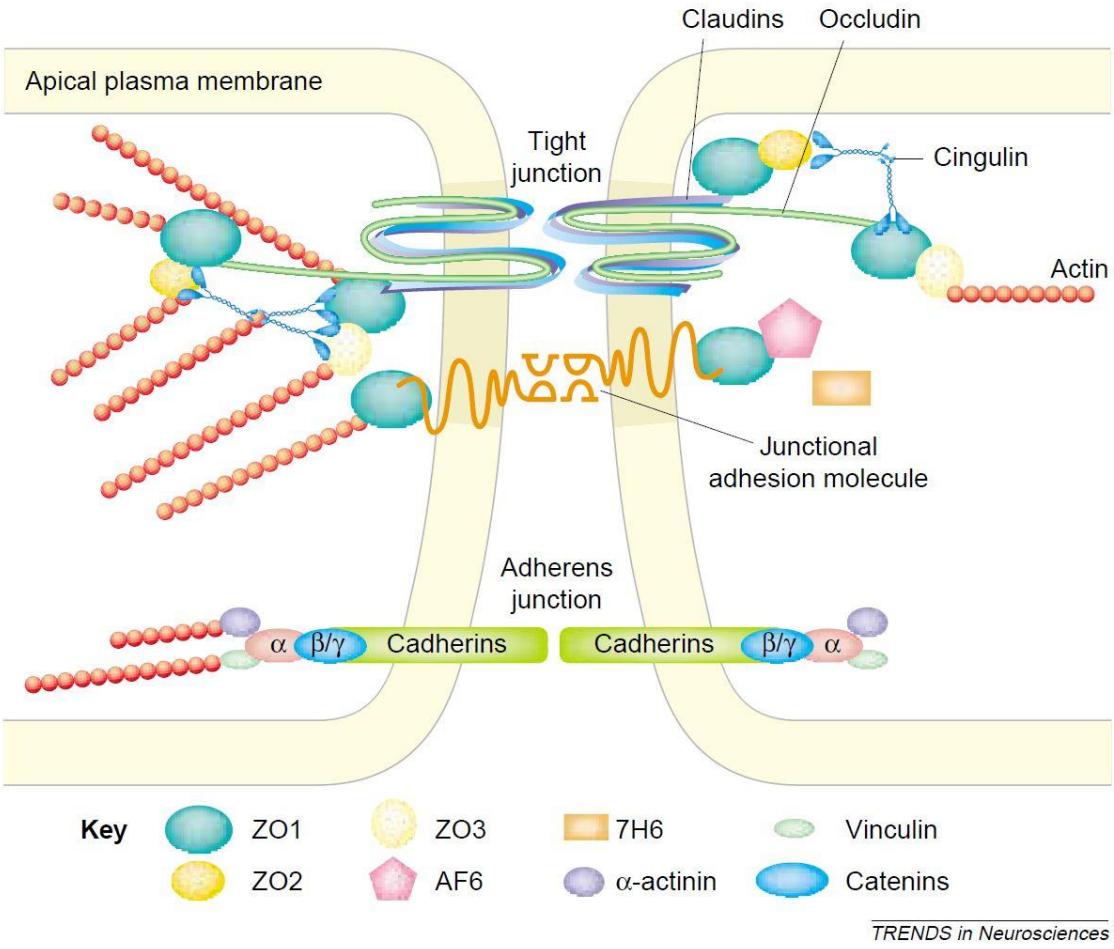

Figure 1.2 A schematic representation of the structure of complex tight junctions expressed between brain endothelial cells. Reproduced, with permission, from (Huber et al. 2001)[3] © (2001) Elsevier (doi:10.1016/S0166-2236(00)02004-X).

[3] Reprinted from Trends in Neurosciences, 24(12), Huber, J. D., Egleton, R. D. and Davis, T. P., "Molecular physiology and pathophysiology of tight junctions in the blood-brain barrier," 719-725, 2001, with permission from Elsevier.

1.2 Primary blast-induced BBB dysfunction

BBB damage associated with TBI results in brain edema and increased cerebrovascular permeability, both of which affect morbidity and mortality in head-injured patients (Unterberg et al. 2004, Ling et al. 2009, Chen and Huang 2011, Magnuson et al. 2012). In particular, in-theater clinical observations of casualties resulting from explosive blast report that edema, intracranial hemorrhage, and vasospasm are characteristic pathophysiological outcomes of bTBI (Bauman et al. 2009, Ling et al. 2009). Brain edema after TBI is closely associated with damage to the BBB, which may permit the influx of serum components through compromised endothelial tight junctions and ultimately result in neuronal dysfunction and degeneration (Liu and Sturner 1988, Unterberg et al. 2004, Shlosberg et al. 2010). The net expansion of brain volume elicits increased intracranial pressure, impaired cerebral perfusion and oxygenation that impact patient outcome (Unterberg et al. 2004). Although the role of vascular pathology in acute neurological dysfunction has only recently been explored, pathologies closely associated with BBB dysfunction – neuroinflammation, excitotoxicity, impaired molecular and ion flux, edema, intracerebral hemorrhage, and others – have become a matter of major clinical importance (Klatzo 1987, Liu and Sturner 1988, Shlosberg et al. 2010, Shetty et al. 2014, Elder et al. 2015).

BBB dysfunction lasting from days to years after the initial injury event has been observed in experimental models of TBI (blast and non-blast) and in clinical studies (Korn et al. 2005, Armonda et al. 2006, Tomkins et al. 2008, Readnower et al. 2010, Garman et al. 2011, Fujita et al. 2012, Abdul-Muneer et al. 2013, Yeoh et al. 2013). Several mechanisms have been proposed to operate during the secondary wave of brain damage following BBB disruption, including altered interactions among the cellular components of the neurovascular unit and deficits in the structural integrity of BBB tight junction complexes (Hawkins and Davis 2005,

Abbott et al. 2006, Shlosberg et al. 2010). Recovery of low permeability and BBB function has been shown to occur within days to weeks following blast injury and concussive injury *in vivo*; however, there is a need for greater quantitative understanding of the relationship between cerebrovascular compromise and the physical initiators of TBI, particularly in primary blast (Shapira et al. 1993, Kirchhoff et al. 2006, Readnower et al. 2010, Garman et al. 2011, Abdul-Muneer et al. 2013, Yeoh et al. 2013). Utilization of our bTBI model to study isolated effects of blast overpressure on the BBB *in vitro* enables determination of more accurate tolerance criteria specifically for the BBB in response to primary blast-loading.

1.3 BBB disruption after repeated blast injury

Repeated exposure to mild blast overpressure may potentially increase the burden of neurobehavioral and cognitive deficits, in part, by lowering the threshold for damage in a subsequent exposure and establishing a temporal window of heightened vulnerability to injury (Elder and Cristian 2009, Rosenfeld and Ford 2010, Kamnaksh et al. 2012). Service personnel exposed to low-intensity blasts in the military setting often exhibit mild symptoms and may return to duty without sufficient recovery-time, placing them at greater risk of sustaining additional blast injuries that may worsen ongoing pathobiological cascades (Trudeau et al. 1998, Kamnaksh et al. 2012, Abdul-Muneer et al. 2013). Although potential effects of multiple blast exposures pose a major challenge to the military healthcare system, results of clinical and experimental investigations have not conclusively demonstrated exacerbated neuropathological, cognitive, or inflammatory outcomes following repeated blast exposure (Trudeau et al. 1998, Elder and Cristian 2009, Saljo et al. 2009, Blennow et al. 2011, Saljo et al. 2011, Wang et al. 2011, Ahlers et al. 2012, Elder et al. 2012, Kane et al. 2012, Abdul-Muneer et al. 2013).

Repeated insults delivered within specific time frames have been shown to aggravate brain pathology in studies utilizing impact- and inertia-driven models of repetitive brain injury (non-blast); however, only a limited number of studies have addressed the potential for concomitant BBB dysfunction (Fujita et al. 2012). Experimental and human TBI case studies report that repeated exposure to mild TBI (mTBI) can lead to dramatic cumulative deficits in behavior, cognition, and cerebral metabolism when they occur within hours to days following the initial insult (Longhi et al. 2005, Friess et al. 2009, Peskind et al. 2011, Shitaka et al. 2011, Fujita et al. 2012, Prins et al. 2013). Athletes receiving a second injury while still symptomatic from a previous head injury presented with evidence of cerebral vascular engorgement, consistent with the clinical scenario of second-impact syndrome whereby exposure to a single mTBI results in elevated risk for damage induced by subsequent mTBIs (Cantu and Gean 2010, Kamnaksh et al. 2012).

Despite a limited number of studies that have assessed the acute effects of a single primary blast on the BBB (Readnower et al. 2010, Garman et al. 2011, Effgen et al. 2012, Abdul-Muneer et al. 2013, Yeoh et al. 2013), only recently have studies shed light on the pathological complexity associated with repeated bTBI on the cerebral microvasculature. In a recent study of officers from the Swedish Armed Forces, repeated exposure to the firing of heavy weapons and explosives produced no neurochemical evidence of neuronal or BBB damage (Blennow et al. 2011). By contrast, primary blast injury in rats induced nitrosative and oxidative damage in the BBB after repeated exposure to low-intensity shock waves, and reduced protein expression levels of tight-junction proteins ZO-1, claudin-5, and occludin (Abdul-Muneer et al. 2013). Others have reported that the pathological changes in rats exposed to multiple mild blast injuries were not cumulative, despite significant neuronal, glial, and vascular damage after a

single mild exposure (Kamnaksh et al. 2012). Therefore, additional work is necessary for developing a more detailed understanding of the cerebrovascular changes that arise following multiple blast injuries and their relation to the neuropathological and behavioral changes associated with bTBI (Blennow et al. 2011, Wang et al. 2011, Fujita et al. 2012).

1.4 Potentiated BBB recovery after blast with glucocorticoid treatment

Given that breakdown of the BBB can induce signaling cascades and downstream interactions among pathological processes in the neurovascular unit that can lead to brain edema, inflammation, and neuronal dysfunction (Unterberg et al. 2004, Hawkins and Davis 2005, Abbott et al. 2006, Shlosberg et al. 2010), there is urgent need for the development of therapeutic strategies to help protect against primary blast-induced damage to the BBB or to potentiate cellular repair processes after exposure. Glucocorticoids have played an important role in the clinical management of CNS disorders associated with a compromised BBB, such as edema, brain tumors, and multiple sclerosis (Miller et al. 1992, Kaal and Vecht 2004), and have been studied extensively in experimental treatment models *in vitro* and *in vivo* (Romero et al. 2003, Cucullo et al. 2004, Forster et al. 2005, Forster et al. 2006, Campolo et al. 2013, Thal et al. 2013). For example, dexamethasone (DEX) promotes BBB integrity by initiating glucocorticoid receptor-mediated signaling, leading to altered gene expression and upregulation of tight junction proteins including occludin, claudin-5, and ZO-1 that strengthen and restore barrier properties (Singer et al. 1994, Romero et al. 2003, Forster et al. 2006, Blecharz et al. 2010, Thal et al. 2013). Greater than three-fold increases in transendothelial electrical resistance (TEER), and similar changes in restriction of water permeability have been attributed to glucocorticoid treatment in epithelial and brain endothelial cell cultures (Underwood et al. 1999, Romero et al. 2003, Forster et al. 2005, Forster et al. 2006). Administration of glucocorticoids also

significantly increased gene expression and protein synthesis of occludin and claudin-5, but not of claudin-1, claudin-3, or VE-cadherin (Forster et al. 2008). Others have also reported that glucocorticoid treatment results in fewer frayed junctions and more uniform arrangement of claudin-5 at the cell borders (Romero et al. 2003). Therefore, interventional strategies to promote BBB recovery after blast injury may be a promising therapeutic strategy to mitigate the damaging consequences of bTBI.

1.5 Blast-induced BBB opening *in vivo*

The phenomenon of BBB breakdown has amassed greater recognition as a hallmark of blast injury, (Readnower et al. 2010, Garman et al. 2011, Logsdon et al. 2014, Lucke-Wold et al. 2014) and in some cases, of pure primary blast injury (Abdul-Muneer et al. 2013, Hue et al. 2013, Skotak et al. 2013, Yeoh et al. 2013, Hue et al. 2014, Hue et al. 2015). *In vivo*, blast-induced BBB opening has been assessed most frequently by the extravasation of Evans blue (EB) (Abdul-Muneer et al. 2013, Logsdon et al. 2014, Lucke-Wold et al. 2014) and IgG (Readnower et al. 2010, Garman et al. 2011, Skotak et al. 2013, Yeoh et al. 2013). Other studies have also suggested that BBB opening after blast exposure is sufficient to permit the infiltration of immune cells such as macrophages, polymorphonuclear leukocytes, and lymphocytes into the brain parenchyma (Abdul-Muneer et al. 2013, Tompkins et al. 2013). Despite these findings, however, a number of investigators have reported inconsistent BBB damage even with efforts to carefully control blast injury parameters (Readnower et al. 2010, Garman et al. 2011, Skotak et al. 2013). The complexity of BBB damage after blast may be further confounded by the variety of loading regimes and biomechanical injury parameters (peak overpressure, duration, and impulse) used in different studies. Together, these challenges underscore the critical need for more quantitative analysis of the time course and pore-size of BBB opening after blast exposure,

further supported by kinematic analysis of blast-induced head motion. Such findings would hold important implications for potentially impaired transport processes across the BBB and the influx of toxic blood-borne constituents (normally excluded by the BBB) that may initiate secondary neuropathological cascades after bTBI.

1.6 Significance

TBI is the leading cause of death in young adults and children in the developed world (Shlosberg et al. 2010). Each year in the United States, approximately 1.7 million people sustain a TBI, accounting for at least 50,000 deaths and 235,000 hospitalizations (Langlois et al. 2003, Coronado et al. 2011). TBI is a chronic disease process known to increase long-term mortality and reduce life expectancy, and an estimated 80,000-90,000 individuals experience long-term or permanent disabilities annually (Thurman et al. 1999, Masel and DeWitt 2010). The Centers for Disease Control and Prevention estimates that the lifetime costs of TBI in the United States, associated with medical expenditures and lost productivity, amount to at least $76 billion annually (Langlois et al. 2006, Shlosberg et al. 2010, Sahler and Greenwald 2012). Therefore, TBI has become a major concern for clinicians, researchers, health care providers, and society at large. The prevention and treatment of TBI to reduce its high incidence and devastating consequences continues to be a public health priority in the United States and worldwide.

Since the start of U.S. military operations in 2001, TBI has been considered the "signature injury" of the wars in Iraq (Operation Iraqi Freedom [OIF]) and Afghanistan (Operation Enduring Freedom [OEF]) (Hoge et al. 2008, Schneiderman et al. 2008). Exposure to blasts caused by IEDs is the most common cause of TBI among contemporary battle injuries (Warden 2006, Zouris et al. 2006, Wade et al. 2007, Brethauer et al. 2008, Galarneau et al.

2008). A recent study of hospitalizations of U.S. Army soldiers on OIF/OEF deployments reported that explosions were the cause of approximately 65% of the most severe form of TBI (Wojcik et al. 2010). In addition, an analysis of data from the US Navy-Marine Corps Combat Trauma Registry found that IEDs were responsible for 52% of all TBI cases (Galarneau et al. 2008). Between 2001 and 2005, IEDs were the source of nearly 80% of all casualties reported to the Joint Theater Trauma Registry (JTTR), a data repository for U.S. Department of Defense trauma-related injuries (Owens et al. 2008). Clearly, head injuries caused by exposure to blast account for a significant proportion of mortality and morbidity in service members, warranting further detailed investigation to better understand the etiology and pathobiology of bTBI.

Effectively addressing the burden to society of TBI, especially that caused by explosive blast, requires a multifaceted approach that facilitates the development of novel helmet designs and treatment strategies to mitigate the effects of bTBI in head-injured patients. Furthermore, because BBB breakdown has frequently been documented in patients with TBI (Loane and Faden 2010, Shlosberg et al. 2010), the prevention and management of blast-induced damage to the BBB may be of clinical importance. Efforts are needed to define the threshold for blast-loading required to impart structural and functional changes to the barrier, which is a major goal of the work described herein. Outcomes from this research strongly suggest that BBB damage is a major mechanism contributing to vascular and neuronal pathology of bTBI at exposure levels above a critical threshold. Such findings contribute to the development of tolerance criteria for the BBB in response to primary blast, and ultimately guide the development of novel armor designs to protect service members and civilians at risk of exposure.

There also exists a pressing need to develop more promising therapeutic strategies to treat TBI-related pathologies of the BBB in order to improve healthcare in the clinic (Shlosberg et al.

2010). The BBB has emerged as a promising therapeutic target for the treatment of bTBI in light of recent studies reporting breakdown of the cerebral microvasculature resulting specifically from blast exposure (Readnower et al. 2010, Garman et al. 2011, Abdul-Muneer et al. 2013, Hue et al. 2013, Skotak et al. 2013, Yeoh et al. 2013, Logsdon et al. 2014, Lucke-Wold et al. 2014, Hue et al. 2015). Delivering treatments that activate specific intracellular signaling cascades known to repair the BBB or induce barrier integrity (Forster et al. 2008, Liebner et al. 2008, Alvarez et al. 2011, Mizee et al. 2013) represents a potential strategy for ameliorating the deleterious consequences of bTBI. Work described in this dissertation has advanced this goal through mechanistic studies of modulating BBB integrity to potentiate functional recovery of the barrier after blast exposure.

2 Blood-brain barrier dysfunction after primary blast injury *in vitro*[4]

2.1 Introduction

Traumatic brain injury (TBI) resulting from explosive blast in modern military conflicts has become the signature wound sustained by both warfighters and civilians working in combat zones (Ling et al. 2009, Kuehn et al. 2011). Recent evidence highlights the growing concern for neuropathological consequences of blast exposure (DePalma et al. 2005, Elder and Cristian 2009, Ling et al. 2009). In this setting, brain injury has been hypothesized to be caused by direct interaction with the shock wave associated with a blast, in a process termed primary blast injury (DePalma et al. 2005, Taber et al. 2006). However, understanding the biophysics that cause blast-induced traumatic brain injury (bTBI) remains elusive. We hypothesize that one potential mechanism of brain injury is mediated by damage to the blood-brain barrier (BBB), which separates capillaries over 600 km in length from the brain parenchyma with a barrier only 300 nm in thickness (Huber et al. 2001, Pardridge 2007).

The BBB is a heterogeneous unit consisting of brain endothelial cells expressing tight junctions that are essential to ensure the barrier's integrity and low permeability (Risau and Wolburg 1990, Wolburg and Lippoldt 2002, Abbott et al. 2006, Simon et al. 2010). Tight junctions are made up of claudins, occludin, and the zonula occludens accessory proteins (ZO-1 and ZO-2), which form the restrictive paracellular diffusion barrier characterized by high

[4] A modified version of this chapter previously appeared in print: Hue, C.D., Cao, S., Haider, S.F., Vo, K.V., Effgen, G.B., Vogel, E., 3rd, Panzer, M.B., Bass, C.R., Meaney, D.F., Morrison, B., 3rd. (2013). Blood-brain barrier dysfunction after primary blast injury in vitro. J Neurotrauma 30, 1652-1663. Reproduced with permission (doi:10.1089/neu.2012.2773).

electrical resistance (Kniesel and Wolburg 2000, Simon et al. 2010). Because the BBB plays a central role in preventing the transport of potentially neurotoxic blood-borne molecules into the neural parenchyma, damage to the barrier has been known to exacerbate several central nervous system (CNS) pathologies such as multiple sclerosis and stroke, and may be an important mediator in bTBI (Huber et al. 2001, Hicks et al. 2010, Readnower et al. 2010, Svetlov et al. 2010, Chen and Huang 2011, Garman et al. 2011). However, further investigation is warranted to understand the physical mechanism responsible for potential BBB breakdown resulting from militarily-relevant levels of blast exposure.

BBB disruption associated with TBI results in brain edema and increased cerebrovascular permeability, both of which affect morbidity and mortality in head-injured patients (Unterberg et al. 2004, Chen and Huang 2011). In-theatre clinical observations of casualties resulting from explosive blast further report that edema, intracranial hemorrhage, and vasospasm are characteristic pathophysiological outcomes of bTBI (Bauman et al. 2009, Ling et al. 2009). Brain edema after TBI is thought to be initiated by BBB rupture, permitting the influx of protein-rich exudate through compromised endothelial tight junctions that may lead to delayed neuronal dysfunction and degeneration (Liu and Sturner 1988, Unterberg et al. 2004, Shlosberg et al. 2010). The net expansion of brain volume elicits increased intracranial pressure, impaired cerebral perfusion and oxygenation that impact patient outcome (Unterberg et al. 2004). Although the role of vascular pathology in acute neurological dysfunction has only recently been explored, such neuropathologies directly linked to BBB breakdown have become a matter of major clinical importance (Klatzo 1987, Liu and Sturner 1988, Shlosberg et al. 2010).

Breakdown of the BBB, lasting from several days to years after the initial injury event, has been observed in animal models of experimental TBI and in clinical studies (Korn et al.

2005, Tomkins et al. 2008). Several mechanisms have been proposed to operate during the secondary wave of brain damage following BBB disruption, including altered interactions among cellular components of the neurovascular unit and deficits in the structural integrity of BBB tight junction complexes (Hawkins and Davis 2005, Abbott et al. 2006, Shlosberg et al. 2010). Restoration of low permeability and BBB function has been shown to occur within days to weeks following concussive injury *in vivo*; however, there is a need for greater quantitative understanding of the relationship between cerebrovascular compromise and the physical initiators of TBI (Shapira et al. 1993, Kirchhoff et al. 2006).

Several studies have demonstrated brain microvasculature and BBB breakdown resulting from blast exposure in rodent and small animal models of bTBI (Readnower et al. 2010, Garman et al. 2011, Kuehn et al. 2011). However, there is incomplete understanding of the mechanism(s) governing BBB damage following primary blast, distinct from a combination of primary and tertiary (acceleration-driven) blast injuries which are typically difficult to separate in animal models. To explore the pathophysiological effects of primary blast exposure alone on the barrier, we subjected an *in vitro* model of the BBB (a brain endothelial monolayer mimicking cell-specific phenotype and functional properties of the BBB), to controlled blast-loading at militarily-relevant exposure levels (Li et al. 2010, Simon et al. 2010, Effgen et al. 2012). We report isolated *primary* blast-induced barrier damage, quantify associated effects on BBB permeability and tight junction breakdown, and describe a time-course for spontaneous barrier recovery. We conclude that primary blast injury alone is capable of acutely disrupting the integrity of an *in vitro* BBB model at realistic blast-loading conditions, suggesting a possible physical mechanism for vascular and subsequent neuronal pathology after blast.

2.2 Materials and Methods

2.2.1 *In vitro* BBB model

Brain endothelial monolayers representing the BBB were cultured using the bEnd.3 mouse brain microvascular cell line (ATCC, Manassas, VA). This cell line has been widely used in other *in vitro* BBB cell culture models for its rapid growth properties and ability to maintain BBB features and functions over multiple passages (Gumbleton and Audus 2001, Li et al. 2010, Simon et al. 2010, Booth and Kim 2012, Naik and Cucullo 2012). For all experiments, a total of 60,000 bEnd.3 cells were seeded on Transwell inserts (1.12 cm^2 membrane growth area) pre-coated with poly-L-lysine (Simon et al. 2010, Effgen et al. 2012). Cultures were maintained for 7 to 8 days at 37º C and 5 % CO_2 to achieve confluence in Dulbecco's Modified Eagle's Medium (DMEM) supplemented with 10 % newborn calf serum and 4 mM GlutaMAX (Life Technologies, Carlsbad, CA). Cultures were fed every 2 to 3 days. Cell monolayers with trans-endothelial electrical resistance (TEER) less than 15 $\Omega*cm^2$ were not included in the study (see Quantification of TEER).

2.2.2 Shock wave-induced injury of the BBB

A recently described *in vitro* bTBI model consisting of a shock tube and fluid-filled sample receiver was used to expose endothelial monolayers to controlled primary blast injury (Effgen et al. 2012). Prior to blast exposure, cultures were enclosed within sterile bags (Whirl Pak, Fort Atkinson, WI) filled with culture medium pre-warmed to 37º C. Any entrapment of air bubbles was meticulously prevented during sample preparation. For every experiment, each culture and bag was submerged in the fluid-filled sample receiver to a pre-determined depth, and oriented perpendicular to the direction of shock wave propagation.

Ideal Friedlander-like shock waves, mimicking overpressure/duration profiles similar to those observed in free-field blasts, were generated using a 76 mm-diameter shock tube with an adjustable-length driver section (25 or 50 mm used for the current study) pressurized with helium or nitrogen gas, and a 1240 mm-long driven section (Figure 2.1A) (Effgen et al. 2012, Panzer et al. 2012). Pressure transducers (8530B, Endevco, San Juan Capistrano, CA) flush-mounted at the tube outlet recorded the incident pressure of the shock wave (Figure 2.1B). A range of loading conditions was tested for the parameters of peak incident overpressure, duration, and impulse (Table 2.1). These blast parameters were determined in the open-tube configuration in the absence of interacting structures downstream, since this arrangement represented an independent and consistent measure of the injury input. Unless otherwise indicated, all blast parameters reported in this study refer to open-tube measurements. A transducer (8530B, Endevco) flush-mounted to the interior of the sample receiver test column measured the fluid pressure history directly beneath the submerged BBB sample (Figure 2.1C). Blast parameters in the receiver fluid were measured for each corresponding open-tube configuration (Table 2.1). A previously published characterization of our *in vitro* bTBI model confirmed that the pressure wave was not attenuated as it passed through the BBB sample (Effgen et al. 2012). Sham controls were also enclosed in sterile bags and submerged in the receiver for a duration matching the injured cultures, but were not exposed to blast (Effgen et al. 2012).

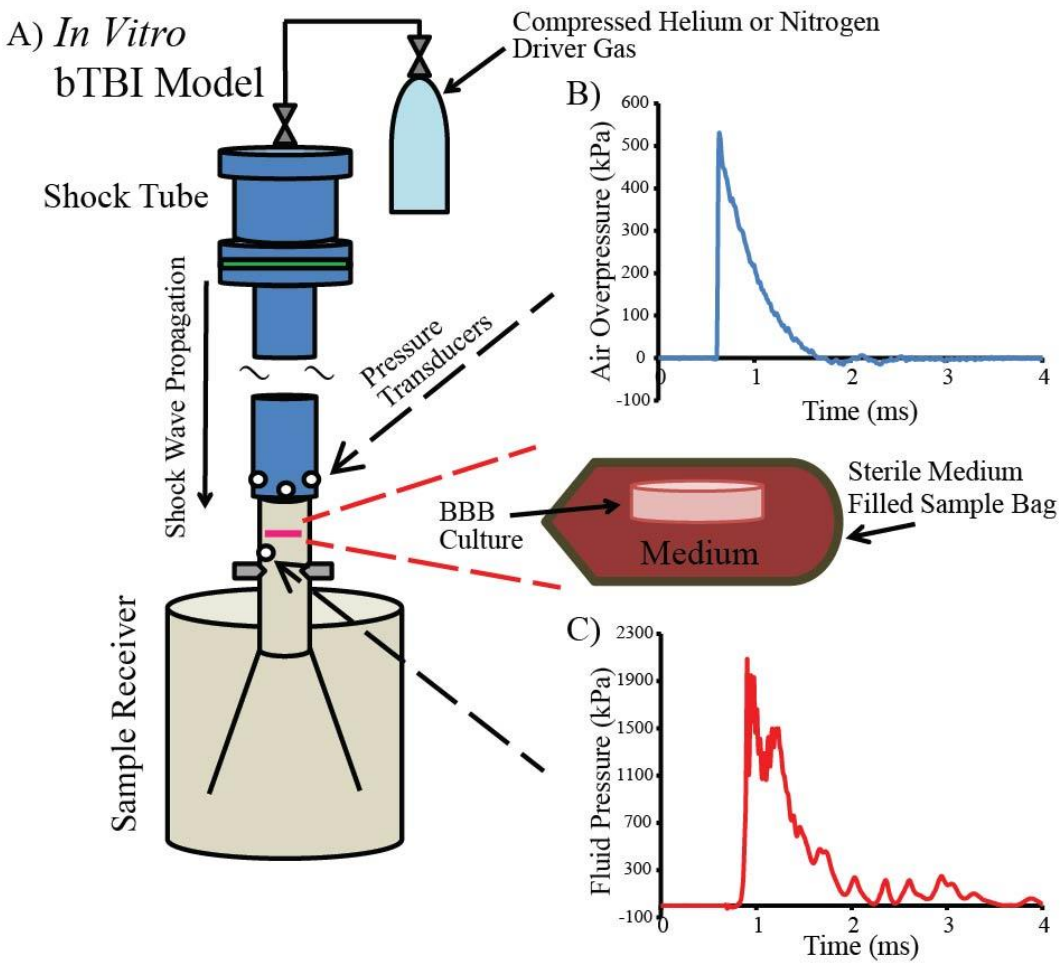

Figure 2.1 *In vitro* bTBI model consisting of shock tube and fluid-filled sample receiver as previously described (Effgen et al. 2012). A) Compressed helium or nitrogen gas was connected to an adjustable driver section of the shock tube. Transducers were flush-mounted at the tube's exit and within the receiver column to measure pressure history of experimental blast injury input. B) An example shock wave recorded in the open-tube configuration by transducers flush-mounted at the exit of the shock tube. Biomechanical injury parameters associated with this example pressure trace include a peak overpressure of 571 kPa, duration of 1.06 ms, and impulse of 186 kPa*ms. C) Example fluid pressure history, associated with 571 kPa shock wave in open-tube configuration, measured by a transducer located directly beneath the submerged BBB culture in sample receiver. Image reproduced with permission (Effgen et al. 2012).

Experimental Blast Injury Parameters

	Peak Overpressure (kPa)	Duration (ms)	Impulse (kPa*ms)	Driver Gas
open-tube	231 ± 11	0.60 ± 0.01	40 ± 0.9	helium
receiver	439 ± 21	1.43 ± 0.02	232 ± 5.5	helium
open-tube	250 ± 5	1.15 ± 0.02	85 ± 3.1	nitrogen
receiver	797 ± 29	1.51 ± 0.02	514 ± 22.5	nitrogen
open-tube	377 ± 8	0.89 ± 0.01	96 ± 1.5	helium
receiver	817 ± 22	1.53 ± 0.04	472 ± 15.5	helium
open-tube	469 ± 21	0.99 ± 0.01	143 ± 1.5	helium
receiver	1258 ± 26	1.46 ± 0.02	658 ± 22.4	helium
open-tube	311 ± 5	1.54 ± 0.02	148 ± 3.4	nitrogen
receiver	1083 ± 57	1.52 ± 0.01	733 ± 2.7	nitrogen
open-tube	571 ± 15	1.06 ± 0.01	186 ± 1.5	helium
receiver	1523 ± 91	1.48 ± 0.03	812 ± 29.3	helium
open-tube	342 ± 8	1.83 ± 0.04	192 ± 6.6	nitrogen
receiver	1223 ± 42	1.62 ± 0.02	852 ± 39.4	nitrogen
open-tube	396 ± 7	2.40 ± 0.06	276 ± 8.3	nitrogen
receiver	1431 ± 22	1.65 ± 0.02	911 ± 9.3	nitrogen

Table 2.1 Experimental primary blast-loading conditions tested in this study were characterized by peak incident overpressure, duration, and impulse, measured in the open-tube configuration and in the fluid-filled sample receiver (mean ± SEM; $n \geq 3$ for open-tube parameters; $n \geq 2$ for receiver parameters).

2.2.3 Quantification of TEER

TEER is a resistance measure dependent on ion flux through the cell monolayer, and thus provides a way to functionally characterize the integrity of the monolayer as well as tight junctions (Gaillard et al. 2001, Brown et al. 2007). TEER was recorded immediately before and between 2 to 10 minutes after blast exposure using an Endohm-12 electrode chamber connected to an EVOMX Epithelial Voltohmmeter (World Precision Instruments, Sarasota, FL). Consistent with TEER calculations for *in vitro* BBB models reported in the literature (Li et al. 2010, Simon et al. 2010, Booth and Kim 2012), all TEER values were corrected for the TEER of a cell-free insert and then normalized for the insert surface area. Measurements reported in this study represent the TEER of each culture normalized to its pre-injury group average. For the time-course evaluation, the TEER of injured cultures was further normalized to age-matched and time point-matched sham controls. Sham control cultures were processed identically to injured cultures, but were not exposed to blast.

2.2.4 Quantification of BBB hydraulic conductivity

Hydraulic conductivity serves as a functional indicator of monolayer tightness, as the BBB restricts water flux from the systemic circulatory system to the brain *in vivo* (Deli et al. 2005, Simon et al. 2010). To measure hydraulic conductivity between 30 minutes to 2 hours post-injury, cultures were placed in a custom-built polycarbonate chamber (Sill et al. 1995, Li et al. 2010, Simon et al. 2010). Each BBB model was then subjected to a known hydrostatic pressure across the monolayer, giving rise to fluid flow through the culture. Water flux was quantified by tracking the displacement of an air bubble through a calibrated glass tube connected to the chamber. Hydraulic conductivity (L_p, cm/s/cmH_2O) was calculated using equation (1) (Li et al. 2010, Simon et al. 2010)

$$L_p = \frac{\frac{\Delta x}{\Delta t} \times F}{S \times \Delta P} \quad (1)$$

where, $\frac{\Delta x}{\Delta t}$ is the displacement of the bubble over time, F is the fluid volume contained in a known length of tubing, S is the surface area of the culture, and ΔP is the hydrostatic pressure across the endothelial monolayer.

2.2.5 Quantification of BBB solute permeability

Solute permeability serves as a quantitative measure of the diffusive permeability of a blast-injured BBB to a range of molecular weights. To measure solute permeability between 30 minutes to 2 hours post-injury, fluorescent solutes of specific molecular weights including fluorescein-labeled 3 and 10 kDa dextrans (Life Technologies; excitation 494 nm, emission 521 nm), and Texas Red®-labeled 40 and 70 kDa dextrans (Life Technologies; excitation 595 nm, emission 615 nm) were added to the upper Transwell compartment above the BBB culture. Every 30 minutes for 4 hours, 100 µL of medium was collected from the lower chamber, and the fluorescence was quantified using a SpectraMax M2 Microplate Reader (Molecular Devices, Sunnyvale, CA). The 100 µL sample was replaced with 100 µL fresh medium, and this change in volume was accounted for when calculating the change in concentration over time. The diffusive solute permeability (P, cm/s) was calculated using equation (2) (Li et al. 2010, Simon et al. 2010)

$$P = \frac{\frac{\Delta C_B}{\Delta t} \times V_B}{S \times C_T} \quad (2)$$

where, $\frac{\Delta C_B}{\Delta t}$ is the change in concentration of dextrans over time in the lower compartment, V_B is the volume contained in the lower compartment, S is the surface area of the culture, and C_T is the concentration in the upper compartment.

2.2.6 Evaluation of ZO-1 morphology

To assess disruption of the structural integrity of tight junctions between 1 to 2 hours following blast exposure, the BBB endothelial cultures were fixed and incubated with anti-ZO-1 rabbit polyclonal antibody (Life Technologies). The presence of ZO-1 tight junction proteins, a standard marker for BBB integrity (Mori et al. 2002, Li et al. 2010, Simon et al. 2010, Booth and Kim 2012), was detected using the Alexa Fluor 488 anti-rabbit secondary antibody (Life Technologies). Cultures were also incubated with 4', 6-diamidino-2-phenylindole (DAPI, Life Technologies) to detect individual cell nuclei and to count the number of cells in each monolayer culture. Using antibodies manufactured from the same lot and applied at the same post-injury time-point, all samples were imaged with an Olympus IX81 (Olympus America, Center Valley, PA) fluorescence microscope and MetaMorph software (Molecular Devices, Sunnyvale, CA). The degree of ZO-1 immunostaining was quantified by applying an identical threshold for ZO-1 immunofluorescence to each of 5 randomly selected images acquired from every sham and injured culture. ZO-1 immunostaining was measured as the area-percentage exhibiting fluorescence above the threshold, normalized to the total number of endothelial cells in each image. This quantification method is similar to published methods on evaluating bEnd.3 barrier

integrity by calculating the percentage of pixels with intensities above a threshold value (Simon et al. 2010).

2.2.7 Statistical analysis

Hydraulic conductivity, ZO-1 immunostaining, and cell-count comparison data were analyzed statistically by one-way ANOVA followed by Dunnett *post hoc* tests to sham controls. Dose-dependent TEER response data were analyzed by repeated-measures to determine the effect of blast on TEER in the acute phase post-injury, followed by one-way ANOVA and Dunnett *post hoc* tests to sham controls. Repeated-measures analysis was used to determine the effect of blast on the temporal recovery of TEER, followed by one-way ANOVA and Dunnett *post hoc* tests to the pre-injury group. Independent samples t-tests between sham and injured cultures were used to analyze solute permeability data (SPSS v. 20, IBM, Armonk, NY, significance * $p < 0.05$).

2.3 Results

2.3.1 Decreased TEER after blast

An initial investigation was conducted to identify a threshold for this disruption as determined by a significant decrease in TEER measured acutely between 2 to 10 minutes after blast exposure. Using helium as the driver gas, TEER acutely decreased in a dose-dependent manner at increasing severities of blast from: 231 to 571 kPa peak incident overpressure, 0.60 to 1.06 ms duration, and 40 to 186 kPa*ms impulse (Figure 2.2A). Following the 469 kPa peak overpressure blast, TEER significantly ($p < 0.05$) decreased to 78 ± 8 % of pre-exposure levels compared to 102 ± 3 % in sham controls (Figure 2.2A). TEER continued to decrease at greater blast levels, while exposure to lower severity blasts with peak overpressure ranging from 231 to

377 kPa, duration of 0.60 to 0.89 ms, and impulse of 40 to 96 kPa*ms did not significantly reduce TEER.

We next sought to identify the most influential biomechanical blast parameter driving damage to the barrier. Changing the driver gas to nitrogen enabled generation of a different combination of parameters that included generally lower peak overpressures at longer durations and higher impulses compared to helium as the driver gas. TEER acutely decreased in a dose-dependent manner as the blast severity increased from: 250 to 396 kPa peak incident overpressure, 1.15 to 2.40 ms duration, and 85 to 276 kPa*ms impulse (Figure 2.2B). Following the 342 kPa peak overpressure blast, TEER significantly decreased to 73 ± 2 % of pre-exposure levels compared to 97 ± 5 % in sham controls (Figure 2.2B). TEER continued to decrease as the blast severity increased, while exposure to milder blasts with peak overpressure ranging from 250 to 311 kPa, duration of 1.15 to 1.54 ms, and impulse of 85 to 148 kPa*ms did not significantly reduce TEER.

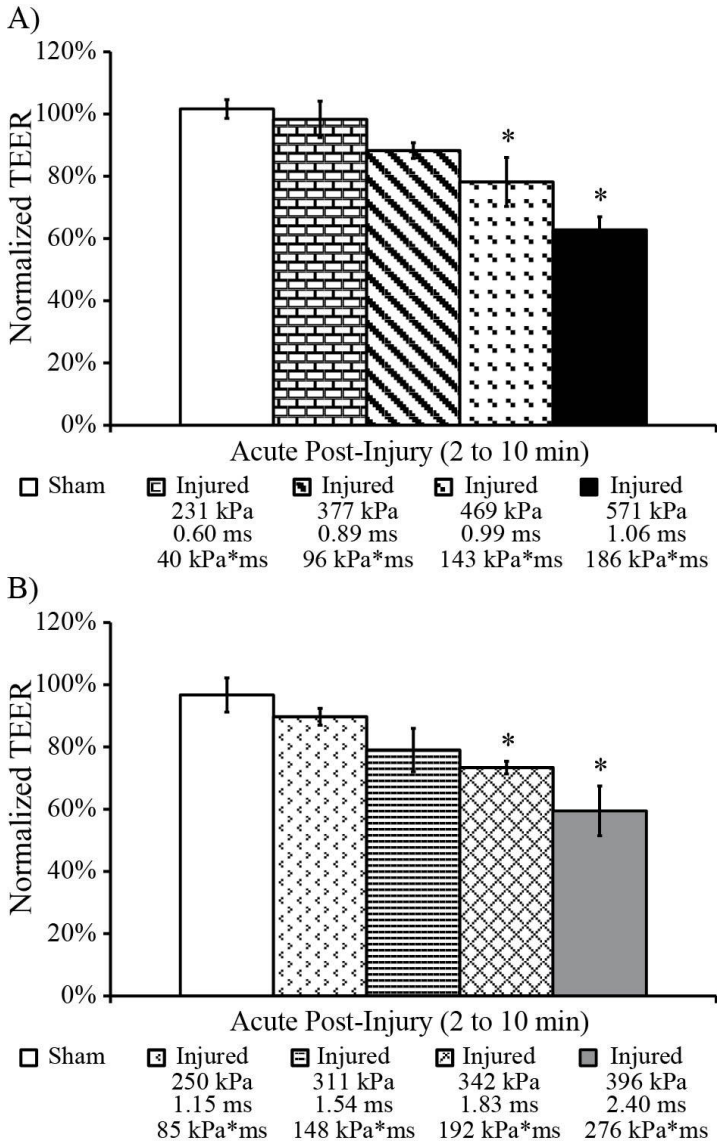

Figure 2.2 Dose-dependent TEER response in endothelial monolayers following exposure to a range of blast-loading conditions. A) Following the 469 kPa peak overpressure blast (helium driver gas), TEER significantly and acutely decreased in injured cultures to 78 ± 8 % of pre-exposure levels. B) Following the 342 kPa peak overpressure blast (nitrogen driver gas), TEER significantly and acutely decreased in injured cultures to 73 ± 2 % of pre-exposure levels. (* $p < 0.05$; ± SEM; Sham $n \geq 8$; Injured $n \geq 6$ per blast condition)

To determine which blast parameter was most critical to BBB disruption, the correlation between changes in TEER and each of the three biomechanical injury parameters – peak overpressure, duration, and impulse – measured in the open-tube configuration (air) and in the

sample receiver (fluid) was determined. As evidenced by the high R^2 values of 0.92 (Figure 2.3A) and 0.88 (Figure 2.3D) for measurements in both the air and fluid, changes in TEER were overall most strongly correlated with impulse. A significant decrease in TEER after blast was observed at an air impulse as low as 143 kPa*ms, indicating functional deficits at TEER levels approximately 80 % of pre-injury values (Figure 2.2A, B). TEER was also strongly correlated with peak overpressure measured in the fluid, as indicated by a high R^2 value of 0.93 (Figure 2.3E). Weaker associations were evident between TEER and air peak overpressure, air duration, and fluid duration, which were all associated with comparatively lower R^2 values of 0.52, 0.52, and 0.34, respectively (Figure 2.3B, C, F).

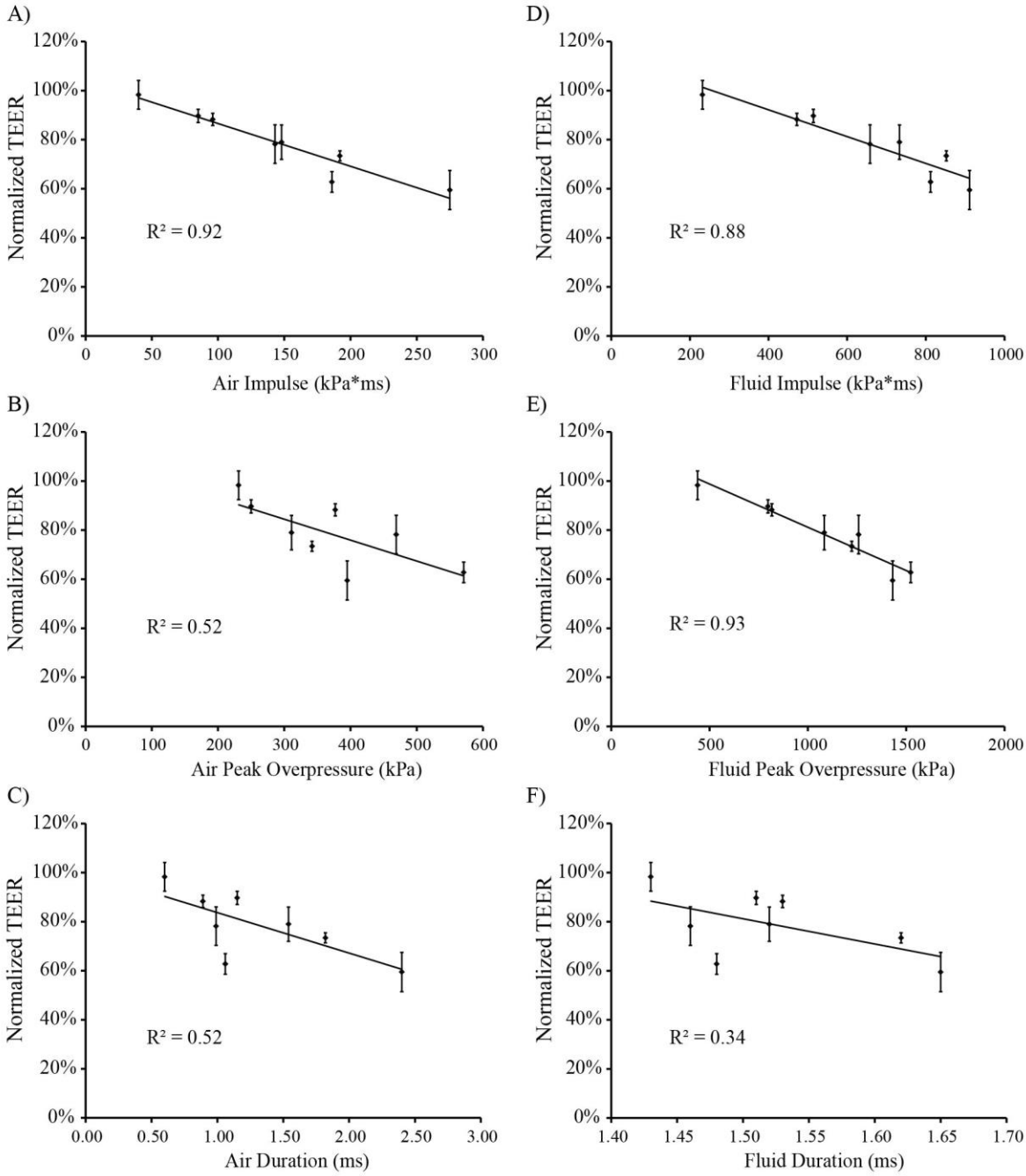

Figure 2.3 Correlations established for changes in TEER with different blast injury parameters measured in the open-tube configuration (air) and in the sample receiver (fluid). Linear functions were fit to the data for each association. A) Correlation between TEER and air impulse, showing $R^2 = 0.92$. B) Correlation between TEER and air peak overpressure, indicating a weaker association with $R^2 = 0.52$. C) Correlation between TEER and air duration, indicating a weaker association with $R^2 = 0.52$. D) Correlation between TEER and fluid impulse, showing $R^2 = 0.88$. E) Correlation between TEER and fluid peak overpressure, showing $R^2 = 0.93$. F) Correlation between TEER and fluid duration, indicating a weaker association with $R^2 = 0.34$.

2.3.2 Increased hydraulic conductivity after blast

Hydraulic conductivity, L_p, was measured between 30 minutes to 2 hours post-injury to quantify water flux through the BBB model. After exposure to blast with a peak overpressure of 571 kPa, duration of 1.06 ms, and impulse of 186 kPa*ms (helium driver gas), hydraulic conductivity was significantly increased to $11.4 \pm 3.5 \times 10^{-7}$ cm/s/cmH_2O compared to $2.9 \pm 0.4 \times 10^{-7}$ cm/s/cmH_2O in sham controls (Figure 2.4). Similarly, blast with a peak overpressure of 396 kPa, duration of 2.40 ms, and impulse of 276 kPa*ms (nitrogen driver gas) significantly increased hydraulic conductivity to $7.5 \pm 1.9 \times 10^{-7}$ cm/s/cmH_2O (Figure 2.4). Blasts with peak overpressures of 469 or 342 kPa, durations of 0.99 or 1.83 ms, and impulses of 143 or 192 kPa*ms did not cause significant increases in hydraulic conductivity.

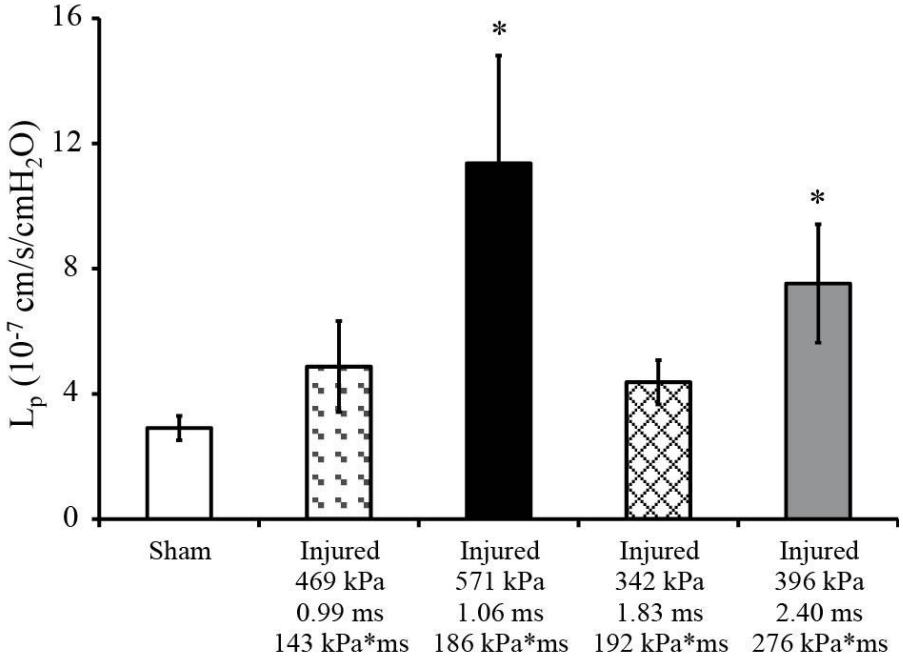

Figure 2.4 Hydraulic conductivity of blast exposed endothelial monolayers. Between 30 minutes to 2 hours after injury, cultures exposed to the 571 and 396 kPa blasts exhibited a significant increase in hydraulic conductivity to $11.4 \pm 3.5 \times 10^{-7}$ cm/s/cmH_2O and $7.5 \pm 1.9 \times 10^{-7}$ cm/s/cmH_2O, respectively, compared to $2.9 \pm 0.4 \times 10^{-7}$ cm/s/cmH_2O in sham controls. (* $p < 0.05$; ± SEM; Sham n = 23; Injured n ≥ 6 per blast condition).

2.3.3 Increased solute permeability after blast

Between 30 minutes to 2 hours of exposure to blast with a peak overpressure of 571 kPa, duration of 1.06 ms, and impulse of 186 kPa*ms (helium driver gas), a trend of increased solute permeability was observed. The permeability of exposed cultures at the 10 kDa group significantly increased to $2.5 \pm 0.3 \times 10^{-6}$ cm/s compared to $1.2 \pm 0.2 \times 10^{-6}$ cm/s in shams (Figure 2.5).

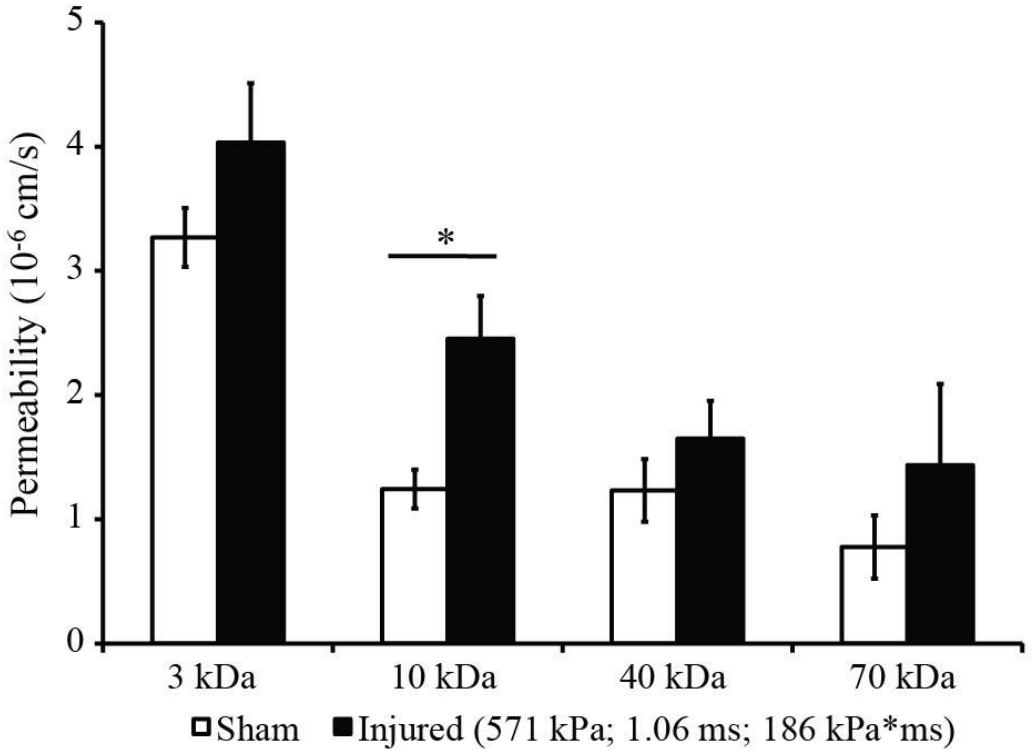

Figure 2.5 Increased solute permeability of 3, 10, 40, and 70 kDa dextran molecules after blast exposure. Injured cultures exhibited a significant increase in solute permeability to $2.5 \pm 0.3 \times 10^{-6}$ cm/s compared to $1.2 \pm 0.2 \times 10^{-6}$ cm/s in shams for the 10 kDa molecular weight tracer. (* $p < 0.05$; ± SEM; Sham n = 6; Injured n = 6)

2.3.4 Disruption of ZO-1 after blast

In sham cultures, ZO-1 immunostaining revealed high levels of ZO-1 protein on the surface of cells and at the junctions between cells, indicating wide-spread expression of tight

junction proteins (Figure 2.6A). Visual examination of immunofluorescence images of the bEnd.3 cultures confirmed confluent cell monolayers exhibiting characteristic, elongated spindle-shape morphology for sham controls (Figure 2.6A), bearing very close resemblance to the cell architecture of confluent bEnd.3 monolayers shown by light microscopy and tight junction immunostaining in previous studies (Omidi et al. 2003, Brown et al. 2007, Li et al. 2010, Simon et al. 2010, Effgen et al. 2012). Between 1 to 2 hours of exposure, a blast with peak overpressure of 571 kPa, duration of 1.06 ms, and impulse of 186 kPa*ms (helium driver gas) substantially decreased ZO-1 staining and altered tight junction morphology (Figure 2.6B). Similarly, a blast with peak overpressure of 396 kPa, duration of 2.40 ms, and impulse of 276 kPa*ms (nitrogen driver gas) substantially compromised ZO-1 staining (Figure 2.6C). The morphology of tight junctions in both injury groups was more punctate and discontinuous, leaving regions between cells devoid of well-formed tight junctions. Consistent with the qualitative imaging data, the area-percentage of ZO-1 immunostaining per cell was significantly decreased in the 571 kPa injured cultures to 0.25 ± .02 % and in the 396 kPa injured cultures to 0.18 ± .01 %, compared to 0.31 ± .02 % in sham controls (Figure 2.6D). Previous characterization of our bTBI model has confirmed cell viability following similar exposure levels, showing the absence of any significant cell death post-injury (Effgen et al. 2012).

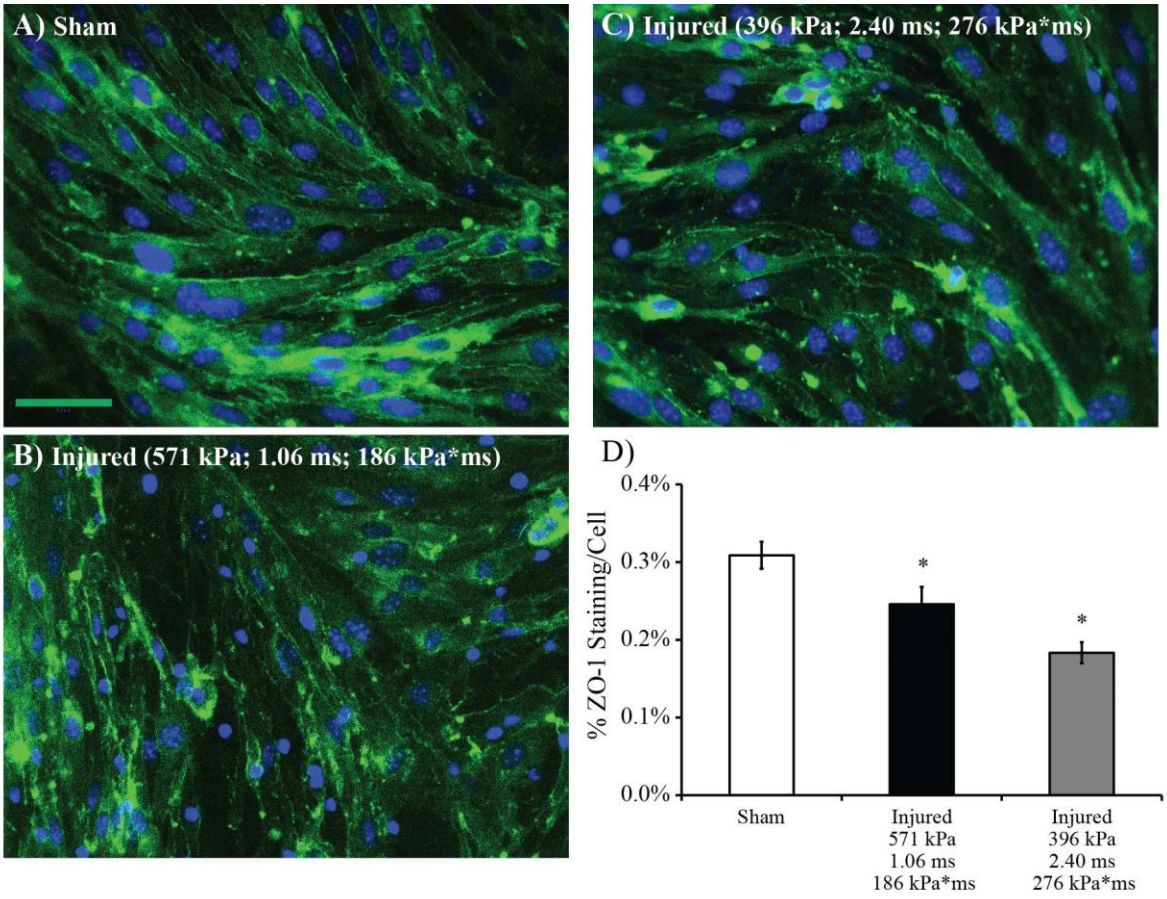

Figure 2.6 Immunostaining of ZO-1 (green), a marker for tight junctions. A) Immunostaining of ZO-1 in sham cultures revealed high levels of ZO-1 expression and well-formed tight junctions. B) Compromised ZO-1 staining in cultures exposed to a blast with a 571 kPa peak overpressure, 1.06 ms duration, and 186 kPa*ms impulse (helium driver gas). C) Compromised ZO-1 staining in cultures exposed to a blast with a 396 kPa peak overpressure, 2.40 ms duration, and 276 kPa*ms impulse (nitrogen driver gas). D) Quantitative analysis of ZO-1 immunostaining showing significantly reduced staining after both levels of blast injury, supporting qualitative interpretation of the immunofluorescence images. (* $p < 0.05$; ± SEM; Sham n = 50; Injured n ≥ 20 per blast condition; Scale bar = 50 µm).

The average number of cells in each immunofluorescence image was quantified to determine the degree of cell detachment between 1 to 2 hours of exposure to the 571 and 396 kPa peak overpressure blasts. In sham controls, the average cell count per field of view was 90 ± 2, while corresponding cell counts for cultures injured at the 571 and 396 kPa overpressure levels

were 87 ± 3 and 79 ± 2, respectively (Figure 2.7). Significant cell detachment compared to sham was only observed for cultures exposed to the highest level blast (396 kPa overpressure, 2.40 ms duration, and 276 kPa*ms impulse, nitrogen driver gas).

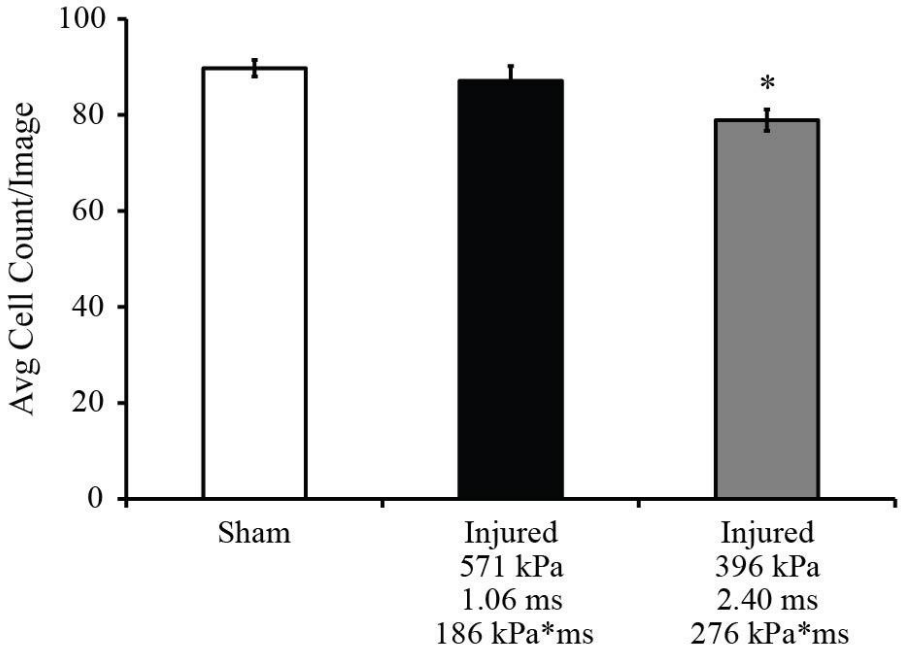

Figure 2.7 Average cell count per immunostained image to quantify cell detachment between 1 to 2 hours of blast exposure. The cell count was significantly reduced by 12 % in cultures exposed to a blast with a 396 kPa peak overpressure, 2.40 ms duration, and 276 kPa*ms impulse (nitrogen driver gas). (* $p < 0.05$; ± SEM; Sham n = 50; Injured n ≥ 20 per blast condition).

2.3.5 Temporal recovery of TEER after blast

The temporal recovery of TEER was measured after a blast with a peak overpressure of 571 kPa, duration of 1.06 ms, and impulse of 186 kPa*ms (helium driver gas). This level was selected because it was shown to cause a robust decrease in TEER based on the dose-dependent response in the *in vitro* BBB model without significant loss of cells (Figure 2.2A). TEER of the injured cultures, normalized to age-matched and time point-matched sham controls, decreased in

the acute phase 30 minutes after injury (Figure 2.8). TEER remained significantly depressed for 2 days after exposure as compared to pre-injury levels (Figure 2.8). Injured cultures recovered over time, and exhibited full-recovery to pre-injury TEER levels at 3 days post-blast (Figure 2.8).

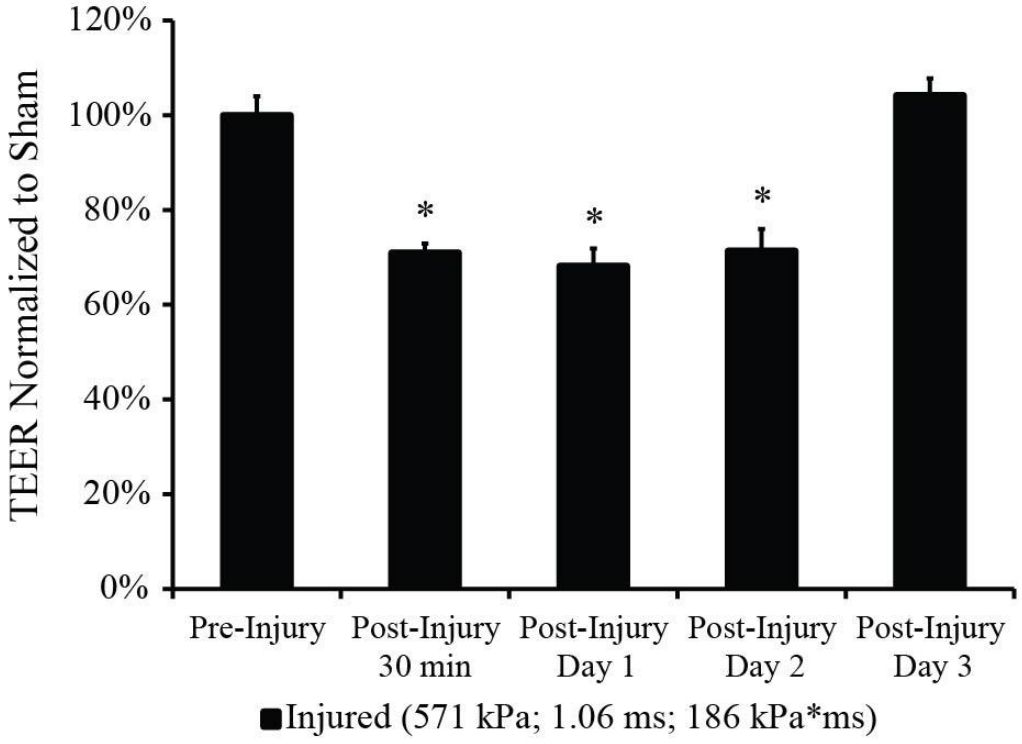

Figure 2.8 TEER time-course of blast-exposed endothelial monolayers normalized to age-matched sham controls. Depressed TEER of injured cultures fully recovered to pre-injury levels at 3 days post-blast. (* $p < 0.05$; ± SEM; n = 3).

2.4 Discussion

There exists a need to quantitatively assess changes in BBB integrity following blast-loading at militarily relevant exposures. Several experimental bTBI models in rodents have demonstrated blast-induced BBB disruption through heightened permeability to endogenous circulating IgG. Elevated IgG immunohistochemical staining has been observed in the rat cortex

after exposure to a 120 kPa peak overpressure blast, but with unreported duration and impulse (Readnower et al. 2010). Increased IgG immunoreactivity was observed in the contralateral cortex of rats 24 hours after exposure to a 241 kPa overpressure blast with approximately a 4 ms duration (Garman et al. 2011). Following a sub-lethal complex blast of 427 to 517 kPa peak overpressure delivered to the head of rats, abnormal IgG immunolabeling in the cerebellum and thalamus signified microvascular dysfunction (Kuehn et al. 2011). Collectively, such evidence provides valuable insight into the vulnerability of the BBB to blast; however, the challenge remains of harmonizing differences between injury parameters used in the models. Analysis of the outcomes is further complicated by the biomechanical complexity of *in vivo* models, making it difficult to separate the specific contributions of shearing and stretching forces due to inertial loading from interaction of a primary blast pressure transient with the brain parenchyma and specialized structures like the BBB (Morrison et al. 2011, Effgen et al. 2012, Panzer et al. 2012). Exposure conditions of the aforementioned studies are also quite different from those used in this study. For instance, blast exposure to the unprotected torso of rats may potentially lead to injury cascades in the thoracic cavity that may affect the BBB and evoke transient effects within the brain (Readnower et al. 2010). The apparatus used in delivery of a complex blast potentially reflected a high-pressure wave off of the closed cranial surface of the rats (Kuehn et al. 2011), while the integrated impulse of longer duration shocks (4 to 5 ms) described by others are substantially larger but may not be representative of operationally-relevant blast conditions (Readnower et al. 2010, Bass et al. 2011, Garman et al. 2011).

A definitive link between mild TBI (mTBI) associated with blast exposure and primary blast injury parameters (peak overpressure, duration, and impulse), has not been established. A mouse model of blast neurotrauma reported in a recent study demonstrated chronic traumatic

encephalopathy (CTE)-related neuropathologies in blast-exposed mice, including tau protein hyperphosphorylation, vascular damage, and neurodegeneration, among others (Goldstein et al. 2012). Functional deficits including hippocampal-dependent learning and memory impairments were also observed after delivery of a single sub-lethal shock wave with 77 kPa peak incident overpressure (Goldstein et al. 2012). The investigators demonstrated that blast winds associated with the shock wave induced oscillating head accelerations sufficient to cause brain injury, as their model permitted free movement of the animal head to mimic real-world blast-loading conditions (Fijalkowski et al. 2007, Goldstein et al. 2012). It is important to note that neurological deficits initially observed after exposure were reduced with head immobilization, suggesting that blast-induced inertial loading on the head (in addition to primary blast effects of the shock wave) was a major mechanism responsible for the ensuing neuropathology.

Capabilities provided by the *in vitro* blast injury model used in our study, however, enable separation of the effects of primary blast from secondary or tertiary (inertial loading) phases of blast injury. Using high-speed video, we have observed minimal to no gross deformation or movement of the sample during blast exposure. Our ability to isolate the shock wave component from confounding influences of the inertial component enables precise investigation of injury thresholds for primary blast, as opposed to the combination of primary and tertiary blast mechanisms. Furthermore, as previously described, our test methodology reproduces the intracranial loading whereby an external shock wave is translated to a fast-rising pressure wave (Effgen et al. 2012). Therefore, our *in vitro* model best represents the dynamic pressures that occur within the head/brain complex during a blast event.

Our results indicate that integrity of the BBB decreases in a dose-dependent manner with increasing severities of primary blast. Correlations established between TEER and each of the

three blast parameters measured in the air and fluid confirmed impulse to be the overall most influential injury parameter responsible for disruption of the *in vitro* BBB model. We observed significant functional disruption of our BBB model after blast with an air impulse of 143 kPa*ms, with minimal alterations to barrier integrity evident at impulse levels as low as 40 kPa*ms. Other reports have suggested that the impulse component of the blast wave is a key parameter influencing severity of the damage and neurological deficits after blast exposure (Chen et al. 2009, Panzer et al. 2012). Interestingly, changes in TEER were much more strongly correlated with peak overpressure in the receiver fluid rather than in air, further implying the importance of measuring intracranial pressure history in addition to the external shock wave for accurately predicting the effects of primary blast injury. The weakest association was found between TEER and fluid duration, likely because material compliance in the sample receiver limited the range of durations that could be achieved with our specific device configuration. Future studies will examine if using more rigid materials of construction for the receiver will enable a broader range of fluid durations to be generated that could potentially be more closely correlated with changes in TEER. Nevertheless, the fact that injury outcome determined by TEER was so highly correlated with fluid impulse and fluid peak overpressure is encouraging, as such insight will inform the development of detailed injury tolerance criteria for brain tissue exposed to primary blast.

It is also encouraging that the threshold values we determined are above the sub-lethal shock wave input of 77 kPa overpressure reported in a previous study that resulted in no functional deficits when the mouse head was immobilized (Goldstein et al. 2012), which is the approximate condition we are modeling in the current study. We also note that our impulse-driven functional disruption may be specific to the ideal Friedlander curve generated by our *in*

vitro bTBI model (Effgen et al. 2012), and is potentially sensitive to more complex loading scenarios with altered pressure histories and frequency content that will be the subject of future studies. Previous characterization of our *in vitro* bTBI model has also demonstrated the absence of significant endothelial cell death following exposure to similar blast levels causing significant decreases in TEER (Effgen et al. 2012).

Real-world blast exposures in the military setting, predicted by the Conventional Weapons Effects Program, span a range of 50 to 1000 kPa peak incident overpressure with 2 to over 8 ms duration (D.W. 2004, Panzer et al. 2012, Panzer et al. 2012). Consistent with this range, loading conditions in this study were sufficient to cause functional changes similar to realistic blast threats. For instance, a blast with 571 kPa peak overpressure and 1.06 ms duration is similar to exposure to a 105 mm artillery round at a standoff distance of 5 to 10 m, which represents a common IED scenario (Nelson et al. 2008, Panzer et al. 2012). Our *in vitro* bTBI model was capable of achieving single overpressure pulses between 0.60 and 2.40 ms in duration, comparable to loading conditions predicted by computational blast studies (Bauman et al. 2009, Panzer et al. 2012, Panzer et al. 2012).

A major function of the BBB *in vivo* is to exclude water flux by the presence of tight junctions (Bershad et al. 2008), and measuring blast-induced modulation of hydraulic conductivity is important for linking exposure to the neuropathological conditions associated with vessel hyper-permeability (Fenstermacher 1984, Olson et al. 1997, Victorino et al. 2003, Diringer and Zazulia 2004, Elliott et al. 2007, Garcia et al. 2011). This study is the first to quantify a blast-induced increase in water flux across an *in vitro* BBB model. Hydraulic conductivity of our sham control cultures was in strong agreement with published values on the order of 10^{-7} cm/s/cmH_2O for similar bEnd.3 culture systems (Li et al. 2010, Simon et al. 2010).

We observed changes in hydraulic conductivity for our *in vitro* BBB cultures between 30 minutes to 2 hours of blast exposure at increasing magnitudes of impulse. While there is a lack of published literature quantifying water flux across the BBB after primary blast, it is possible that this relatively long time-window – coupled with potential differences in the time-course of blast-induced BBB opening – accounts for why our hydraulic conductivity results did not mirror the acute TEER dose-dependent response observed (between 2 to 10 minutes after exposure) with increasing impulse levels. A previous study comparing the progression of BBB opening in different rat models of TBI demonstrated that impact acceleration resulted in immediate BBB opening followed by rapid closing of the barrier, whereas lateral cortical impact was associated with prolonged BBB opening for up to 4 hours (Beaumont et al. 2000). Therefore, we anticipate that more precisely defining the time point at which hydraulic conductivity is measured after injury will allow for improved mechanistic understanding of the high incidence of brain edema following bTBI (Ling et al. 2009, Mac Donald et al. 2011).

A normally functioning BBB *in vivo* is capable of impeding the diffusion of molecules greater than 500 Da between the systemic and brain compartments (van Asperen et al. 1997). Others have demonstrated shock-wave induced membrane permeabilization of *in vitro* cell culture systems by increased uptake of molecules of varying weights including calcein (622 Da), propidium iodide (668 Da), trypan blue (873 Da), and fluorescein isothiocyanate-dextran (72 kDa) (Gambihler and Delius 1992, Kodama et al. 2000, Sonden et al. 2000, Sonden et al. 2002). Importantly, it was found that permeability of solutes did not depend on peak pressure of the shock waves, but was critically dependent on impulse (Kodama et al. 2000). It is also vital to note that shock waves tested in these studies were of peak overpressures exceeding 1 MPa with

durations on the order of microseconds (Kodama et al. 2000, Sonden et al. 2000, Sonden et al. 2002), which are not applicable to real-world blast events.

Following blast exposure, significantly increased permeability of 10 kDa dextrans in our exposed BBB cultures suggested impaired ability of the monolayers to restrict the passage of solutes equal to or below this molecular weight. However, because our endothelial cultures do not form permeability barriers as restrictive as those observed *in vivo* or in primary cell culture systems (Gumbleton and Audus 2001, Omidi et al. 2003, Yuan et al. 2010), the baseline permeability of the 3 kDa dextrans was high in shams and not significantly elevated in blast-injured cultures. The permeabilities of other *in vitro* BBB models (incorporating bEnd.3 cells) to similar dextran tracers ranging from 3 to 70 kDa were in close agreement with permeability values observed in our sham cultures (Li et al. 2010, Simon et al. 2010, Booth and Kim 2012). Clinical studies have used dynamic magnetic resonance imaging of gadolinium diethylenetriaminepentaacetate (Gd-DTPA; 550 Da) (Hawkins et al. 1990) to identify areas of BBB breakdown in neurological diseases such as multiple sclerosis (Larsson et al. 1990, Tofts and Kermode 1991). Permeability values for multiple sclerosis lesions in patients ranged from 4 to 17×10^{-6} cm/s (Tofts and Kermode 1991), which is comparable to our measured permeabilities for 3 and 10 kDa solutes in blast-exposed cultures. Increased solute permeability post-injury holds implications for neurotoxic serum constituents that may infiltrate the brain, potentially leading to neuronal dysfunction or death.

A potential limitation of the current study is that at one of the highest exposures tested, endothelial cells may have detached from the Transwell membrane. The counting of nuclei (representing individual cells) in immunostaining images of sham and injured cultures resulted in a non-significant difference in cultures exposed to the 571 kPa peak overpressure blast, but a

significant difference ($p < .05$) in cultures exposed to the 396 kPa overpressure blast. Detachment was minimal, however, as the average number of cells between sham and injured images differed by no more than 11 cells (12 % of total cells in shams), and is likely only applicable to the highest impulse exposure level tested in this study (396 kPa overpressure, 2.40 ms duration, 276 kPa*ms impulse, nitrogen driver gas). Others utilizing *in vitro* cell monoculture systems have reported some degree of cell detachment after shock wave exposure (Sonden et al. 2000, Sonden et al. 2002), which is thought to resemble *in vivo* lesions associated with pathophysiological processes of bTBI (Sonden et al. 2000). Denuded regions of cell loss have been observed after exposure to shock wave pulse trains, sometimes in conjunction with cavitation, in extracorporeal lithotripsy models (Sonden et al. 2000). We did not observe denuded patches in our cultures using our blast injury model.

BBB dysfunction and the disruption of tight junctions is a common phenomenon following TBI (Morganti-Kossmann et al. 1999, Huber et al. 2001, Vilalta et al. 2008, Blyth et al. 2011). The ZO-1 accessory protein is extensively studied because its interactions with the cytoskeleton are thought to dictate the localization and functional expression of tight junctions (Willis et al. 2004, Lai et al. 2005, Fanning et al. 2007, Simard et al. 2008). Activation of pro-inflammatory factors and MMPs are implicated in elevated BBB permeability following TBI, causing degradation of tight junction proteins including ZO-1, an MMP-9 substrate (Mori et al. 2002, Grossetete et al. 2009, Hayashi et al. 2009, Vajtr et al. 2009). ZO-1 levels have been shown to decrease by up to 50 % of baseline at 24 hours post-injury using a controlled cortical impact model (Mori et al. 2002). This effect is comparable to our approximately 55 % decrease in ZO-1 staining after exposure to a 276 kPa*ms impulse blast, suggesting similar BBB disruption under dramatically different physical loading conditions.

The bEnd.3 mouse brain microvascular cell line was used in our *in vitro* BBB model for its ability to retain phenotypic stability, preserve physiologic cell architecture, and form a functional paracellular barrier (Gumbleton and Audus 2001, Omidi et al. 2003, Brown et al. 2007, Simon et al. 2010). While our model consisted of only one cell type, the BBB is commonly thought of as a three-cell archetype that includes the brain capillary endothelial cell, astrocyte, and supporting pericyte, to help mediate full expression of the BBB phenotype (Gumbleton and Audus 2001). Brain endothelial tight junctions in rats establish a rate-limiting diffusion barrier resulting in sucrose (342 Da) (Deli et al. 1995) permeability ranging from 0.03 to 0.10×10^{-6} cm/s (Ohno et al. 1978, Gumbleton and Audus 2001, Huber et al. 2001). By comparison, the measured permeability of 3 kDa dextrans through our sham control cultures was at least an order of magnitude higher, at 3.3×10^{-6} cm/s. TEER values reported *in vivo* exceed 1000 $\Omega*cm^2$ (Pardridge 1999, Gumbleton and Audus 2001), whereas typical values achieved by our *in vitro* culture system are approximately 20 to 30 $\Omega*cm^2$ (Li et al. 2010, Simon et al. 2010, Booth and Kim 2012). Primary cerebromicrovascular endothelial cells more closely resemble the BBB phenotype *in vivo* due to their ability to form tight monolayers with higher TEER and lower permeability (Gumbleton and Audus 2001, Omidi et al. 2003, Li et al. 2010, Simon et al. 2010); however, their vulnerability to contamination by other neurovascular unit cells, lack of phenotypic stability over multiple passages *in vitro,* and inter- and intra-batch variability between cultures may hamper sensitivity for identification of injury thresholds (Gumbleton and Audus 2001, Omidi et al. 2003).

The endothelial monolayer exhibited an intrinsic capacity for spontaneous recovery as demonstrated by the full recovery of TEER at 3 days post-injury. *In vivo* bTBI studies reporting BBB damage marked by increased IgG levels in the brain have shown return to control levels 3

days post-exposure, which is in close agreement with our TEER recovery period (Readnower et al. 2010, Garman et al. 2011). Self-repair mechanisms leading to restoration of BBB integrity after the biomechanical insult have been described in other TBI models like fluid percussion injury, where initial increases in BBB permeability (detected by IgG brain localization) was followed by barrier recovery preventing further influx of the circulating proteins (Enters et al. 1992, Tanno et al. 1992, Fukuda et al. 1995). These results help provide insight on standing controversy as to whether damaged endothelial cells can undergo functional recovery (Landis 1994), and suggest value in developing acute therapeutic strategies to repair the blast-injured BBB.

In summary, this study is the first to demonstrate disruption of an *in vitro* model of the BBB after exposure solely to primary blast injury. The acute dose-dependent TEER response following exposure to a range of blast-loading conditions revealed compromised monolayer integrity that was most strongly correlated with impulse. BBB opening after exposure was confirmed by significantly increased hydraulic conductivity and solute permeability. The physical breakdown of tight junctions was identified with compromised ZO-1 immunostaining. The temporal recovery of TEER post-blast highlighted that acute treatments to repair the blast-injured BBB may provide clinical utility. Taken together, these results indicate that BBB damage could be a major mechanism contributing to vascular and neuronal pathology of bTBI at blast levels above a critical threshold, and hold implications for novel helmet designs to mitigate the effects of blast in humans.

3 Repeated primary blast injury causes delayed recovery, but not additive disruption, in an *in vitro* blood-brain barrier model[5]

3.1 Introduction

Prevalent use of improvised explosive devices (IEDs) in recent military conflicts has motivated study of the underlying neuropathological mechanisms associated with mild traumatic brain injury (mTBI) resulting from one or more exposures to blast overpressure (Warden 2006, Hoge et al. 2008, Ahlers et al. 2012). Epidemiological studies have reported that repeated exposure to mild blast overpressure may potentially increase the burden of neurobehavioral and cognitive deficits, in part, by lowering the threshold for damage and establishing a temporal window of heightened vulnerability (Elder and Cristian 2009, Rosenfeld and Ford 2010, Kamnaksh et al. 2012). In the military setting, personnel exposed to low-intensity blasts often exhibit mild symptoms and may return to duty without sufficient recovery-time, placing them at greater risk of sustaining additional blast injuries that may worsen ongoing pathobiological cascades (Trudeau et al. 1998, Kamnaksh et al. 2012, Abdul-Muneer et al. 2013). Though potential effects of multiple blast exposures pose a major challenge to the military healthcare system, results of clinical and experimental investigations have not conclusively demonstrated exacerbated neuropathological, cognitive, or inflammatory outcomes following repeated blast exposure (Trudeau et al. 1998, Elder and Cristian 2009, Saljo et al. 2009, Blennow et al. 2011,

[5] A modified version of this chapter previously appeared in print: Hue, C.D., Cao, S., Dale Bass, C.R., Meaney, D.F., Morrison, B., 3rd. (2014). Repeated primary blast injury causes delayed recovery, but not additive disruption, in an in vitro blood-brain barrier model. J Neurotrauma 31, 951-960. Reproduced with permission (doi:10.1089/neu.2013.3149).

Saljo et al. 2011, Wang et al. 2011, Ahlers et al. 2012, Elder et al. 2012, Kane et al. 2012, Abdul-Muneer et al. 2013).

Studies utilizing impact- and inertia-driven models of repetitive brain injury (non-blast) have shown that repeated insults delivered within specific time frames can aggravate brain pathology; however, only a limited number of studies have addressed the potential for concomitant blood-brain barrier (BBB) dysfunction (Fujita et al. 2012). Experimental and human traumatic brain injury (TBI) case studies have shown that repeated exposure to mTBI can lead to dramatic cumulative deficits in behavior, cognition, and cerebral metabolism when they occur within hours to days following the initial insult (Longhi et al. 2005, Friess et al. 2009, Peskind et al. 2011, Shitaka et al. 2011, Fujita et al. 2012, Prins et al. 2013). Athletes receiving a second injury while still symptomatic from a previous head injury presented with evidence of cerebral vascular engorgement, consistent with the clinical scenario of second-impact syndrome whereby exposure to a single mTBI results in elevated risk for severe damage induced by subsequent mTBIs (Cantu and Gean 2010, Kamnaksh et al. 2012).

Although previous work from our laboratory and others has assessed the acute effects of a single primary blast on the BBB (Readnower et al. 2010, Garman et al. 2011, Effgen et al. 2012, Abdul-Muneer et al. 2013, Hue et al. 2013, Yeoh et al. 2013), only recently have studies started to shed light on the pathological complexity associated with repeated bTBI on the cerebral microvasculature. In a recent study of officers from the Swedish Armed Forces, repeated exposure to the firing of heavy weapons and explosives produced no neurochemical evidence of neuronal or BBB damage (Blennow et al. 2011). In contrast, primary blast injury in rats induced nitrosative and oxidative damage in the BBB after repeated exposure to low-intensity shock waves, as well as reduced the tight-junction proteins zonula occludens-1 (ZO-1),

claudin-5, and occluding (Abdul-Muneer et al. 2013). Others have reported that the pathological changes observed in rats exposed to multiple mild blast injuries were not cumulative, despite findings of significant neuronal, glial, and vascular damage after a single mild exposure (Kamnaksh et al. 2012). Therefore, additional work is needed to develop a more detailed understanding of the cerebrovascular changes that arise following multiple blast injuries, and their relation to the neuropathological and behavioral changes associated with bTBI (Blennow et al. 2011, Wang et al. 2011, Fujita et al. 2012).

In this study, we investigate the consequences of repeated bTBI by subjecting an *in vitro* model of the BBB (consisting of a monolayer of brain endothelial cells) (Hue et al. 2013) to controlled primary blast-loading at realistic exposure levels (Effgen et al. 2012, Panzer et al. 2012, Hue et al. 2013). We test the hypothesis that exposure to two blast injuries administered within a short time frame leads to cumulative functional deficits in the BBB compared to a single exposure. The resulting outcome on BBB integrity was found to be dependent on the severity of the injury and time-interval between insults. We report that damage to the BBB following two blast injuries, as opposed to one, was not additive. Importantly, we find that repeated blast delayed the spontaneous recovery of BBB function. With a prolonged inter-injury interval, the effects of multiple injuries on the BBB were found to be independent given sufficient recovery time between consecutive injuries. Defining the window of vulnerability for damage to the cerebral microvasculature may hold important implications for mandatory resting periods for service members exposed to blast, prior to returning to duty.

3.2 Materials and Methods

3.2.1 BBB cell culture model

Monolayers of immortalized mouse brain endothelial cells, bEnd.3 (ATCC, Manassas, VA), were cultured in Dulbecco's Modified Eagle's Medium (DMEM; Mediatech, Manassas, VA) supplemented with 10 % newborn calf serum (Thermo Scientific, Logan, UT) and 4 mM GlutaMAX (Life Technologies, Carlsbad, CA). A total of 60,000 cells were seeded in Transwell inserts (1.12 cm^2 surface area) pre-coated with poly-L-lysine, and grown to confluence to represent *in vitro* models of the BBB (Hue et al. 2013). Cell cultures were maintained for 7 days prior to experimentation to achieve confluent, integral monolayers in a cell-culture incubator at 37º C and 5 % CO_2/95 % O_2, and were fed with new medium every 2-3 days (Effgen et al. 2012, Hue et al. 2013).

3.2.2 Repeated exposure of BBB to primary blast injury

As described previously in detail, an *in vitro* bTBI model comprised of a shock tube and fluid-filled sample receiver was used to expose BBB cultures to controlled primary blast injury (Effgen et al. 2012, Hue et al. 2013). For repeated blast exposures, *in vitro* BBB cultures were subjected to two consecutive blasts at pre-determined severity levels, separated by either a 24 hour or extended 72 hour interval. Prior to injury, cultures were placed in sterile bags (Whirl Pak, Fort Atkinson, WI) filled with medium pre-warmed to 37º C. In accordance with previously published methods (Effgen et al. 2012, Hue et al. 2013), samples were then loaded into the fluid-filled receiver and secured above a perforated polytetrafluoroethylene (PTFE) membrane held at a pre-determined depth. Cultures were oriented in the receiver to allow propagation of the fluid pressure transient in the direction perpendicular to the endothelial monolayer. The double injury group was exposed to an initial blast (injury 1) as well as a

subsequent blast (injury 2). The single injury group was exposed to an initial blast (injury 1), but treated as a sham control for the subsequent blast (injury 2). Sham controls were processed identically to blast-injured cultures at both injury 1 and injury 2, but were not exposed to blast overpressure at either injury time point.

Primary blast overpressure was generated using a 76 mm-diameter shock tube with an adjustable-length driver section (25 mm used for current study) pressurized with compressed helium gas, and a 1240 mm-long driven section. A detailed schematic of the blast-injury device, along with example pressure traces recorded in the open-tube configuration and in the fluid-filled receiver, are described in a previous investigation (Hue et al. 2013). The incident pressure of the shock wave was recorded by pressure transducers (8530B, Endevco, San Juan Capistrano, CA) flush-mounted at the exit of the tube. The fluid pressure history located at the level of the BBB culture was recorded by a pressure transducer (8530B, Endevco) flush-mounted to the interior of the receiver test column. The blast severities ranged from mild to moderate intensity levels (Table 3.1), previously reported to cause acute *in vitro* BBB disruption (Hue et al. 2013). The mild exposure was associated with nominal acute deficits in TEER, while the moderate exposure was associated with greater decreases in TEER signifying moderate acute damage to the barrier (Hue et al. 2013). The biomechanical injury parameters were characterized by peak incident overpressure, duration, and impulse determined in the sample receiver and in the open tube configuration. Because open-tube pressure recordings represent independent measurements uninfluenced by interactions with structures positioned downstream, all blast exposure conditions tested in this study will be identified by their open-tube parameters, unless otherwise noted.

Experimental Repeated Blast Injury Parameters

	Peak Overpressure (kPa)	Duration (ms)	Impulse (kPa*ms)	Severity
open-tube	377 ± 8	0.89 ± 0.01	96 ± 1.5	mild
receiver	902 ± 12	1.38 ± 0.02	483 ± 2.6	
open-tube	402 ± 9	0.92 ± 0.01	118 ± 2.2	moderate
receiver	1196 ± 26	1.35 ± 0.02	580 ± 6.6	

Table 3.1 Primary blast-loading conditions for repeated blast exposure were characterized by peak incident overpressure, duration, and impulse. Parameters were measured in the open-tube (in-air) configuration and in the fluid-filled sample receiver (in-fluid) in close proximity to the sample (mean ± SEM; $n \geq 3$).

3.2.3 Measurement of trans-endothelial electrical resistance (TEER)

The functional integrity of the BBB can be determined by TEER, a sensitive measure of ion flux through the brain endothelial monolayer (Li et al. 2010, Simon et al. 2010, Hue et al. 2013). All TEER values were recorded by placing the *in vitro* BBB model into an Endohm-12 electrode chamber connected to an EVOMX Epithelial Voltohmmeter (World Precision Instruments, Sarasota, FL). TEER was measured immediately prior to delivery of the first blast, and approximately 5 minutes following exposure to the first and second blasts (or sham exposures). For measuring time course changes, TEER was recorded 5 minutes after the first (day 1) and second (day 2) blast injuries, and once every 24 hours until day 6 from the initial injury. For experiments involving an extended inter-injury interval, TEER was recorded 5

minutes after the first (day 1) blast injury, and once every 24 hours thereafter, including 5 minutes following the second (day 4) blast injury. As previously described, each individual TEER measurement was corrected for the TEER of a cell-free Transwell insert and adjusted to account for the membrane surface area (Effgen et al. 2012, Hue et al. 2013). All TEER data presented in this manuscript are normalized as the ratio of each culture's post-injury TEER values to its individual TEER value prior to the initial insult. For time course measurements, the TEER values of injured cultures were compared to age-matched and time point-matched sham controls. In accordance with our previous work (Effgen et al. 2012, Hue et al. 2013), cultures exhibiting TEER values less than 15 Ω*cm^2 before experimentation were deemed to be in suboptimal health and excluded from the study.

3.2.4 Measurement of solute permeability

The intact BBB forms a restrictive barrier to the paracellular permeation of larger solutes (Madara 1998). Quantifying permeability of a range of molecular weights across the endothelial monolayer provides one method to assess BBB dysfunction after repeated blast injury. Approximately 30 minutes after exposure to the second blast injury or sham exposure, fluorescein-labeled dextrans of 3 and 10 kDa (Life Technologies; ex/em: 494/521 nm), and Texas Red®-labeled dextrans of 40 kDa (Life Technologies; ex/em: 595/615 nm) were added to the upper compartment above the endothelial monolayer. Every 60 minutes for 4 hours, 100 µL of medium from the compartment below the endothelial culture was collected and replaced with 100 µL of fresh medium. The change in volume associated with sampling at multiple time points was accounted for when calculating the change in solute concentration over time. Fluorescence of the collected samples was quantified using a SpectraMax M2 Microplate Reader

(Molecular Devices, Sunnyvale, CA). As previously described, the diffusive solute permeability (P, cm/s) was calculated using equation (1) (Li et al. 2010, Simon et al. 2010, Hue et al. 2013)

$$P = \frac{\frac{\Delta C_B}{\Delta t} \times V_B}{S \times C_T} \quad (1)$$

where, $\frac{\Delta C_B}{\Delta t}$ represents the change in concentration of dextrans over time in the compartment below the endothelial culture, V_B the volume contained in the compartment below the endothelial culture, S the surface area of the culture, and C_T is the concentration in the compartment above the culture.

3.2.5 Assessment of tight junction morphology

The presence and morphology of tight junction proteins, ZO-1 and claudin-5, between adjacent endothelial cells serve as indicators of BBB integrity (Brown et al. 2007, Li et al. 2010, Simon et al. 2010, Abdul-Muneer et al. 2013, Hue et al. 2013). Approximately 30 minutes after exposure to the second blast injury or sham exposure, the BBB endothelial cultures were fixed and incubated with either anti-ZO-1 rabbit polyclonal antibody or anti-claudin-5 mouse monoclonal antibody (Life Technologies). In separate experiments to determine presence of each tight junction protein, ZO-1 was detected using the Alexa Fluor 488 anti-rabbit secondary antibody and claudin-5 was detected using the Alexa Fluor 488 anti-mouse secondary antibody (Life Technologies). Endothelial monolayers were also incubated with 4', 6-diamidino-2-phenylindole (DAPI; Life Technologies) to detect individual cell nuclei and to quantify the number of cells in each BBB culture. All antibodies used were manufactured from the same lot and applied at the same post-injury time point. Following the immunostaining procedure, cultures were imaged using an Olympus IX81 (Olympus America, Center Valley, PA)

fluorescence microscope and MetaMorph software (Molecular Devices, Sunnyvale, CA). As previously described (Hue et al. 2013), the degree of tight junction immunostaining was measured by applying the same threshold for ZO-1 or claudin-5 immunofluorescence to each of 5 randomly selected images taken from every sham control or injured culture. Immunostaining for ZO-1 or claudin-5 was quantified as the area-percentage of an image exhibiting fluorescence above an identical threshold, normalized to the total number of endothelial cells in each image.

3.2.6 Measurement of hydraulic conductivity

Exposure to primary blast has been found to enhance the leakiness of the BBB, which promotes vascular fluid influx and brain edema (Abdul-Muneer et al. 2013). Hydraulic conductivity provides a quantitative measure of water flux through the BBB model (Li et al. 2010, Simon et al. 2010, Hue et al. 2013). Approximately 15 to 30 minutes after exposure to the second blast injury or sham exposure, cultures were placed in a custom-built permeability device similar to one described previously (Sill et al. 1995, Li et al. 2010, Simon et al. 2010, Hue et al. 2013). Each Transwell culture was tightly secured in a polycarbonate chamber connected to a lower fluid reservoir, establishing a known hydrostatic pressure (approximately 20 cm H_2O) across the endothelial monolayer. Hydrostatically-induced fluid flow was quantified by tracking the linear displacement of an air bubble through a calibrated glass tube. Hydraulic conductivity (L_p, cm/s/cmH_2O) was calculated using equation (2) (Li et al. 2010, Simon et al. 2010, Hue et al. 2013)

$$L_p = \frac{\frac{\Delta x}{\Delta t} \times F}{S \times \Delta P} \quad (2)$$

where, $\frac{\Delta x}{\Delta t}$ represents the linear displacement of the bubble over time, F the fluid volume of the calibrated glass tube, S the surface area of the culture, and ΔP the hydrostatic pressure across the endothelial culture.

3.2.7 Statistical analysis

Repeated-measures statistical analysis followed by one-way ANOVA and Bonferroni *post hoc* tests to sham controls was used to determine the overall effect of blast on TEER response for repeated exposures delivered 24 or 72 hours apart, as well as for temporal TEER recovery associated with repeated blast exposures. Hydraulic conductivity and tight junction immunostaining data were analyzed statistically by one-way ANOVA followed by Bonferroni *post hoc* tests to sham controls. Solute permeability data were analyzed by independent samples t-tests between sham and injured cultures. (SPSS v. 20, IBM, Armonk, NY, significance * $p < 0.05$).

3.3 Results

3.3.1 Severity dependent TEER response after repeated blast

The *in vitro* BBB model was subjected to two blasts delivered 24 hours apart at a severity level previously determined to result in mild functional disruption of the endothelial monolayer (377 kPa peak overpressure, 0.89 ms duration, and 96 kPa*ms impulse) (Hue et al. 2013). In the single injury group receiving one mild blast (injury 1), TEER decreased significantly compared to sham to 91 ± 3 % (mean ± SEM), and was not significantly different at 92 ± 6 % following the

second sham injury time point (Figure 3.1A). In the double injury group receiving two mild blasts delivered 24 hours apart, TEER was significantly decreased compared to sham to 84 ± 4 % after injury 1 and 78 ± 4 % after injury 2 (Figure 3.1A). There was no significant difference in TEER between the double and single injury groups following the second injury time point, indicating mild effects of repeated exposure to a mild intensity blast. Sham control TEER levels were statistically unchanged at 102 ± 2 % following the first sham exposure and 99 ± 6 % following the second (Figure 3.1A).

When the blast severity was increased to a level previously determined to result in moderate functional disruption of the endothelial monolayer (402 kPa peak overpressure, 0.92 ms duration, and 118 kPa*ms impulse) (Hue et al. 2013), more dramatic compromises in BBB integrity were observed. In the single injury group receiving one moderate blast, TEER decreased significantly compared to sham to 52 ± 7 % after the initial injury and remained significantly depressed at 71 ± 4 % after the second sham injury; compared to after the first injury, TEER was slightly increased (not significantly) after the second sham injury due to spontaneous recovery of the monolayer (Figure 3.1B). In the double injury group (24 hour inter-injury interval), TEER was significantly decreased to 54 ± 7 % after injury 1 and similarly to 44 ± 7 % after injury 2 (Figure 3.1B), demonstrating sustained, but not additive, disruption of the monolayer with repeated injuries. TEER of the double injury group was significantly more depressed than the single injury group after the second injury time point due to persistent damage in the double injury group and partial recovery in the single injury group. TEER of sham controls was consistently high at 94 ± 3 % and 101 ± 5 % following the first and second sham injuries, respectively (Figure 3.1B). It is important to note that previous characterization of our blast injury model confirmed the absence of any significant cell death or cell detachment from

the Transwell membrane after blast exposure at higher severity levels than those tested in the current study (Effgen et al. 2012, Hue et al. 2013).

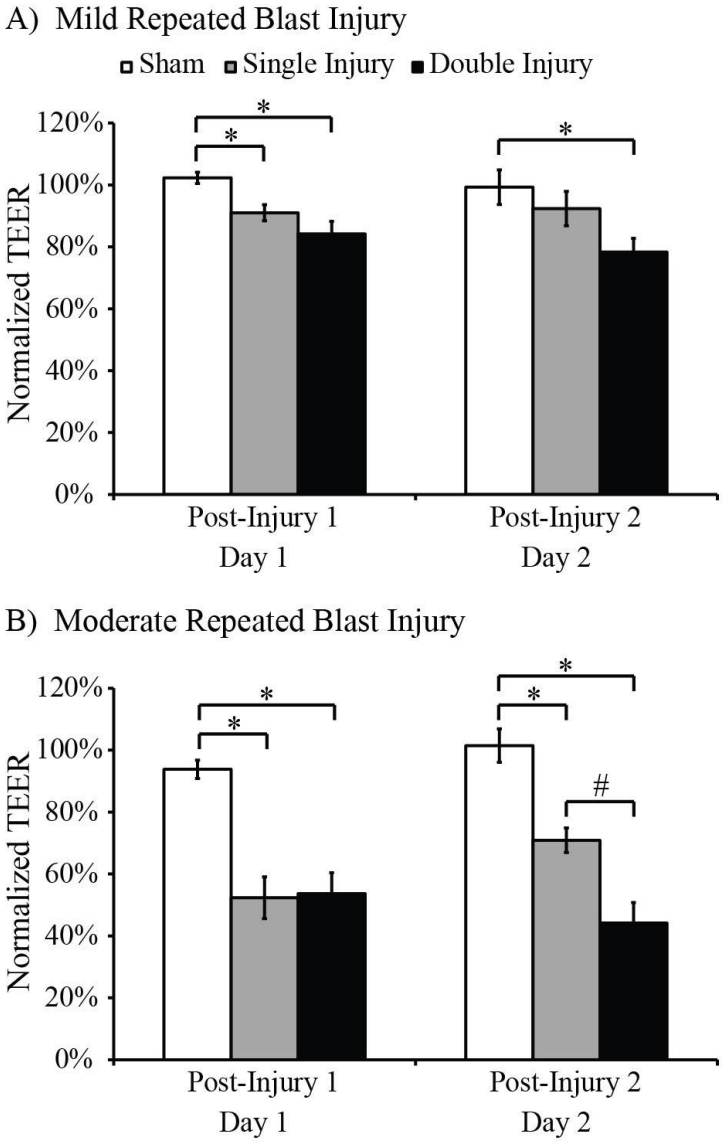

Figure 3.1 Acute TEER response of *in vitro* BBB model to repeated mild and moderate blast injuries. A) Mild, sustained disruption of the BBB following repeated mild blast with a 377 kPa peak overpressure, 0.89 ms duration, and 96 kPa*ms impulse. B) Pronounced, sustained disruption of BBB following exposure to repeated moderate blast with a 402 kPa peak overpressure, 0.92 ms duration, and 118 kPa*ms impulse. ($^{*,\#}$ $p < 0.05$; ± SEM; Sham n = 12; Single Injury n ≥ 11; Double Injury n = 12).

3.3.2 Unaltered solute permeability after repeated blast

Despite slightly elevated permeability of the 3 kDa dextran in the single and double injury groups after exposure to moderate blast compared to sham, there was no significant difference among the experimental groups for the 3, 10, or 40 kDa molecular weight tracers (Figure 3.2). Solute permeability of all groups was measured 30 minutes after exposure to the second blast injury or sham exposure. As a positive control, endothelial monolayers were exposed to a single blast with a 571 kPa peak overpressure, 1.06 ms duration, and 186 kPa*ms, previously reported to significantly increase permeability of 10 kDa dextrans through the barrier (Hue et al. 2013). Following acute exposure to the same blast level in the current study, solute permeability significantly increased to $1.77 \pm 0.25 \times 10^{-6}$ cm/s compared to $0.90 \pm 0.05 \times 10^{-6}$ cm/s in sham controls (data not shown), which is in agreement with our previously published data (Hue et al. 2013).

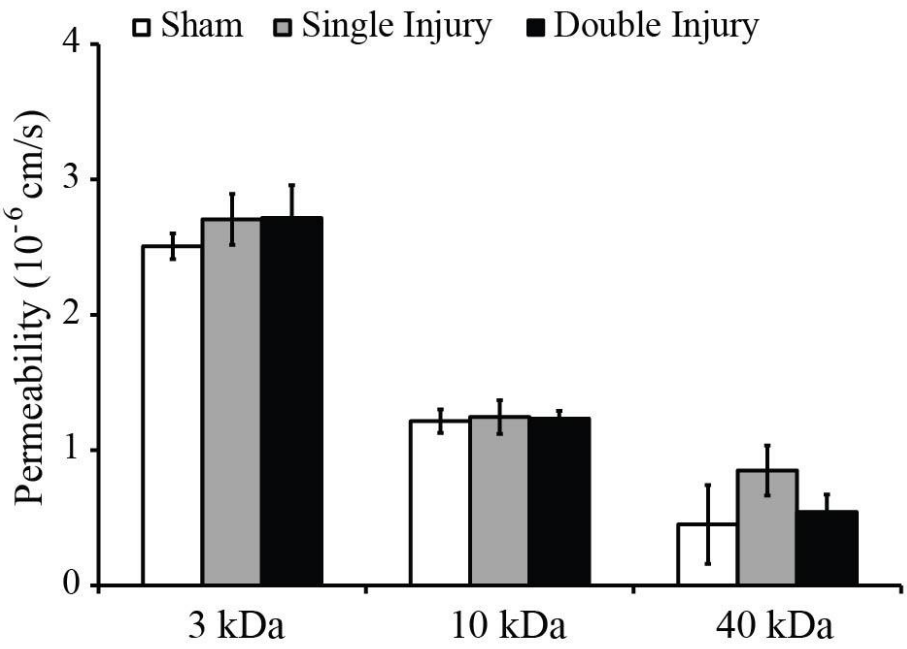

Figure 3.2 Unaltered solute permeability after repeated blast injury in BBB cultures. After exposure to moderate levels of blast with a 402 kPa peak overpressure, 0.92 ms duration, and 118 kPa*ms impulse, no significant difference in solute permeability was observed between sham and the single or double injury groups. (* $p < 0.05$; ± SEM; Sham n = 10; Single Injury n = 10; Double Injury n ≥ 9).

3.3.3 Tight junction disruption after repeated blast

Wide-spread and integral expression of tight junction proteins was indicated by high levels of ZO-1 and claudin-5 staining in sham control cultures (Figure 3.3A, E). As described previously, visual inspection of bright-field and immunostained images of sham control cultures confirmed the formation of confluent monolayers exhibiting spindle-shape morphology that was characteristic of bEnd.3 cells and the brain endothelial cell phenotype (Omidi et al. 2003, Brown et al. 2007, Li et al. 2010, Simon et al. 2010, Effgen et al. 2012, Hue et al. 2013). Approximately 30 minutes after exposure to the second moderate injury or sham exposure, tight junction protein-staining for the single and double injury groups appeared less intense and slightly more punctate in morphology as compared to sham controls. The area-percentage of ZO-1

immunostaining per cell was significantly decreased to 0.09 ± 0.01 % in the single injury group and to 0.08 ± 0.01 % in the double injury group, as compared to 0.15 ± 0.02 % in sham controls (Figure 3.3D). Levels of ZO-1 immunostaining were not significantly different between the single and double injury groups, showing no cumulative disruption of the ZO-1 tight junction protein. Similarly, the area-percentage of claudin-5 immunostaining per cell was significantly decreased to 0.15 ± 0.01 % in the single injury group and to 0.18 ± 0.02 % in the double injury group, as compared to 0.24 ± 0.02 % in sham controls (Figure 3.3H). Levels of claudin-5 immunostaining were not significantly different between the single and double injury groups. Overall, the altered tight junction morphology in both single and double injury groups subtly resembled the more punctate and discontinuous appearance of tight junctions previously observed after single blast exposure at higher severity levels (Hue et al. 2013). We also note that our previous work reported healthy cell morphology in bright-field micrographs and no significant cell death for injured and sham-exposed cultures following exposure to a more severe level of blast (Effgen et al. 2012).

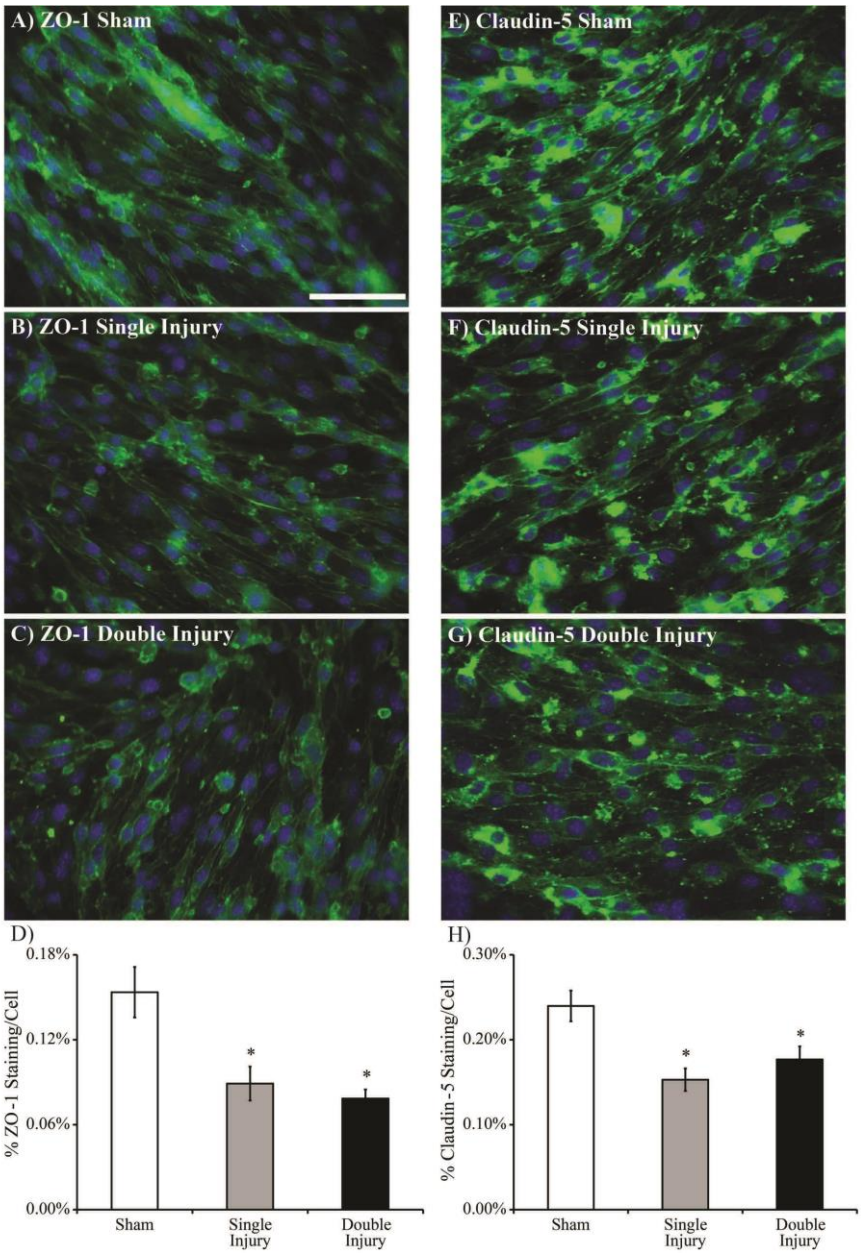

Figure 3.3 Immunostaining of tight junction proteins ZO-1 (green) and claudin-5 (green) following repeated moderate blast injury with a 402 kPa peak overpressure, 0.92 ms duration, and 118 kPa*ms impulse. A, E) ZO-1 and claudin-5 staining was high in sham cultures, together indicating the presence of well-formed tight junctions. B, F) Exposure to a single blast injury compromised ZO-1 and claudin-5 staining as compared to sham controls. C, G) Exposure to repeated blast injury compromised ZO-1 and claudin-5 staining as compared to sham controls, but not compared to the single injury group. D, H) Quantified ZO-1 and claudin-5 staining in the single and double injury groups was significantly reduced as compared to sham, consistent with qualitative depictions in immunofluorescence images. (* $p < 0.05$; ± SEM; Sham n = 6 cultures (30 images); Single Injury n = 6 cultures (30 images); Double Injury n = 6 cultures (30 images) for ZO-1 or claudin-5; Scale bar = 70 µm).

3.3.4 Delayed TEER recovery after repeated blast

Recovery of TEER in cultures exposed to moderate, repeated blast injury was delayed compared to cultures exposed to a single blast. TEER of the single injury group was significantly depressed compared to age-matched shams for up to one day after the initial injury delivered on day 1, but was no longer significantly different by day 2 due to recovery of the monolayer (Figure 3.4). Recovery of TEER in the double injury group was delayed such that TEER remained significantly lower compared to age-matched shams up to day 3 after exposure to the initial insult (Figure 3.4). TEER of all cultures was monitored out to day 6 following the initial exposure, and there were no significant differences among the sham, single, or double injury groups from days 4 to 6.

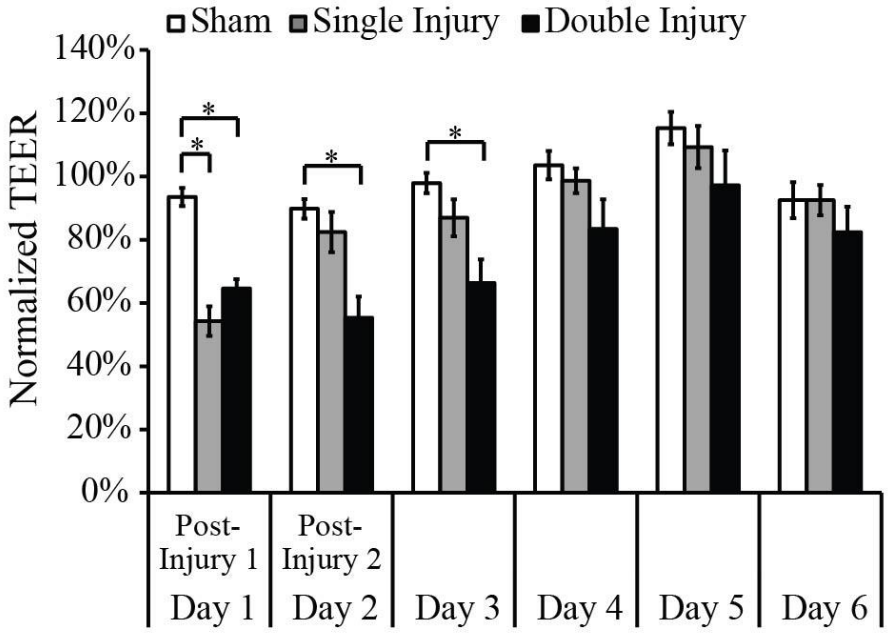

Figure 3.4 Endothelial monolayers exhibited delayed recovery in TEER following exposure to repeated moderate blast with a 402 kPa peak overpressure, 0.92 ms duration, and 118 kPa*ms impulse. TEER in the single injury group remained significantly depressed compared to shams for up to 1 day following the initial injury. TEER of the double injury group remained significantly depressed compared to shams for 3 days following the first injury. (* $p < 0.05$; ± SEM; Sham n = 6; Single Injury n = 6; Double Injury n = 6).

3.3.5 Increased hydraulic conductivity after repeated blast

Hydraulic conductivity, L_p, was measured 15 to 30 minutes after the second moderate blast or sham injury (similar measurement time point as solute permeability and tight junction immunostaining) to quantify water flux through the BBB model. In the single injury group, L_p was slightly elevated but not significantly different compared to sham at 24 hours following exposure to one mild blast – i.e. immediately after the second sham injury time point (Figure 3.5). In the double injury group, L_p was significantly elevated to $2.14 \pm 0.54 \times 10^{-7}$ cm/s/cmH_2O compared to $0.83 \pm 0.18 \times 10^{-7}$ cm/s/cmH_2O in sham controls immediately after a second blast – i.e. the same measurement time point as the single injury group (Figure 3.5). However, there was no significant difference in hydraulic conductivity between the single and double injury groups. These results suggest that L_p spontaneously recovers over time similarly to the observed changes in TEER.

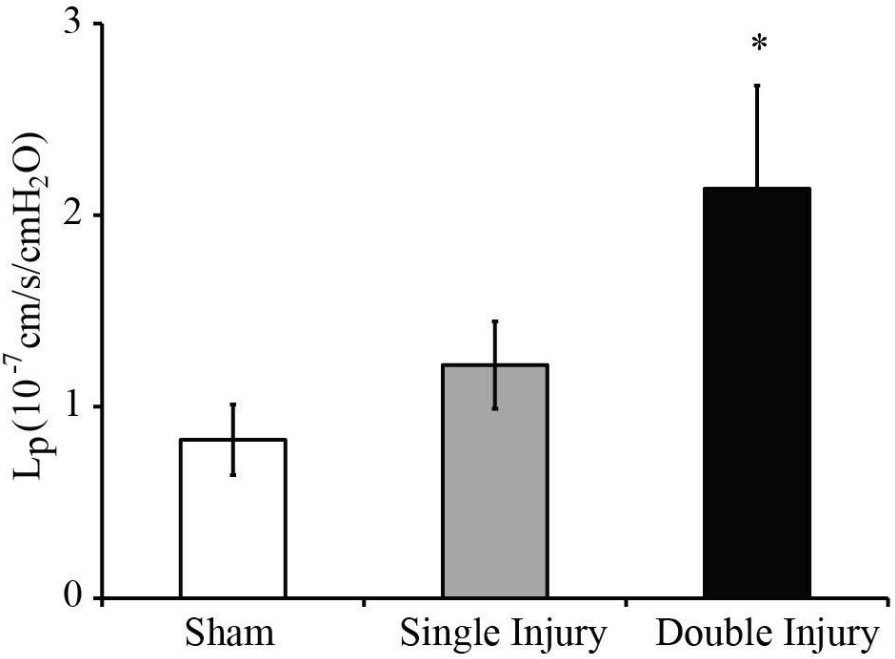

Figure 3.5 Increased hydraulic conductivity following repeated blast injury in BBB cultures. Hydraulic conductivity of endothelial monolayers exposed to consecutive moderate blasts with a 402 kPa peak overpressure, 0.92 ms duration, and 118 kPa*ms impulse was significantly increased to $2.14 \pm 0.54 \times 10^{-7}$ cm/s/cmH_2O compared to $0.83 \pm 0.18 \times 10^{-7}$ cm/s/cmH_2O in sham controls. Hydraulic conductivity in cultures sustaining two blast injuries was not significantly different from sham controls or the single injury group when measured at the same time point (i.e. after the second sham injury). (* $p < 0.05$; ± SEM; Sham n = 11; Single Injury n = 12; Double Injury n = 12).

3.3.6 Independent effects of repeated blast on TEER with prolonged interval

To investigate the interval-specific effects of repeated blast injury in the BBB cultures, the time between injuries was extended to 72 hours. After the first exposure to moderate blast, TEER of injured cultures decreased by 25 to 30 % compared to sham controls (Figure 3.6). Injured cultures recovered at a similar rate over time, exhibiting full recovery of TEER by day 3. Following the second injury time point on day 4, TEER of the double injury group was significantly decreased by a consistent 25 to 30 % in comparison to age-matched shams; this change in TEER was not significantly different than the change in TEER after the first injury

(Figure 3.6). The similar decrease in TEER between the double injury group and sham cultures following both the initial (day 1) and subsequent (day 4) injuries suggests that the effect of the subsequent injury on the BBB is independent (i.e. as a new single insult without residual effects from the initial exposure) given enough recovery time between the two injuries.

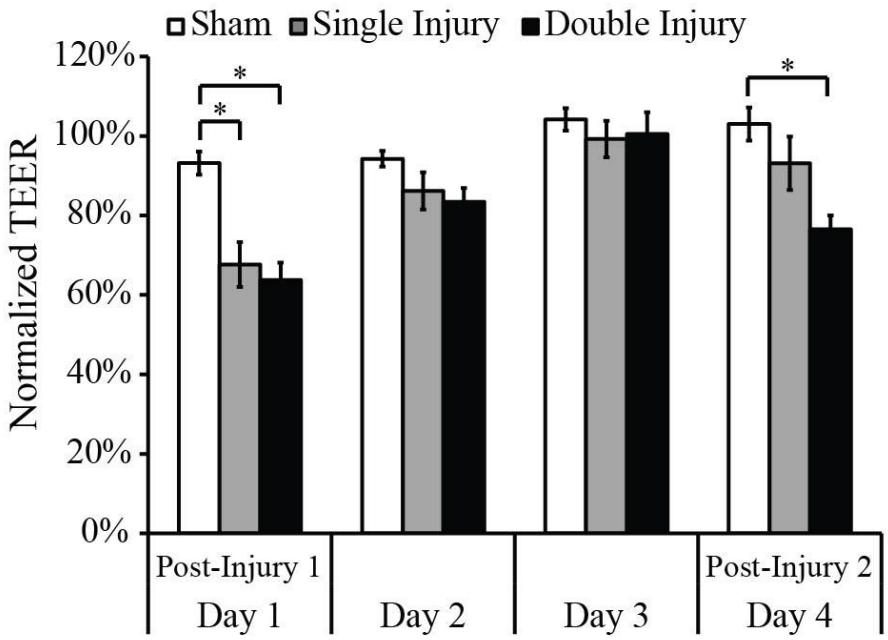

Figure 3.6 Independent effects of blast on BBB cultures over an extended 72 hour inter-injury interval between consecutive moderate blasts with a 402 kPa peak overpressure, 0.92 ms duration, and 118 kPa*ms impulse. The consistently similar 25 to 30 % difference in TEER between the double injury and sham groups after the first (day 1) and second (day 4) injuries suggests that the effects of repeated injuries are independent (i.e. no residual effects from the initial exposure) given a sufficiently prolonged inter-injury interval. (* $p < 0.05$; ± SEM; Sham n = 6; Single Injury n = 6; Double Injury n = 6).

3.4 Discussion

Augmented brain pathology is considered to be a consequence of repetitive brain injury, and our results extend this understanding to repeated, primary blast exposure in an *in vitro* BBB model. The significant difference in TEER which we observed between cultures exposed to two

moderate injuries demonstrated sustained, but not additive, effects associated with the subsequent insult (Figure 3.1B). Our results add to published findings of worsened axonal and microvascular damage evoked by severity- and interval-specific repetitive TBI (Fujita et al. 2012). In an animal model of impact acceleration injury, sub-threshold injuries administered in repeated fashion caused neither axonal nor vascular changes, whereas supra-threshold insults resulted in cumulative axonal damage and microvascular dysfunction (Fujita et al. 2012). It is important to note, however, that our results demonstrated sustained depression in TEER representing persistent injury to the BBB following multiple insults, which is distinct from additive damage to the barrier. This discrepancy may underscore fundamental differences between primary blast injury and inertial- and impact-driven injuries.

Clinically, the diagnosis of repeated mild blast exposure is challenging due to the difficulty in assessing damage using conventional neuroimaging or by impairments determined by neurobehavioral assessments (Belanger et al. 2007, Brenner et al. 2009). Repeated exposure to mild explosive blast presents a significant challenge to the military healthcare system due to the frequency of this type of exposure, the potential for cumulative effects of multiple injuries, and the delayed onset of cognitive and behavioral impairments experienced by warfighters (Brenner et al. 2009, Rosenfeld and Ford 2010, Kamnaksh et al. 2011). In neurosurgical (severe) cases of bTBI due to IEDs, cerebral vasospasm was detected in a substantial number of patients who generally experienced poorer outcomes (Armonda et al. 2006, Long et al. 2009). The constriction of blood vessels has also been confirmed experimentally in a mouse model of repeated blast-induced neurotrauma (Valiyaveettil et al. 2013). Observations of exacerbated vascular dysfunction are consistent with the second-impact syndrome reported in humans, whereby subsequent brain injuries may cause significant abnormalities including vasoparalysis

and vascular engorgement (Cantu and Gean 2010, Fujita et al. 2012). BBB dysfunction caused by multiple exposures to bTBI, as reported in our study, may compromise the barrier's ability to maintain ion homeostasis and limit the entry of neurotoxic and inflammatory serum constituents – functions required to preserve the health of neurons, physiologic neural signaling, and network connectivity (Abbott and Friedman 2012). By extending the duration of the opening of the BBB with multiple exposures, the influx of serum components and their subsequent pathophysiological effect could be increased without necessarily causing more severe BBB breakdown.

Increased BBB permeability has been reported after bTBI (Readnower et al. 2010, Garman et al. 2011, Yeoh et al. 2013), but it is still unknown whether repeated mild blast exposure has the potential to exacerbate leakiness of the barrier. A prior study from our laboratory demonstrated significantly increased permeability of 10 kDa dextrans through an *in vitro* BBB model after exposure to a single severe blast (571 kPa peak overpressure, 1.06 ms duration, and 186 kPa*ms impulse) (Hue et al. 2013). In other studies, permeability of the BBB was enhanced following a single primary blast exposure *in vivo* as measured by increased extravasation of sodium fluorescein (376 Da), Evans blue (70 kDa when bound to plasma albumin) (Greish 2007), and IgG (approximately 150 kDa) (Readnower et al. 2010, Garman et al. 2011, Kuehn et al. 2011, Abdul-Muneer et al. 2013, Yeoh et al. 2013). A detailed understanding of blast-induced disruption of cerebral vascular integrity is of clinical importance because greater adhesion and infiltration of immune cells, including macrophages, can promote neurovascular inflammation and degeneration *in vivo* (Abdul-Muneer et al. 2013). Interestingly, exposure to moderate blast (402 kPa) in the current study did not increase solute permeability, even after repeated exposure over a 24 hour interval. These data suggest that repeated blast

exposure at mild or moderate levels may establish intercellular structural voids not sufficient to permit an influx of larger solutes (≥ 3kDa) through the barrier, but large enough to allow changes in paracellular ion-flux as previously observed in TEER measurements.

The effect of multiple blast exposures on tight junctions that mediate the restrictive properties of the BBB is still an area of active investigation. Previously, we demonstrated that exposure to a single, severe blast injury significantly compromised ZO-1 immunostaining in a brain endothelial monolayer (Hue et al. 2013). Results from the current study also demonstrate that repeated blast exposure at lower intensities can significantly reduce immunostaining of the ZO-1 and claudin-5 tight junction proteins compared to sham controls; however, the degree of staining after exposure to two injuries did not significantly differ from that after a single injury. Another investigation of exposure to a single primary blast with a 123 kPa peak overpressure (estimated 5 ms duration) in rats reported significant reductions in expression of ZO-1, claudin-5, and occluding (Abdul-Muneer et al. 2013). Consistent with our results *in vitro,* the same study reported that two consecutive blast injuries delivered 24 hours apart in rats reduced immunostaining for tight junction proteins compared to controls, but not compared to cultures sustaining a single blast (Abdul-Muneer et al. 2013). These data strongly suggest that the effects of repeated blast on the integrity of the BBB are not associated with significantly worse tight junction damage over consecutive insults experienced within a 24 hour timeframe.

The time course we measured for changes in TEER suggests that repeated blast exposure delays recovery of the damaged BBB. A recent study revealed that exposure to two mild primary blast injuries with a 123 kPa peak overpressure and 4 to 5 ms duration, separated by 24 hours, prolonged vascular damage as opposed to significantly exacerbating it (Abdul-Muneer et al. 2013). In our BBB culture, repeated exposure to moderate blast (402 kPa) delayed

spontaneous recovery of the injured monolayer. TEER of cultures exposed to a single insult remained significantly depressed for 1 day after the injury, whereas in cultures exposed to two insults, TEER remained significantly depressed for 3 days after the initial injury. We are the first to report delayed recovery of TEER following repeated, pure primary blast injury, and our time course for *in vitro* barrier recovery is reasonably similar to that observed *in vivo* at comparable blast exposure levels (Readnower et al. 2010, Garman et al. 2011). Previous investigations of BBB disruption induced by single blast exposure in small animals have reported peak IgG extravasation at 3 and 24 hours post-injury, with complete resolution by 3 days after exposure (Readnower et al. 2010, Garman et al. 2011). Future work will examine the cellular mechanisms responsible for BBB recovery, but it has been suggested that shock wave-induced injury to the cerebral vasculature gradually diminishes over time potentially because of repair processes that help mitigate subsequent damage from consecutive blast exposures (Kamnaksh et al. 2012, Abdul-Muneer et al. 2013).

Brain edema has been reported to be a characteristic outcome of bTBI (Cernak and Noble-Haeusslein 2010, Mac Donald et al. 2011). In the current investigation, hydraulic conductivity in our *in vitro* BBB model was significantly increased immediately after a second injury compared to sham controls. Similar to the time course of TEER, hydraulic conductivity recovered 24 hours after a single injury to lower pre-injury levels. Although in this study we did not measure changes in water flux acutely after the initial injury time point, our previous study describes changes in hydraulic conductivity in response to a single blast over a range of severity levels (Hue et al. 2013). These results are supported by previous findings that mice exposed to three consecutive blast injuries with an estimated 142 kPa peak overpressure (unreported duration) separated by 1 and 30 minute intervals had significantly increased brain water content

compared to sham controls (Wang et al. 2011). Changes in brain edema were detected 4 hours post-injury, and were no longer apparent at 24 and 48 hours after blast exposure (Wang et al. 2011). Multiple exposures to low-level blasts in rats and pigs were associated with increased intracranial pressure, which may be attributed to edema, hemorrhage, and BBB damage (Saljo et al. 2008, Saljo et al. 2009, Saljo et al. 2011, Wang et al. 2011). The development of cerebral edema around the vasculature is often associated with enhanced expression of the water channel protein, AQP4, in the perivascular region following impact- and blast-induced injuries to the head (Higashida et al. 2011, Abdul-Muneer et al. 2013). Further studies are warranted to identify the underlying mechanisms responsible for increased water flux through the barrier following blast exposure.

An important outcome of the current study is that extension of the interval between the initial and subsequent blast injuries from 24 to 72 hours allowed TEER to fully recover prior to delivery of the subsequent insult. It is worth noting that microvascular restoration in the inter-injury interval has been reported by others using an impact-driven repetitive TBI model (Fujita et al. 2012). After the second injury in our study, TEER decreased by 25-30 % compared to sham controls, which was equivalent to the change in TEER observed acutely after the first blast. Together, these results suggest that the BBB response to repeated blasts may be independent; that is, there is no evidence of residual effects across consecutive exposures given a sufficient delay between injuries. The ability to ameliorate the persistent burden of BBB disruption is supported by published studies reporting the reduction or complete elimination of axonal damage, vascular dysfunction, and compromises in cerebral metabolism when the interval between consecutive injuries was sufficiently extended (Longhi et al. 2005, Vagnozzi et al. 2008, Fujita et al. 2012, Prins et al. 2013). Overall, such findings support the existence of a window of

heightened vulnerability of the BBB to repetitive primary blast injury, which holds implications for a minimum mandatory rest-period (several days) for blast-injured service members prior to returning to duty. We note that our results were from an isolated component of the BBB and do not preclude the possibility that repeated primary blast may have cumulative and direct effects on other components of the brain, such as neurons or glia or on their interactions. *In vivo*, the BBB is a heterogeneous structure consisting of brain capillary endothelial cells (e.g. bEnd.3 cells), which together with astrocytes, pericytes, microglia, neurons, and the extracellular matrix, make up the neurovascular unit (Gumbleton and Audus 2001, Shlosberg et al. 2010). Following brain injury, such as TBI, the physiological interactions among the various cellular components of this unit are significantly altered. Such changes can lead to abnormal tight junction protein expression, an inflammatory response mediated by astrocytes and microglia, and altered neuronal activity, among others (Shlosberg et al. 2010). Consistent with this, exposure to a pure shock wave in rats induced free radical-generating enzymes, oxidative damage markers, a reduction in tight junction proteins, BBB leakage, upregulation of perivascular matrix metalloproteinases, and an increase in fluid channel aquaporin-4 expression in astrocytes, ultimately leading to neuroinflammation (Abdul-Muneer et al. 2013). While our previous work describes in greater detail the advantages and limitations of using an *in vitro* model to study the effects of primary blast on the BBB (Hue et al. 2013), the need to better understand the influence of other cell types of the neurovascular unit on BBB dysfunction after blast injury motivates further study *in vivo*.

Comparison of our results to those published in the literature may be limited by variability in the blast parameters tested among different experimental blast injury models. For example, one recent investigation of bTBI demonstrated BBB breakdown by the presence of

focal lesions following exposure to low-impulse primary blast with short durations on the order of microseconds (Yeoh et al. 2013), whereas typical free-field explosions have durations spanning several milliseconds (Bauman et al. 2009). BBB breakdown in animals has also been demonstrated in studies following exposure to lower levels of peak overpressure, but longer durations of approximately 4 to 5 ms (Readnower et al. 2010, Garman et al. 2011, Abdul-Muneer et al. 2013). In addition, despite efforts to restrain head motion during blast exposure, it is difficult to completely rule out possible contributions of concomitant inertial head injuries in the absence of high-speed video recordings (Saljo et al. 2009, Readnower et al. 2010, Garman et al. 2011, Wang et al. 2011). A previous investigation highlighted that the effects of pure primary blast exposure could be vastly different from those of blast-induced inertial loading of the head, as neurological deficits disappeared when the head was immobilized (Goldstein et al. 2012). As reported previously, we have used high-speed video analysis (data not shown) to confirm the absence of gross movement of our *in vitro* BBB cultures during primary blast exposure (Hue et al. 2013). An advantage of our blast injury model is the ability to study damage to an *in vitro* model of the BBB purely as a result of primary blast injury, in the absence of confounding contributions from inertial loading mechanisms (Effgen et al. 2012, Hue et al. 2013). A prior study using finite element modeling to simulate biomechanical parameters of our *in vitro* blast injury model predicted tissue strain rates less than 80 s^{-1} and principal strains not exceeding 5 % (Panzer et al. 2012, Panzer et al. 2012), which are levels significantly below the thresholds for functional deficits and axonal death reported for living brain tissue (Bain and Meaney 2000, Morrison et al. 2003). Together, these previous investigations provide further support that the injuries modeled using our methodology are due to overpressure-loading and not strain-loading in the sample. A limitation to consider is that our repeated blast-paradigm consisted of only 2

consecutive injuries, so caution should be exercised when extending our results to situations with more blasts.

In conclusion, this study contributes to a growing body of work indicating that brain microvascular dysfunction can result from repetitive injuries at specific severity levels applied within a well-defined timeframe. Our results do not support the hypothesis that damage to the BBB by repeated blasts is cumulative, at least for 2 blast exposures delivered within 24 hours of one another. Results of our investigation are in strong agreement with studies reporting that, despite dramatic pathological changes observed after a single injury, multiple exposures delivered within a short time frame delay recovery, rather than cause additive damage to the barrier (Abdul-Muneer et al. 2013). By extending the interval between injuries from 24 to 72 hours, the BBB fully recovered to pre-injury levels prior to experiencing similar damage after the second injury as that observed after the first, together demonstrating independent effects of multiple injuries given a sufficiently prolonged inter-injury interval. Future work will examine the cellular and molecular mechanisms that underpin the observed changes in BBB integrity and function.

4 Dexamethasone potentiates *in vitro* blood-brain barrier recovery after primary blast injury by glucocorticoid receptor-mediated upregulation of ZO-1 tight junction protein[6]

4.1 Introduction

Widespread use of improvised explosive devices (IEDs) in recent military conflicts has been a major source of mortality and morbidity associated with blast-induced traumatic brain injury (bTBI) (Warden 2006, Hoge et al. 2008). Recent evidence suggests that blood-brain barrier (BBB) disruption occurs after blast exposure (Readnower et al. 2010, Garman et al. 2011), and specifically, after primary blast exposure (Abdul-Muneer et al. 2013, Hue et al. 2013, Skotak et al. 2013, Yeoh et al. 2013, Hue et al. 2014). *In vivo*, the BBB serves as a highly restrictive interface between the systemic circulatory system and the brain (Cucullo et al. 2004, Abbott et al. 2010), making the BBB a promising therapeutic target for the treatment of traumatic brain injury (TBI) caused by explosive blast. There may be clinical utility in developing therapies to enhance repair of the damaged BBB to maintain brain homeostasis and protect neuronal activity and function (Forster et al. 2006, Shlosberg et al. 2010).

Glucocorticoids have played an important role in the clinical management of central nervous system (CNS) disorders associated with a compromised BBB, such as edema, brain tumors, and multiple sclerosis (Miller et al. 1992, Kaal and Vecht 2004), and have been studied

[6] A modified version of this chapter previously appeared in print: Hue, C.D., Cho, F.S., Cao, S., Dale Bass, C.R., Meaney, D.F., Morrison Iii, B. (2015). Dexamethasone potentiates in vitro blood-brain barrier recovery after primary blast injury by glucocorticoid receptor-mediated upregulation of ZO-1 tight junction protein. J Cereb Blood Flow Metab. Epub ahead of print. Reproduced with permission (doi: 10.1038/jcbfm.2015.38).

extensively in experimental treatment models *in vitro* and *in vivo* (Romero et al. 2003, Cucullo et al. 2004, Forster et al. 2005, Forster et al. 2006, Campolo et al. 2013, Thal et al. 2013). For example, dexamethasone (DEX) promotes BBB integrity by initiating glucocorticoid receptor-mediated signaling, leading to altered gene expression and upregulation of tight junction proteins including occludin, claudin-5, and zonula occludens (ZO)-1 that strengthen and restore barrier properties (Singer et al. 1994, Romero et al. 2003, Forster et al. 2006, Blecharz et al. 2010, Thal et al. 2013). Greater than 3-fold increases in transendothelial electrical resistance (TEER), and similar changes in restriction of water permeability have been attributed to glucocorticoid treatment in epithelial and brain endothelial cell cultures (Underwood et al. 1999, Romero et al. 2003, Forster et al. 2005, Forster et al. 2006).

Upregulated expression of ZO-1 has been linked specifically to the proper functioning of tight junctions and heightened resistance to paracellular transport in epithelial and endothelial monolayers (Singer et al. 1994, Underwood et al. 1999). ZO-1 is a 220 kDa protein localized to the intracellular surface of the tight junctional complex and is expressed in a wide variety of mammalian tissues (Balda and Anderson 1993, Singer et al. 1994). ZO-1 is expressed in α^+ and α^- isoforms, termed ZO-1α^+ and ZO-1α^-, that result from alternative RNA splicing and can exist in different distributions within a single cell type (Willott et al. 1992, Balda and Anderson 1993, Alvarado et al. 2004). ZO-1α^+ contains an 80 amino acid α domain, which is absent in ZO-1α^- (Willott et al. 1992, Balda and Anderson 1993). Some studies have suggested that expression specifically of ZO-1α^+ is associated with more restrictive barrier properties (Underwood et al. 1999, Alvarado et al. 2004).

Despite evidence supporting treatment with steroids for mitigating vasogenic edema, raised intracranial pressure, and damage to the BBB after brain injury, their use in the clinic

remains controversial (Poungvarin 2004, Thal et al. 2013). Glucocorticoid therapy failed to demonstrate substantial benefit in reducing post-injury sequelae in head-injured patients, stroke patients, and in some animal models of TBI (Poungvarin 2004, Roberts et al. 2004, Chen et al. 2010). However, more recent experimental evidence suggests that concomitantly inhibiting proteasomal degradation of the glucocorticoid receptor and delivering DEX after TBI promoted BBB recovery and improved neurological outcomes (Thal et al. 2013). Other *in vivo* studies clearly indicate that combination therapy with melatonin and DEX synergistically reduced brain injury and promoted BBB recovery after TBI, while minimizing the required dosage and potential side effects of glucocorticoids (Campolo et al. 2013). Taken together, these reports suggest that factors influencing glucocorticoid effectiveness after traumatic insult are numerous and their interactions are complex. As such, positive results obtained by using more refined approaches support further study and development of glucocorticoid therapies in the ongoing search for improved treatments for TBI and other disorders of the CNS.

In the current study, we provide evidence that treatment with DEX after primary blast injury promotes faster recovery of a monolayer of mouse brain microvascular cells (bEnd.3) representing an *in vitro* model of the BBB. We used a previously described primary blast injury model to precisely control the biomechanical initiators of injury and measure subsequent changes to barrier integrity by methods not possible *in vivo* (Effgen et al. 2012, Hue et al. 2013, Hue et al. 2014). We report, for the first time, that treatment with DEX after primary blast exposure potentiated recovery of TEER and hydraulic conductivity of the BBB *in vitro*, and that glucocorticoid receptor activation accelerated barrier restoration. We further demonstrate that DEX-induced BBB recovery was accompanied by increased ZO-1 tight junction immunostaining and expression, specifically associated with upregulation of the ZO-1α^+ isoform but not ZO-1α^-.

These findings hold important implications for development of a potential therapy for restoring BBB integrity and function after bTBI.

4.2 Materials and Methods

4.2.1 BBB cell culture model

In vitro models of the BBB were generated using monolayers of immortalized mouse brain endothelial cells, bEnd.3 (ATCC, Manassas, VA, USA), as previously described (Hue et al. 2013, Hue et al. 2014). Cells were cultured in Dulbecco's Modified Eagle's Medium (DMEM; ATCC) supplemented with 10 % newborn calf serum (Hyclone Laboratories, Logan, UT, USA). Each Transwell insert (1.12 cm^2 surface area) was pre-coated with poly-L-lysine and seeded with a total of 60,000 bEnd.3 cells. Transwell cultures were grown for 8 days to reach confluency in a cell culture incubator at 37℃ and 5 % CO_2 / 95 % O_2. Cells were fed with new medium every 2-3 days.

4.2.2 Exposure of BBB to primary blast injury

Endothelial cultures were exposed to primary blast injury using an *in vitro* bTBI model, as described previously in detail (Effgen et al. 2012, Hue et al. 2013, Hue et al. 2014). Briefly, Transwells were secured within a fluid-filled receiver, designed to mimic the surrounding skull-brain complex, and exposed to a fast-rising pressure transient induced by external shock wave loading. Shock waves were generated using a 76 mm-diameter shock tube with a 25 mm-length driver section pressurized with compressed helium gas, and a 1240 mm-long driven section. The bTBI model is capable of isolating interactions between the BBB culture and blast overpressure alone, substantially reducing the influence of inertial loading, thereby enabling precise investigation of primary blast injury (Effgen et al. 2012, Hue et al. 2013, Hue et al. 2014).

Cultures were exposed to one blast condition, characterized by a shock wave with a 571 ± 15 (mean ± SEM) kPa peak incident overpressure, 1.06 ± 0.01 ms duration, and 186 ± 1.5 kPa*ms impulse in the open-tube configuration (Effgen et al. 2012, Hue et al. 2013). The corresponding biomechanical injury parameters measured at the location of the sample in the fluid-filled sample receiver were 1523 ± 91 kPa peak overpressure, 1.48 ± 0.03 ms duration, and 812 ± 29.3 kPa*ms impulse (Hue et al. 2013). This injury severity level was previously reported to cause disruption of the BBB *in vitro*, and is comparable to exposure to a 105 mm artillery round at a standoff distance of 5-10 m (Hue et al. 2013).

4.2.3 Post-injury treatment

DEX is a synthetic glucocorticoid compound known to improve BBB properties by inducing glucocorticoid receptor-mediated signaling activity (Sigma-Aldrich, St. Louis, MO, USA) (Cucullo et al. 2004, Forster et al. 2006). RU486 (mifepristone) is an antagonist to the glucocorticoid receptor and inhibits glucocorticoid-induced cell signaling activity (Cayman Chemical, Ann Arbor, Michigan, USA) (Forster et al. 2005). Endothelial cultures were treated with DEX, DEX and RU486, or vehicle (pure ethyl alcohol; Sigma-Aldrich) 30 minutes after exposure to primary blast injury, and treatment was continued once per day after injury. To determine the optimal dosage for post-injury functional recovery, cultures were treated with a range of DEX concentrations (0, 1, 10, 100 μM) based on concentrations from the literature (Romero et al. 2003, Cucullo et al. 2004). For all subsequent experiments, cultures were treated with 10 μM DEX; to inhibit effects of DEX, cultures were co-treated with 10 μM DEX and 20 μM RU486.

4.2.4 Measurement of TEER

To quantify changes in ion flux through the endothelial monolayer, TEER values across monolayers of endothelial cultures were measured with an Endohm-12 electrode chamber connected to an EVOMX Epithelial Voltohmmeter (World Precision Instruments, Sarasota, FL, USA). TEER of each culture was measured 5 minutes prior to exposure to blast and 5 minutes after exposure. To assess time course changes, TEER was measured in the same cultures once per day for up to 3 days after exposure to blast injury (delivered on day 0). All recorded TEER values were corrected for the TEER of a cell-free Transwell and adjusted to account for the membrane surface area, as previously described (Hue et al. 2013, Hue et al. 2014). Normalized TEER was determined as the ratio of each culture's post-injury TEER value to its pre-injury TEER value. Age-matched and time point-matched sham controls were used for all time course TEER data comparisons. Endothelial cultures were only included in experiments if their pre-injury TEER was $\geq 10\ \Omega*cm^2$, indicating a healthy and integral bEnd.3 monolayer.

4.2.5 Measurement of hydraulic conductivity

To quantify changes in water flux through the endothelial monolayer, hydraulic conductivity was measured once for a given sample, at each time point from days 1-3 after blast exposure (delivered on day 0) (Hue et al. 2013, Hue et al. 2014). Transwell cultures were placed in a custom-built permeability device, as previously described (Li et al. 2010, Hue et al. 2013). A known hydrostatic pressure of approximately 20 cm H_2O was applied across the endothelial monolayer, and hydrostatically-driven fluid flow was tracked using the linear displacement of an air bubble through a calibrated glass tube. Hydraulic conductivity (L_p, $cm/s/cmH_2O$) was calculated using equation (1) (Li et al. 2010, Hue et al. 2013).

$$L_p = \frac{\frac{\Delta x}{\Delta t} \times F}{S \times \Delta P} \quad (1)$$

where, $\frac{\Delta x}{\Delta t}$ represents the linear displacement of the bubble over time, F the fluid volume of the calibrated glass tube, S the surface area of the culture, and ΔP the hydrostatic pressure across the endothelial culture. Endothelial cultures were only included in experiments if the average L_p of shams was $\leq 4 \times 1/10^7$ cm/s/cmH_2O; otherwise, all samples from the same experimental batch were discarded due to suboptimal culture health.

4.2.6 Assessment of ZO-1 tight junction morphology

The expression and localization of ZO-1 tight junction protein at the border between adjacent endothelial cells is crucial to the function and maintenance of tight junctions (Abbott et al. 2010, Hue et al. 2013, Hue et al. 2014). One day after exposure to blast injury, endothelial cultures were fixed in 1 % formaldehyde and incubated with rabbit anti-ZO-1 polyclonal antibody (Life Technologies, Carlsbad, CA, USA; # 61-7300). The presence of ZO-1 was detected using donkey anti-rabbit Alexa Fluor 488 secondary antibody (Life Technologies). Cultures were also incubated with 4',6-diamidino-2-phenylindole (DAPI; Life Technologies) to detect cell nuclei to determine cell counts for each sample. Endothelial monolayers were imaged using an Olympus IX81 (Olympus America, Center Valley, PA) fluorescence microscope and analyzed using MetaMorph software (Molecular Devices, Sunnyvale, CA). ZO-1 tight junction immunostaining was quantified by applying an identical threshold for ZO-1 immunofluorescence to five randomly selected images of each endothelial culture. Consistent with methods previously described (Hue et al. 2013, Hue et al. 2014), ZO-1 immunostaining was quantified as the area-percentage of an image with fluorescence above a pre-determined threshold, normalized to the total number of cells in each image. Immunostaining images were randomly selected from

each experimental condition, and an identical quantitative analysis method was applied to all samples.

4.2.7 Western blot analysis of ZO-1 tight junction protein

Western blot analysis was performed similarly to our previously published methods (Lamprecht and Morrison 2014), but with slight modifications. At 1 day after injury, endothelial monolayers from 2-3 Transwell cultures representing each experimental condition were washed twice with ice-cold PBS and immediately placed in lysis buffer with inhibitors (40 mM HEPES, 120 mM sodium chloride, 1 mM EDTA, 1 % Triton X-100, 10 mM sodium pyrophosphate decahydrate, 50 mM sodium fluoride, 0.5 mM sodium orthovanadate, 10 mM β-glycerophosphate, 3 % sodium dodecyl sulfate, 1 % sodium deoxycholate, 1 % protease inhibitor cocktail, 1 % phosphatase inhibitor cocktails 2 and 3, and 2 mM phenylmethanesulfonyl fluoride; Sigma-Aldrich). Lysed cell samples were collected and sonicated (Sonicator 3000; Misonix, NY, USA), incubated on ice, then centrifuged to remove cell debris. Approximately 130-150 μg of protein per experimental group was separated by gel electrophoresis on a 4-12 % Bis-Tris gel (Life Technologies). A semidry blotting apparatus (Fisher Scientific, Pittsburgh, PA, USA) was then used to transfer proteins to a nitrocellulose membrane (Life Technologies). The membrane was blocked in Tris-buffered saline (TBS, pH 7.4) with 5 % bovine serum albumin (BSA), and then incubated overnight at 4℃ with rabbit anti-ZO-1 primary antibody (Life Technologies; # 61-7300) and mouse anti-β-tubulin (Life Technologies; # 32-2600) in TBS-T (0.1 % Tween-20, pH 7.4) with 5 % BSA. The primary antibody to ZO-1 recognizes amino acids 463-1109 of human ZO-1 cDNA, and is known to react with both the α^+ and α^- isoforms of ZO-1, as previously reported (Underwood et al. 1999, Alvarado et al. 2004). Membranes were then washed, labeled with corresponding secondary antibody (donkey anti-

rabbit Alexa Fluor 488 or goat anti-mouse Alexa Fluor 647; Life Technologies), and washed. Membranes were imaged using a CRi Maestro 2 Imaging System (Perkin Elmer, Waltham, MA, USA). Densitometric analysis of western blots was performed using National Institutes of Health ImageJ software (v. 1.48; NIH, Bethesda, Maryland, USA). Expression of ZO-1α^+ and ZO-1α^- were each normalized to β-tubulin expression, and experimental groups were further normalized to vehicle-treated sham for each independent experiment.

To detect and verify the identity of the ZO-1α^+ isoform, western blotting was performed with rabbit anti-ZO-1α^+ polyclonal antibody (Hycult Biotech, Plymouth Meeting, PA, USA; # HP9044). The rabbit polyclonal antibody, raised against amino acids 886-995 of human ZO-1, only recognizes the ZO-1α^+ isoform (Willott et al. 1992, Alvarado et al. 2004).

4.2.8 Statistical analysis

Repeated-measures analysis followed by Bonferroni *post hoc* tests were used to determine the overall effect of blast on the dose-dependent response and time course of TEER after exposure. Hydraulic conductivity, tight junction immunostaining, and western blotting data were analyzed by one-way ANOVA followed by Bonferroni *post hoc* tests. (SPSS v. 22, IBM, Armonk, NY, USA; significance * $p < 0.05$).

4.3 Results

4.3.1 Potentiated TEER recovery with DEX treatment after blast

In vitro BBB cultures were exposed to blast with a 571 kPa peak overpressure, 1.06 ms duration, and 186 kPa*ms impulse (Hue et al. 2013). Following blast exposure (day 0), TEER of injured cultures decreased acutely to approximately 80 % of pre-exposure levels compared with 102 ± 1 % in sham controls (Figure 4.1). One day following blast exposure (day 1), TEER

increased in a dose-dependent manner after DEX treatment at a concentration range of 0-10 µM, with no significant increase after a 100 µM treatment (Figure 4.1). TEER decreased to 80 ± 4 % acutely after blast, and after treatment with 10 µM DEX, TEER recovered to 117 ± 5 % 1 day after injury (Figure 4.1). Administration of 10 µM DEX produced a maximal TEER increase (of the treatment concentrations tested) in the *in vitro* BBB culture, which was consistent with published results (Cucullo et al. 2004). Therefore, 10 µM DEX was selected as the treatment concentration for all subsequent experiments.

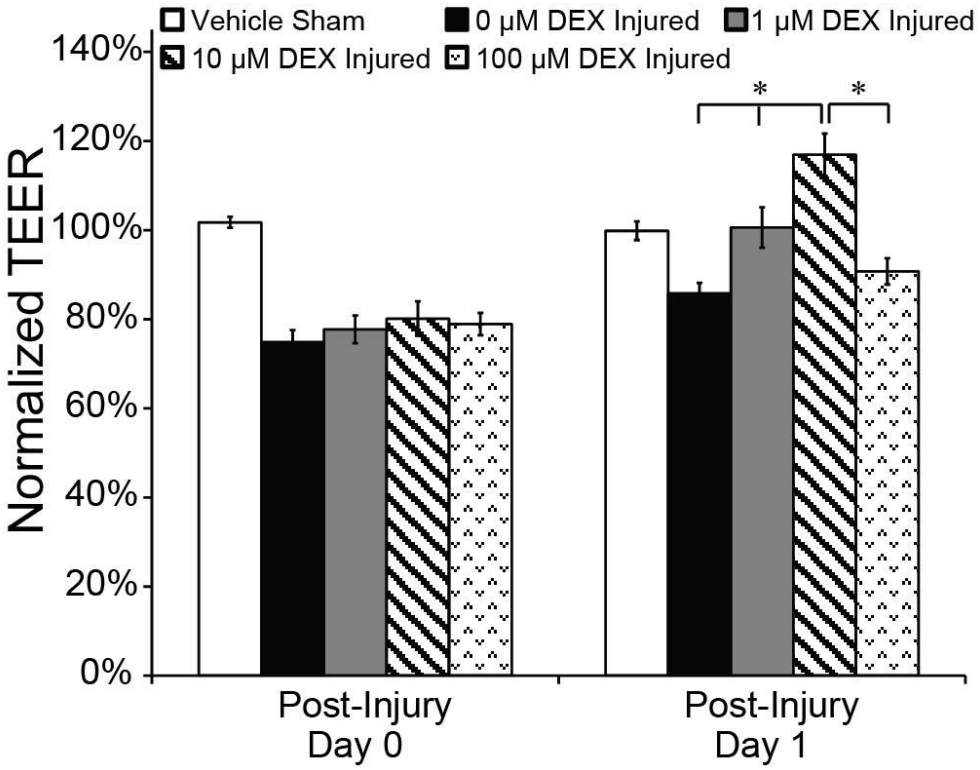

Figure 4.1 Dose-dependent effect of DEX on TEER after blast injury. Cultures were exposed to blast with a 571 kPa peak overpressure, 1.06 ms duration, and 186 kPa*ms impulse. Post-injury treatment with 10 µM DEX resulted in the greatest TEER recovery 1 day after blast exposure compared with all other treatment concentrations. (* $p < 0.05$; ± SEM; $n \geq 9$ per group).

TEER of vehicle-treated injured cultures required 3 days to fully recover spontaneously, compared with 1 day in DEX-treated (10 µM) injured cultures, demonstrating faster BBB

recovery due to treatment (Figure 4.2). TEER of vehicle-treated injured cultures increased from 75 ± 2 % to 85 ± 2 % 1 day after exposure, whereas TEER of DEX-treated injured cultures increased from 78 ± 2 % to 115 ± 2 % at the same time point (Figure 4.2). Vehicle-treated shams maintained consistently high TEER levels at approximately 100 % for 3 days after sham-exposure. TEER of DEX-treated shams increased to 119 ± 2 % 1 day after sham-exposure, which was a level comparable to that of DEX-treated injured cultures at the same time point, and was sustained for 3 days (Figure 4.2). These results support that in addition to potentiated TEER recovery after blast exposure, DEX treatment resulted in overall strengthening of the barrier and a more differentiated BBB phenotype (Romero et al. 2003, Cucullo et al. 2004). Absolute pre-injury TEER values were 13 ± 1.3 $\Omega*cm^2$ (mean ± SD), which were representative of TEER values previously reported for bEnd.3 cultures (Li et al. 2010). In addition, absolute TEER decreased to 10 ± 1.9 $\Omega*cm^2$ on day 0 post-injury, and recovered to 15 ± 1.1 $\Omega*cm^2$ at day 1 in DEX-treated injured cultures.

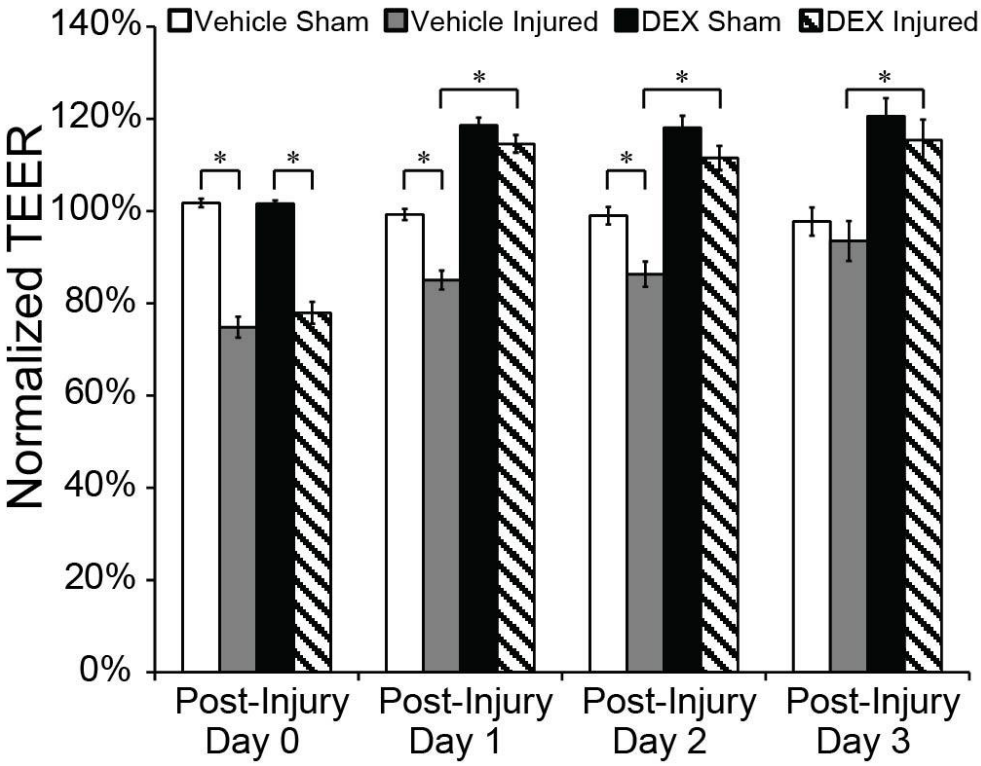

Figure 4.2 Potentiated TEER recovery induced by DEX treatment (10 μM) after blast injury. TEER of vehicle-treated injured cultures required 3 days to fully recover spontaneously, whereas TEER of DEX-treated injured cultures fully recovered 1 day after blast exposure. Effects of DEX treatment were sustained for at least 3 days after injury. (* $p < 0.05$; ± SEM; $n \geq 10$ per group).

4.3.2 Reduced hydraulic conductivity (L_p) with DEX treatment after blast

L_p was significantly decreased – indicating a tighter barrier – in DEX-treated injured cultures and sham cultures compared with vehicle-treated injured cultures from days 1-3 after blast. L_p was elevated to $3.51 \pm 0.89 \times 1/10^7$ cm/s/cmH_2O in vehicle-treated injured cultures compared with $1.74 \pm 0.15 \times 1/10^7$ cm/s/cmH_2O in vehicle-treated shams 1 day post-injury (Figure 4.3; not significant). L_p remained elevated at $4.10 \pm 0.94 \times 1/10^7$ cm/s/cmH_2O in vehicle-treated injured cultures compared with $1.76 \pm 0.46 \times 1/10^7$ cm/s/cmH_2O in vehicle-treated shams 2 days post-injury (Figure 4.3; not significant). Vehicle-treated injured cultures

spontaneously recovered to 2.18 ± 0.44 × $1/10^7$ cm/s/cmH_2O by 3 days post-injury, which was very close to 2.00 ± 0.52 × $1/10^7$ cm/s/cmH_2O in vehicle-treated shams (Figure 4.3). However, L_p of DEX-treated injured cultures fully recovered to 1.44 ± 0.22 × $1/10^7$ cm/s/cmH_2O by day 1 after blast, and remained significantly decreased compared with vehicle-treated injured cultures from days 1-3 after injury (Figure 4.3). Overall, these L_p results support the post-injury time course of TEER recovery (Figure 4.2), demonstrating potentiated and sustained recovery of BBB integrity in DEX-treated injured cultures lasting for at least 3 days after blast.

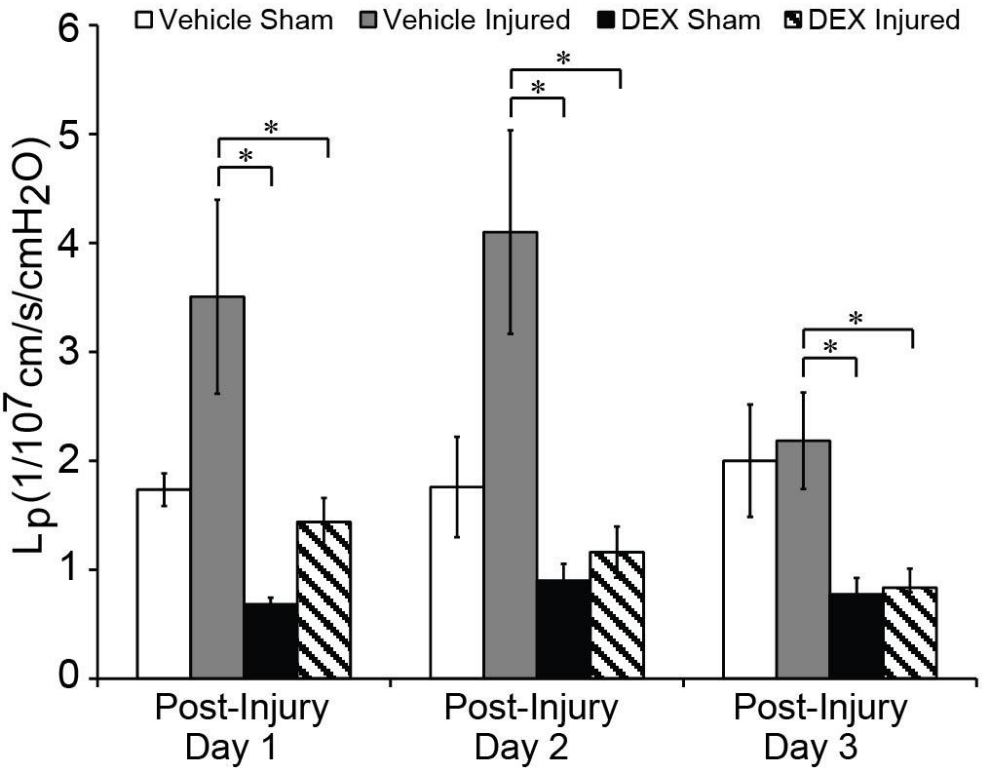

Figure 4.3 Decreased hydraulic conductivity (L_p) due to DEX treatment after blast injury. L_p was significantly reduced – indicating a tighter barrier – in DEX-treated cultures compared with vehicle-treated injured cultures from days 1-3 after injury. Elevated L_p of vehicle-treated injured cultures spontaneously recovered to vehicle-treated sham levels by day 3 post-injury. (* $p < 0.05$; ± SEM; $n \geq 7$ per group).

4.3.3 Inhibition of DEX-induced potentiated BBB recovery

Co-treatment with DEX and the glucocorticoid receptor antagonist, RU486, inhibited potentiated TEER recovery attributed to DEX treatment alone (Figure 4.4A). DEX-treated injured cultures recovered 1 day after injury, compared with 3 days in injured cultures receiving both DEX and RU486. TEER of DEX-treated injured cultures increased from 79 ± 3 % to 119 ± 2 % 1 day after exposure, whereas TEER of DEX and RU486-treated injured cultures increased from 77 ± 3 % to 88 ± 2 % at the same time point (Figure 4.4A). The time course for TEER recovery in injured cultures receiving co-treatment of DEX and RU486 matched the spontaneous recovery time course in vehicle-treated injured cultures (Figure 4.2). In addition, sham cultures treated with RU486 maintained high TEER levels at approximately 100 % for the duration of the time course, confirming that RU486 alone did not negatively affect TEER. Co-treatment with DEX and RU486 also inhibited the reduction in L_p (tightening of the barrier) effected by DEX treatment alone (Figure 4.4B). L_p of DEX-treated injured cultures recovered 1 day after injury to $1.12 \pm 0.08 \times 1/10^7$ cm/s/cmH_2O, whereas L_p of DEX and RU486-treated injured cultures was significantly elevated to $3.03 \pm 0.62 \times 1/10^7$ cm/s/cmH_2O, which was similar to L_p of vehicle-treated injured cultures 1 day post-injury (Figure 4.3).

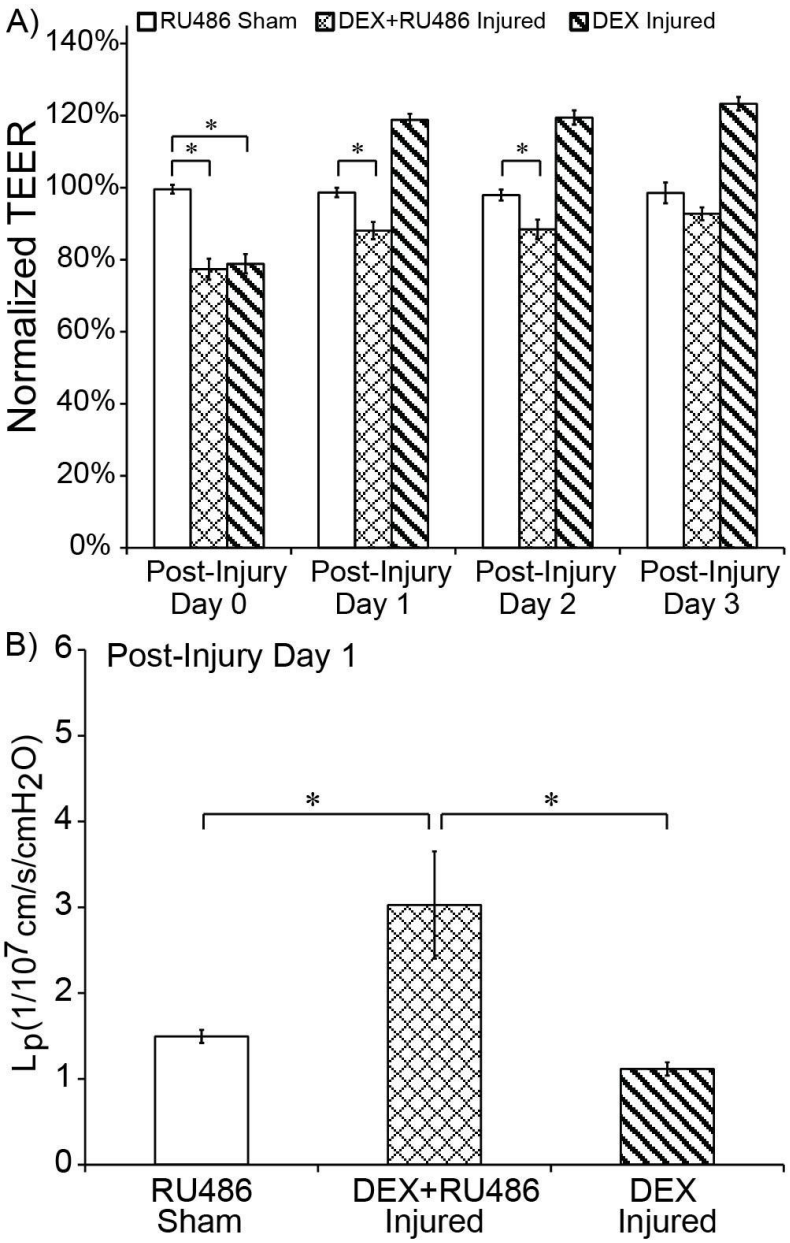

Figure 4.4 Inhibition of DEX-induced potentiated BBB recovery. (**A**) Co-treatment with DEX and RU486 inhibited potentiated TEER recovery attributed to DEX treatment alone. TEER of DEX-treated injured cultures recovered 1 day after injury, compared with 3 days in injured cultures co-treated with DEX and RU486. (**B**) Co-treatment with DEX and RU486 inhibited the reduction in L_p attributed to DEX treatment alone. L_p of DEX-treated injured cultures recovered 1 day after injury, whereas L_p of injured cultures receiving DEX and RU486 was significantly elevated compared with sham and DEX-treated injured groups. (* $p < 0.05$; ± SEM; $n \geq 9$ per group in **A** and **B**).

4.3.4 Increased ZO-1 tight junction immunostaining with DEX treatment after blast

Characteristic morphology and localized staining of the tight junction protein, ZO-1, were visible in vehicle-treated shams (Figure 4.5A). Bearing close resemblance to integral endothelial monolayers described in our previous publications (Hue et al. 2013, Hue et al. 2014), cells from vehicle-treated shams formed a characteristically elongated, spindle-shaped morphology with widespread expression of ZO-1 protein at the cytoplasmic membrane surface and at junctions between adjacent cells. ZO-1 staining was visibly compromised in vehicle-treated injured cultures, consistent with our previously reported results (Figure 4.5B) (Hue et al. 2013, Hue et al. 2014). ZO-1 immunofluorescence was visibly stronger and recovered at the cell periphery in DEX-treated injured cultures, suggesting that increased ZO-1 at tight junctions is a structural correlate to potentiated recovery of the BBB after blast exposure (Figure 4.5C). Co-treatment with DEX and RU486 inhibited DEX-induced increases in ZO-1 after injury (Figure 4.5D). The area-percentage of ZO-1 immunostaining per cell significantly decreased to 0.09 ± 0.01 % in vehicle-treated injured cultures compared with 0.14 ± 0.01 % in vehicle-treated shams, consistent with our previous study (Figure 4.5E) (Hue et al. 2014). ZO-1 staining in DEX-treated injured cultures significantly recovered to 0.15 ± 0.01 %, whereas staining remained significantly depressed at 0.09 ± 0.01 % in injured cultures co-treated with DEX and RU486 (Figure 4.5E). Therefore, the quantified area-percentage of ZO-1 immunostaining per cell confirmed qualitative trends observed in the immunofluorescence images acquired 1 day after blast exposure, further supporting the critical role of ZO-1 in mediating DEX-induced functional recovery of the BBB.

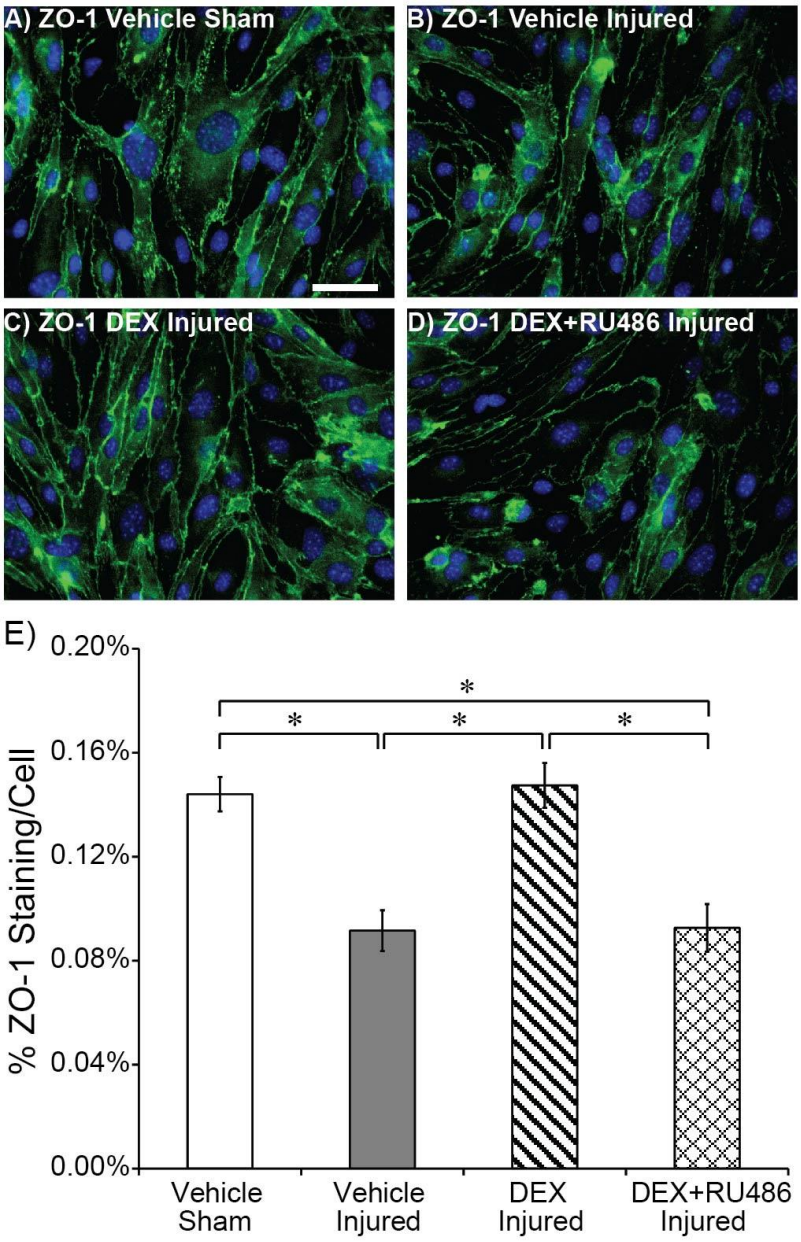

Figure 4.5 Increased tight junction immunostaining due to DEX treatment 1 day after blast injury. (**A**) Characteristic staining of the ZO-1 tight junction protein was present in vehicle-treated shams. (**B**) Reduced ZO-1 staining was evident in vehicle-treated injured cultures after blast exposure. (**C**) Stronger ZO-1 tight junction staining in DEX-treated injured cultures. (**D**) Reduced ZO-1 staining in injured cultures treated with DEX and RU486. (**E**) Quantified ZO-1 staining per cell was consistent with qualitative changes depicted in immunofluorescence images, confirming recovered ZO-1 tight junction immunostaining in DEX-treated injured cultures. (* $p < 0.05$; ± SEM; $n \geq 6$ cultures (≥ 30 images) per group; ZO-1 immunostaining (green); cell nuclei (blue); scale bar = 50 µm).

4.3.5 Increased ZO-1 tight junction protein expression with DEX treatment after blast

The influence of DEX treatment on ZO-1 protein expression 1 day after injury was assessed by western blot analysis. ZO-1 expression was detected by two immunoreactive bands corresponding to the α^+ and α^- isoforms of ZO-1, as previously reported (Willott et al. 1992, Balda and Anderson 1993, Sheth et al. 1997, Underwood et al. 1999, Alvarado et al. 2004). DEX treatment in injured cultures increased the intensity of the ZO-1α^+ band compared with all other experimental conditions, but did not affect the intensity of the ZO-1α^- band (Figure 4.6A). As determined by densitometric analysis, normalized ZO-1α^+ expression was significantly increased in DEX-treated injured cultures to 573 ± 189 % compared with 100 ± 25 % in vehicle-treated shams, 104 ± 30 % in vehicle-treated injured cultures, and 159 ± 11 % in DEX and RU486-treated injured cultures (Figure 4.6B). However, there were no significant changes in normalized ZO-1α^- levels due to DEX treatment (Figure 4.6C). Using an antibody specific to ZO-1α^+, only the protein band of higher molecular mass corresponding to ZO-1α^+ was detected, verifying identity of the isoform (Figure 4.7).

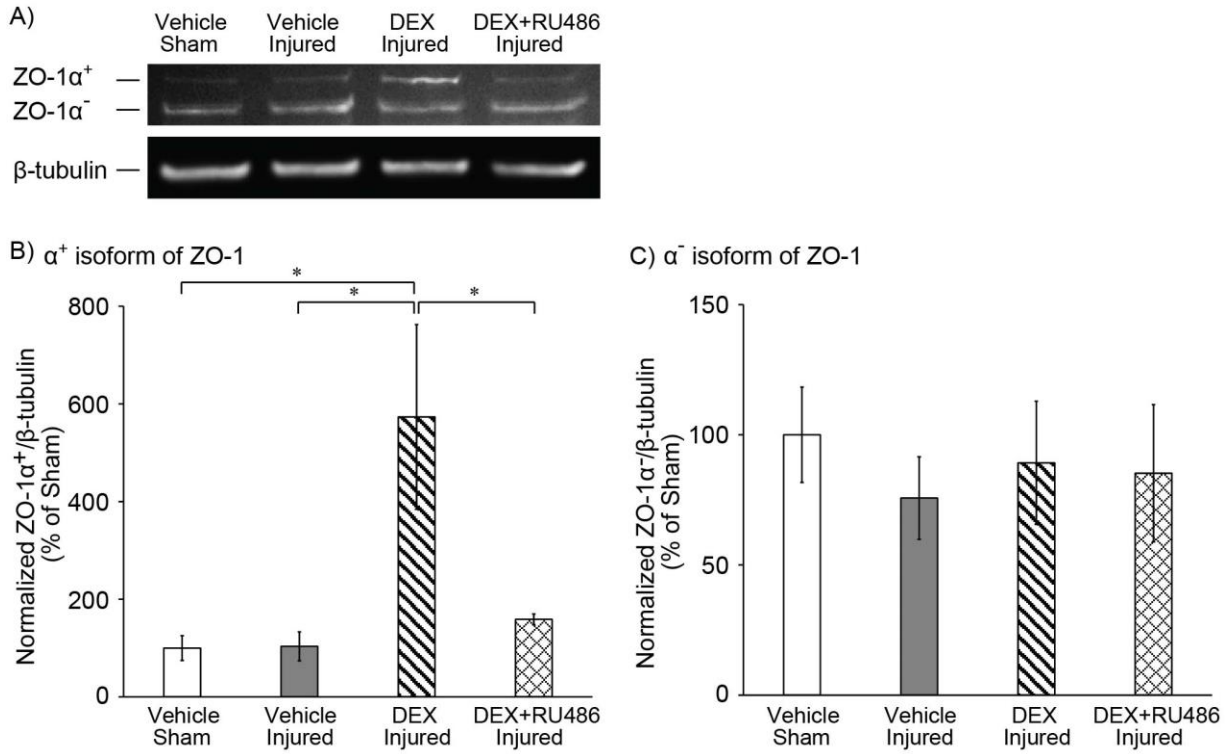

Figure 4.6 Upregulation of ZO-1α^+ tight junction protein with DEX treatment 1 day after blast injury. (**A**) Representative western blot of ZO-1 expression after blast or sham exposure, showing immunoreactive bands for the α^+ and α^- isoforms of ZO-1, and associated β-tubulin expression. DEX treatment in injured cultures increased intensity of the ZO-1α^+ band compared with all other experimental conditions, but did not affect intensity of the ZO-1α^- band. (**B**) Significant upregulation of ZO-1α^+ with DEX treatment after blast injury, as quantified by western blot analysis. The expression of ZO-1α^+ was normalized to β-tubulin expression, and experimental groups were further normalized to vehicle-treated sham. (**C**) No significant changes to ZO-1α^- after blast injury, as quantified by western blot analysis. The expression of ZO-1α^- was normalized to β-tubulin expression, and experimental groups were further normalized to vehicle-treated sham. (* $p < 0.05$; ± SEM; n ≥ 5 independent experiments per group in **B** and **C**).

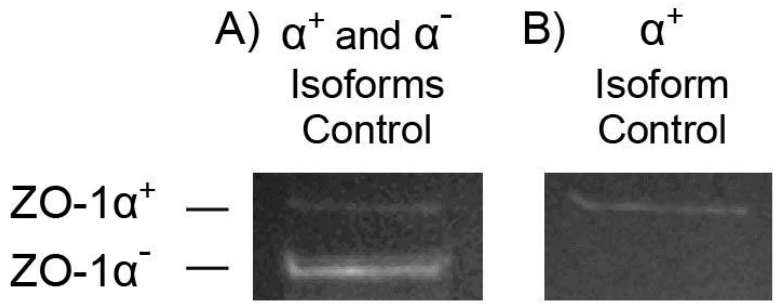

Figure 4.7 Verification of identity of the ZO-1α^+ isoform. (**A**) Representative western blot of ZO-1 expression in control endothelial cultures, showing immunoreactive bands for the α^+ and α^- isoforms of ZO-1. The rabbit anti-ZO-1 primary antibody (Life Technologies; # 61-7300) is known to recognize both isoforms of ZO-1. (**B**) Representative western blot of ZO-1α^+ expression in control endothelial cultures, without an immunoreactive band for ZO-1α^-. The rabbit anti-ZO-1α^+ antibody (Hycult Biotech; # HP9044) only recognizes the ZO-1α^+ isoform, specifically confirming expression of ZO-1α^+ in bEnd.3 cells.

4.4 Discussion

Treatment with DEX promotes BBB formation and functional recovery after injury by upregulating synthesis of tight junction proteins ZO-1, occludin, claudin-5, and other cell junction-related proteins (Romero et al. 2003, Forster et al. 2005, Forster et al. 2006, Blecharz et al. 2010, Campolo et al. 2013, Thal et al. 2013). Increased protein expression at the tight junctional complex induced by glucocorticoid treatment correlates with reduced paracellular permeability and augmented electrical resistance in epithelial and endothelial cells (Singer et al. 1994, Underwood et al. 1999, Romero et al. 2003, Cucullo et al. 2004, Forster et al. 2005, Forster et al. 2006, Blecharz et al. 2010). At the molecular level, ZO-1 acts as an intracellular scaffolding protein that critically regulates the integrity of tight junctions by anchoring transmembrane proteins, occludin and claudin-5, to the cytoskeleton (Abbott et al. 2010). Together, these findings described in the literature strongly support results of our current study,

which is the first to report that increased ZO-1 with DEX treatment after exposure to primary blast injury is linked to potentiated functional recovery of an *in vitro* BBB model.

Effects of glucocorticoid treatment are generally mediated by glucocorticoid receptor signaling activity and modulated expression of target genes (Romero et al. 2003, Forster et al. 2005, Rhen and Cidlowski 2005, Forster et al. 2006). To confirm glucocorticoid receptor-mediated upregulation of ZO-1 and potentiated recovery of the *in vitro* BBB model, we blocked DEX treatment effects with RU486, a potent and specific glucocorticoid receptor antagonist. Specifically, co-treatment with DEX and RU486 after injury eliminated the effects of potentiated recovery of TEER and hydraulic conductivity due to DEX treatment alone, and inhibited DEX-induced increases in ZO-1 immunostaining and protein expression. These results provide a mechanistic basis for signaling pathways affected by DEX treatment that facilitate functional BBB recovery after blast injury. Upon entering the cell, glucocorticoids can act in three ways: 1) complex with the glucocorticoid receptor to directly initiate transcription of target genes; 2) complex with the glucocorticoid receptor and interact with transcription factors including nuclear factor-κB (NF-κB); or 3) initiate non-genomic signaling pathways through membrane-associated receptors and second messengers (Rhen and Cidlowski 2005). It is unlikely that restoration of BBB integrity after injury was influenced by non-genomic pathways, as related studies strongly suggest the prominent role of glucocorticoid receptor signaling in initiating transcriptional and translational activity to regulate tight junction-related proteins and BBB integrity (Forster et al. 2005, Forster et al. 2006, Thal et al. 2013). More detailed biochemical and molecular investigation of these signaling mechanisms will help to identify promising targets for regulating recovery of the BBB after blast exposure.

Although DEX treatment after blast injury induced significant changes in TEER and hydraulic conductivity in the endothelial cultures, bEnd.3 cells may be limited in their ability to form tight monolayers relative to other cell lines and primary cell culture preparations. TEER of the BBB *in vivo* is expected to range from approximately 2000 – 5000 $\Omega*cm^2$, whereas TEER of immortalized brain capillary endothelial cells used to generate *in vitro* models of the BBB range from about 50 – 100 $\Omega*cm^2$ (Forster et al. 2005). Other studies have utilized an immortalized human brain microvascular endothelial cell line, hCMEC/D3, which has been reported to retain key morphological and brain endothelial markers, and form tight monolayers (Forster et al. 2008). Treatment of hCMEC/D3 cells with the glucocorticoid, hydrocortisone, resulted in an increase in TEER from approximately 70 $\Omega*cm^2$ to 200 $\Omega*cm^2$ (Forster et al. 2008). Experimental use of the human-derived cell line would be highly advantageous to the potential translation of findings from *in vitro* studies to the human condition. However, it is important to note that a more recent study reported that the maximum TEER of hCMEC/D3 (and other) human brain endothelial cells was only about 12 $\Omega*cm^2$ under representative culture conditions (Eigenmann et al. 2013), suggesting potentially wide variability in culture quality and glucocorticoid responsiveness in hCMEC/D3 cells. In the current study, absolute TEER values of bEnd.3 cultures were close to the typical reported range of 20-30 $\Omega*cm^2$, and had similar DEX-induced changes in TEER as a comparable endothelial cell line (Cucullo et al. 2004, Li et al. 2010). We also note that the measured time course of TEER was strongly supported by the parallel time course of hydraulic conductivity, demonstrating sustained recovery to sham levels by 1 day post-injury (Figure 4.3). The 2- to 3-fold decrease in hydraulic conductivity (barrier tightening) due to DEX treatment was strongly supported by previous studies describing

glucocorticoid-mediated regulation of endothelial fluid-flow resistance and tight junction formation (Underwood et al. 1999).

Administration of DEX as early as 30 minutes after TBI in mice has been shown to result in therapeutic effects on BBB integrity, neurological function, and secondary brain damage by 24 hours post-injury (Campolo et al. 2013, Thal et al. 2013). Other studies have also reported increases in tight junction proteins and associated BBB recovery 24 hours after DEX treatment *in vitro* and *in vivo* (Forster et al. 2006, Thal et al. 2013), which supports our findings of potentiated recovery of TEER, hydraulic conductivity, and ZO-1 expression 1 day after treatment. Our DEX treatment regimen was also prolonged, with a new dose administered once per day after injury. DEX-induced changes in TEER and hydraulic conductivity were permanent for at least 3 days after injury, the last time point tested. Enhanced tight junction protein expression and barrier properties have been observed in endothelial cells with continual DEX treatment lasting for weeks or months, without adverse effects on culture health (Underwood et al. 1999, Alvarado et al. 2004, Forster et al. 2005), However, DEX is described as a long-acting glucocorticoid with biological half-life of 36-54 hours and potency greater than other glucocorticoids including hydrocortisone and methylprednisolone (Walsh and Avashia 1992), so it may be possible that a reduction in the DEX treatment regimen (concentration and duration) would have yielded similar effects on BBB recovery. Future studies will investigate a therapeutic time window for glucocorticoid delivery to help optimize dosing strategy to rapidly restore BBB integrity and reduce treatment duration.

For over 30 years, treatment with corticosteroids was standard clinical practice for patients with head injuries and cerebral edema (Roberts et al. 2004). However, early results of the multicenter CRASH trial, released in 2004, reported that 48 hour infusion of

methylprednisolone within 8 hours of head injury increased the risk of mortality in enrolled patients (Roberts et al. 2004). Despite the unfavorable outcome, the exact cause and mechanism of increased mortality associated with methylprednisolone treatment remain unclear, as multiple complicating factors related to trauma were present (Roberts et al. 2004). Furthermore, enrollment criteria of the trial were broadly defined, inclusive of patients with mild to severe TBI and a Glasgow coma score (GCS) of 14 or less, making it difficult to appreciate the influence of different severities and etiologies of head injury on outcome. Unlike head injuries sustained by patients of the CRASH trial, the current study investigated effects of DEX treatment in the context of blast-induced TBI, which is a fundamentally different biomechanical injury mechanism that warrants further study of the potential therapeutic benefit of corticosteroids after blast exposure.

Due to potent anti-inflammatory and immunosuppressant effects, glucocorticoids have been widely used in the clinic to treat brain edema, autoimmune disorders like rheumatoid arthritis, and disorders characterized by a leaky BBB like multiple sclerosis (Cucullo et al. 2004, Blecharz et al. 2010, Thal et al. 2013). In some cases, however, steroidal treatments have been ineffective in restoring the damaged BBB in human trauma and stroke patients (Poungvarin 2004). DEX treatment at high doses has also been reported to exacerbate cognitive deficits in a spatial acquisition task after TBI in rodents (Chen et al. 2010). In addition, treatment with DEX or other glucocorticoids has been hampered by reports of toxicity and side effects including osteoporosis, candidiasis, insulin resistance, hypertension, increased intraocular pressure, and gastrointestinal bleeding, especially after chronic treatment (Kimberly 1991, Walsh and Avashia 1992, Schacke et al. 2002, Cucullo et al. 2004, Forster et al. 2006, Zhuo et al. 2010). It is important to note, nonetheless, that the toxicity of glucocorticoids is dependent on the dosage

and duration of treatment, with higher dosages and longer therapies associated with greater toxicity (Walsh and Avashia 1992). Therefore, efforts to elucidate molecular mechanisms underlying the effects of glucocorticoids on the BBB may contribute to the identification of novel therapeutic targets and treatment strategies to help circumvent known side effects.

A limitation of this study is that treatment-induced regulation of other proteins essential for tight junction formation and function of the BBB, such as occludin and claudin-5 (Abbott et al. 2010), were not examined. In addition to ZO-1, glucocorticoid treatment has been reported to result in heightened expression of occludin and claudin-5, ultimately enhancing barrier restriction (Forster et al. 2005, Blecharz et al. 2010). However, it should be noted that cell type plays an important role in determining the specific biological signaling activity triggered by glucocorticoid treatment (Romero et al. 2003). For example, specific increases in occludin, but not claudin-5, were observed 24 hours after DEX treatment in a mouse brain endothelial cell line (Forster et al. 2006). Interpretation of these results therefore requires careful consideration of multiple factors, including cell type and species, when assessing the molecular and functional effects of glucocorticoid treatment. Despite the variable influence of treatment on tight junction protein regulation, it is remarkable that DEX-induced tightening of the BBB was abolished by inhibiting ZO-1 expression with antisense phosphorothioate oligonucleotides – supporting the critical role of ZO-1 in the formation and functional maintenance of tight junctions (Underwood et al. 1999).

Recent evidence supports that BBB breakdown occurs after blast injury, but detailed understanding of this phenomenon and subsequent barrier recovery remain limited. BBB damage after blast exposure has been observed by IgG and Evans blue extravasation (Readnower et al. 2010, Garman et al. 2011, Skotak et al. 2013, Yeoh et al. 2013, Lucke-Wold et al. 2014),

along with reduced immunostaining and protein expression of ZO-1, occludin, and claudin-5 (Abdul-Muneer et al. 2013, Hue et al. 2013, Hue et al. 2014). On the contrary, others have reported BBB damage with no significant reductions in occludin or ZO-1 after blast injury in rats; however, upregulation of the same proteins with byrostatin-1 treatment resulted in restoration of barrier integrity (Lucke-Wold et al. 2014). In our current study, ZO-1 immunostaining was compromised by blast exposure while ZO-1 protein expression was unaltered by blast. It is interesting that in the absence of blast-induced changes to protein levels, upregulation of ZO-1 with DEX treatment in injured cultures resulted in potentiated BBB recovery. To place our results in context of recent studies, it is possible that blast injury disrupted barrier integrity by modifying localization or cellular distribution of ZO-1, without altering total protein expression. Our results are supported by published findings that BBB breakdown in rats exposed to blast triggered acute upregulation of the protein kinase C α (PKCα) isozyme, which has been reported to influence the redistribution of tight junction proteins and brain endothelial permeability (Lucke-Wold et al. 2014). Taken together, these results emphasize that blast injury is a complex phenomenon likely associated with subtle structural changes to tight junctions that underlie BBB breakdown. Broader neuropathological implications of blast-induced changes in BBB integrity include increased oxidative and nitrosative stress, astrocyte reactivity, and microglial activation (Readnower et al. 2010, Abdul-Muneer et al. 2013). Future studies will mechanistically examine molecular alterations to tight junction proteins responsible for compromised BBB integrity after blast exposure.

Although ZO-1 tight junction immunostaining recovered in DEX-treated injured cultures, changes in ZO-1 protein expression provided additional mechanistic insight that upregulation of the ZO-1α^+ isoform critically contributed to potentiated BBB recovery. Specific and dramatic

upregulation of ZO-1α^+ effected by DEX treatment has previously been demonstrated in human trabecular meshwork endothelial cells that express both isoforms of ZO-1 (Alvarado et al. 2004, Zhuo et al. 2010). Our results strongly agree with the literature that ZO-1α^+ may play a crucial role in the restrictive permeability of endothelial barriers (Underwood et al. 1999, Alvarado et al. 2004, Zhuo et al. 2010).

The α^+ and α^- isoforms of ZO-1 are known to be differentially expressed, depending on cell type (Balda and Anderson 1993, Underwood et al. 1999, Alvarado et al. 2004, Zhuo et al. 2010). Consistent with this, we observed relatively less expression of ZO-1α^+ compared with ZO-1α^- in uninjured cells. Differential distribution of the two ZO-1 isoforms may provide a molecular distinction between two functional classes of tight junctions (Balda and Anderson 1993). Although the specific function of the 80 amino acid α domain is unclear, ZO-1α^+ is predominantly expressed in epithelial cells, while ZO-1α^- is more widely expressed in endothelial cells (Balda and Anderson 1993, Sheth et al. 1997, Zhuo et al. 2010). Some studies suggest that ZO-1α^+ plays a distinct role in tight junction assembly and stabilization, and may be associated with higher-resistance junctions (Balda and Anderson 1993, Sheth et al. 1997, Alvarado et al. 2004). In addition, later expression of the ZO-1α^+ isoform, following ZO-1α^- expression, is reported to be a final step in tight junction synthesis and sealing during mouse blastocyst formation (Sheth et al. 1997).

Treatment with DEX *in vivo*, especially when administered as part of a combination therapy with other supplements, can exert neuroprotection after TBI (Campolo et al. 2013, Thal et al. 2013). The use of DEX as part of a combination therapy may help to enhance neuroprotection and minimize unwanted side effects by lowering the required dosage and duration of treatment (Campolo et al. 2013). For example, combination treatment with

melatonin (10 mg/kg) and DEX (0.025 mg/kg) 1 and 6 hours after injury reduced the overall degree of brain injury caused by controlled cortical impact (CCI) in mice (Campolo et al. 2013). It is important to note that DEX treatment alone also significantly attenuated infarct size, mitigated motor deficits, and prevented expression of apoptosis proteins iNOS, MMP-2, and -9 (Campolo et al. 2013). Combined treatment with DEX (10 mg/kg) and bortezomib (0.2 mg/kg; a proteasome inhibitor) 30 minutes post-injury prevented proteasomal degradation of the glucocorticoid receptor after TBI, which was necessary to enable glucocorticoid-mediated recovery of BBB function (Thal et al. 2013). After stabilizing glucocorticoid receptor function, DEX treatment increased occludin expression, and decreased neurological impairment, brain edema, and lesion size after CCI in mice (Thal et al. 2013). Such recent insights and new mechanistic understanding may stimulate renewed clinical interest in the development of glucocorticoid therapies for TBI and disorders of the CNS.

In summary, this study has elucidated important cellular mechanisms underlying potentiated barrier recovery with DEX treatment after primary blast exposure, demonstrating that glucocorticoid-mediated upregulation of ZO-1 tight junction protein was associated with functional restoration of an *in vitro* BBB model. These findings hold important implications for future development of glucocorticoid therapies and for potentially reducing mandatory rest periods for personnel exposed to blast injury.

5 Time course and size of blood-brain barrier opening in a mouse model of blast-induced traumatic brain injury[7]

5.1 Introduction

There have been over 300,000 medical diagnoses of traumatic brain injury (TBI) among U.S. Armed Forces alone, which have been largely attributed to blast exposure in recent military conflicts in Iraq and Afghanistan (Magnuson et al. 2012, Chen et al. 2013). The exact biophysical determinants of bTBI are still an area of active investigation, but an increasing number of studies assert that the direct interaction with blast overpressure (i.e. a shock wave) is sufficient to cause damage to the brain and blood-brain barrier (BBB) (Readnower et al. 2010, Garman et al. 2011, Abdul-Muneer et al. 2013, Hue et al. 2013, Yeoh et al. 2013, Hue et al. 2014, Logsdon et al. 2014). Clinical observations of patients who have sustained blast-induced traumatic brain injury (bTBI) confirm the frequent occurrence of brain edema, vasospasm, and intracranial hemorrhage, implicating insult to the neurovascular unit (Armonda et al. 2006, Ling et al. 2009, Magnuson et al. 2012, Chen et al. 2013). Traumatic cerebral vasospasm has been reported to last for up to 30 days in patients with moderate to severe bTBI (Armonda et al. 2006, Ling et al. 2009). Microhemorrhage may cause glial scarring and white matter degeneration, which may be linked to chronic traumatic encephalopathy (CTE), vascular dementia, and Alzheimer's disease (Wu et al. 2012, Glushakova et al. 2014). Therefore, damage to the BBB may be a major hallmark of bTBI that initiates secondary injury mechanisms and symptoms related to cerebrovascular dysfunction, emphasizing that the loss of BBB integrity may be a

[7] A modified version of this chapter has been submitted for publication and is under review: Hue, C.D., Cho, F.S., Cao, S., Nicholls, R.E., Vogel, E.W., 3rd., Sibindi, C., Arancio, O., Bass, C.R., Meaney, D.F., Morrison, B., 3rd. (2015). Time course and size of blood-brain barrier opening in a mouse model of blast-induced traumatic brain injury.

clinically important facilitator of the pathophysiology of blast injury (Readnower et al. 2010, Chen and Huang 2011, Abdul-Muneer et al. 2013, Chen et al. 2013, Logsdon et al. 2014).

The rapidly growing body of experimental evidence *in vivo* and *in vitro* supports that BBB breakdown is a characteristic outcome of blast exposure (Readnower et al. 2010, Garman et al. 2011, Logsdon et al. 2014, Lucke-Wold et al. 2014), and in some cases, of pure primary blast injury (Abdul-Muneer et al. 2013, Hue et al. 2013, Skotak et al. 2013, Yeoh et al. 2013, Hue et al. 2014, Hue et al. 2015). In murine models of bTBI, BBB opening has been assessed most frequently by extravasation of Evans blue (EB) (Abdul-Muneer et al. 2013, Logsdon et al. 2014, Lucke-Wold et al. 2014), and IgG (Readnower et al. 2010, Garman et al. 2011, Skotak et al. 2013, Yeoh et al. 2013). Recent reports suggest that the loss of restrictive barrier properties is mediated by reduced expression or pathological reorganization of tight junction proteins including zonula occludens (ZO)-1, claudin-5, and occluding (Abdul-Muneer et al. 2013, Hue et al. 2013, Hue et al. 2014, Lucke-Wold et al. 2014, Hue et al. 2015). It is important to note, however, that others have also reported inconsistent BBB damage despite efforts to precisely control blast injury parameters (Readnower et al. 2010, Garman et al. 2011, Skotak et al. 2013), as evidenced in one study by negligible BBB breakdown in approximately half of injured animals (Skotak et al. 2013). Together, this evidence points to the complexity of BBB breakdown after blast injury, which may be further confounded by the variety of loading regimes and biomechanical injury parameters (peak overpressure, duration, and impulse) used in different studies.

To help shed necessary insight on the extent of BBB disruption after blast injury, we characterized the pore-size of BBB opening and its time course for spontaneous recovery after exposure to blast injury by measuring extravasation of sodium fluorescein (NaFl), EB, and

dextrans of distinct molecular masses (3, 70, and 500 kDa). We utilized a previously described *in vivo* blast injury model with high-speed video to control and report the biomechanics of injury and minimize head motion associated with blast exposure (Gullotti et al. 2014, Patel et al. 2014). We report that BBB opening was sufficient to permit significant extravasation of molecules less than approximately 70 kDa in the acute period after blast, with recovery of BBB integrity by 1 day post-injury. This study is the first to characterize the time course and pore-size of BBB opening after blast exposure, and holds important implications for the influx of serum constituents into the brain that may initiate secondary pathological cascades after bTBI.

5.2 Materials and Methods

5.2.1 Animal preparation

All experiments using mice were conducted in accordance with animal welfare guidelines established by the Institutional Animal Care and Use Committee (IACUC) of Columbia University. Wild-type adult mice (male and female, 10 – 14 weeks old, 20 – 30 g), were a Filial 1 (F1) hybrid of C57BL/6 mice obtained from The Jackson Laboratory (Bar Harbor, ME, USA) and 129SvEv mice obtained from Taconic (Germantown, NY, USA). A total of 103 animals were used for this study and divided among sham and injured groups for NaFl, three different-size dextrans (3, 70, and 500 kDa), and EB at each post-injury time point (days 0 and 1).

5.2.2 *In vivo* blast-induced traumatic brain injury model

Our bTBI model consisted of a 76 mm-diameter shock tube that was previously described in detail (Gullotti et al. 2014), with a 25 mm-length driver section pressurized with helium gas, and a 1,240 mm-long driven section (Panzer et al. 2012). The body of the mouse was secured within a rigid pipe to protect the torso but expose the head 15 mm away from the shock tube exit

where the shock wave is still nearly planar (Figure 5.1) (Panzer et al. 2012, Gullotti et al. 2014, Patel et al. 2014). The head was further restrained using an adjustable, metal nose bar to minimize motion of the head during blast exposure. Pressure transducers (Meggitt Sensing Systems, Irvine, CA, USA; Endevco 8530B-1000) were flush-mounted at the shock tube exit, as well as inside the mouse holder in close proximity to the animal torso (Gullotti et al. 2014).

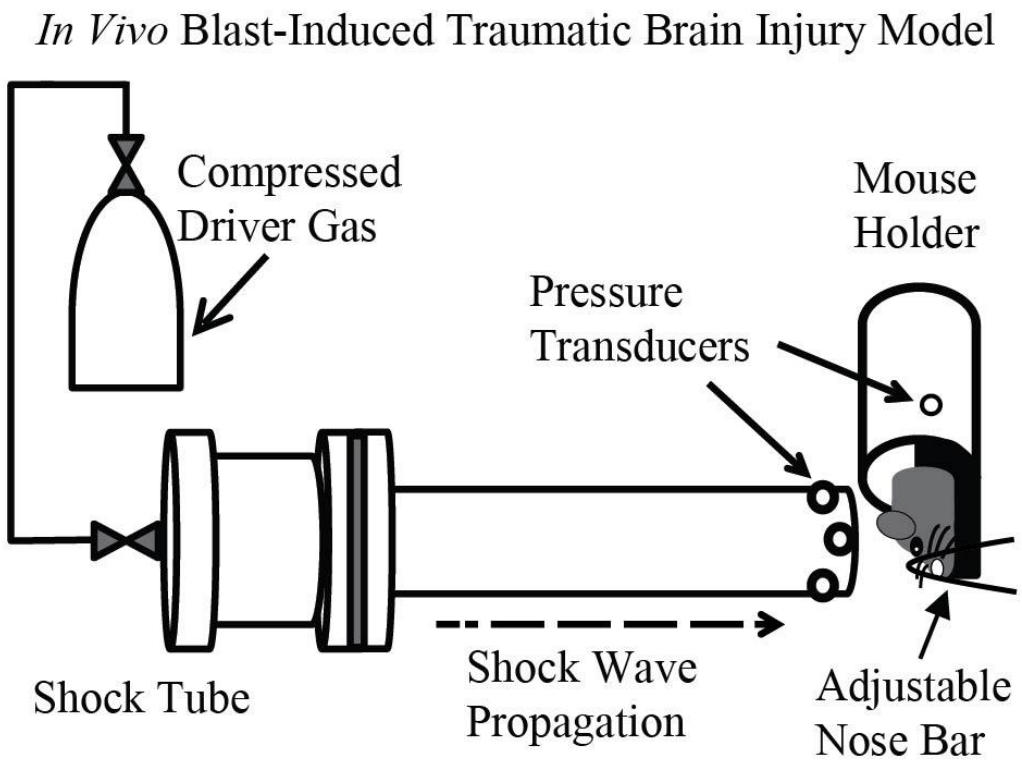

Figure 5.1 *In vivo* blast-induced traumatic brain injury (bTBI) model consisting of a shock tube and custom-designed mouse holder (Gullotti et al. 2014). Pressure transducers were flush-mounted at the exit of the tube and within the mouse holder. The mouse head was aligned 15 mm away from the exit of the tube. An adjustable nose bar was used to restrain the mouse head and minimize head motion during blast exposure. (Figure not drawn to scale)

5.2.3 Exposure to blast and administration of tracers

Prior to blast exposure, animals were anesthetized with isoflurane (Henry Schein Animal Health, Dublin, Ohio, USA) until completely secured and oriented in the custom mouse holder.

Animals were then exposed to a single blast. Animal cohorts were injected by tail vein either immediately prior to blast (day 0) or 1 day post-blast with different tracers. Sham controls were processed identically to injured animals, but were not exposed to blast.

Tracers of different molecular masses were used to determine blast-induced BBB opening. For NaFl, animals received 4 µL/g of a 10 % solution of NaFl (376 Da) dissolved in PBS (Yen et al. 2013). For biotinylated dextrans (Life Technologies, Carlsbad, CA), each animal received 0.16 mg/g of dextran (3, 70, or 500 kDa) dissolved in phosphate buffered saline (PBS). The hydrodynamic diameters (D_H) were previously determined by dynamic light scattering: 3 kDa (D7135; D_H ~ 2 nm), 70 kDa (D1957; D_H ~ 10 nm), 500 kDa (D7142; D_H ~ 30 nm) (Choi et al. 2010, Chen and Konofagou 2014). For EB, animals received 4 µL/g of a 2 % solution of EB (69 kDa when bound to serum albumin) dissolved in PBS (Yen et al. 2013).

5.2.4 Tissue preparation and *ex vivo* fluorescence imaging and analysis

Animals were perfusion-fixed 4 hours after administration of tracers. Animals were perfused with PBS for 6 minutes at 21 ml/min to remove tracers from the vasculature, followed by perfusion fixation with 4 % paraformaldehyde (PFA, dissolved in PBS) for 6 minutes at 21 ml/min. Brains were then extracted and sliced using a vibrating blade microtome (Vibratome 1000 Plus, Leica Biosystems, St. Louis, MO). A total of 10 coronal sections were cut (sections labeled S1-S10), each 1 mm-thick, excluding the olfactory bulbs and brain stem. Brain samples containing biotinylated dextrans were fluorescently labeled during a 1 hour incubation with a 1:100 dilution (in PBS) of streptavidin-Alexa Fluor® 647 conjugate (S32357; Life Technologies). All fluorescently-labeled dextran brain sections (Ex: 650 nm/Em: 668 nm), EB brain sections (Ex: 540 nm/Em: 680 nm), and NaFl brain sections (Ex: 440 nm/Em: 525 nm) were imaged using a CRi Maestro 2 Imaging System (Perkin Elmer, Waltham, MA, USA). A

custom image analysis script was developed using MATLAB (R2014b, MathWorks, Natick, MA, USA) to automate detection of the individual area in pixels and mean fluorescence intensity of each brain section.

5.2.5 High-speed video analysis

A Phantom v4.2 high-speed camera (Vision Research, Wayne, NJ) was used to record a frontal view of head motion associated with blast exposure. Videos were acquired at a resolution of 256 x 256 and a frame rate of 7,407 frames per second. Similar to our previous publication (Gullotti et al. 2014), a custom image processing script was developed using MATLAB (MathWorks) to track changes in eye position to quantify head kinematics (displacement, velocity, and acceleration) over time.

5.2.6 Confocal microscopy

High-resolution fluorescence images of EB-labeled sections were captured using a Leica TCS SP5 laser scanning confocal microscope equipped with a Leica HI Plan 4 x, 0.10 numerical aperture (NA) dry objective and a DMI6000 B inverted microscope (Leica Microsystems, Wetzlar, Germany). Brain sections were imaged with a helium-neon (HeNe) 543 nm laser, and emitted light was captured at a range of 620 nm – 700 nm. A total of 12 tile-scan images per section were acquired at a resolution of 1024 x 1024 with a scanning speed of 10 Hz, and were stitched together using Leica Application Suite software (Leica Microsystems) to generate a composite image of a complete coronal section.

5.2.7 Statistical analysis

All data are presented as mean ± SEM. Statistical significance was determined using one-way analysis of variance (ANOVA) to compare the mean fluorescence intensity of NaFl, EB, and dextrans (3, 70, 500 kDa) between corresponding sham and injured brain sections.

Statistical comparisons were also performed for each time point after blast injury. (SPSS v. 22, IBM, Armonk, NY, significance * $p < 0.05$).

5.3 Results

5.3.1 Kinematic analysis of blast-induced head motion

Animals were exposed to a shock wave with a 272 ± 6 kPa peak overpressure, 0.69 ± 0.01 ms duration, and 65 ± 1 kPa*ms impulse. Consistent with our previous study (Gullotti et al. 2014), head motion was generally characterized by rapid head movement in the direction parallel to the incident shock wave, followed by a slower and prolonged movement in the reverse direction, and a slow lateral evolution of the head as it reached its final position. The peak displacement, velocity, and acceleration of the head were all dramatically greater in the direction parallel to the incident shock wave (x component) than in the perpendicular direction (y component) (Table 5.1). Blast-induced head motion of a representative mouse, using head restraint, is presented in Figure 5.2. The peak pressure measured inside of the animal holder, adjacent to the torso, was 24 ± 1 kPa, which was well below reported thresholds for pulmonary injury (Bass et al. 2008). We also note that after injury, we did not observe any gross macroscopic pulmonary injury (data not shown) (Gullotti et al. 2014).

Kinematic Analysis of Head Motion

	Displacement (m)	Velocity (m/s)	Acceleration (m/s^2)
Maximum Total	0.003 ± 0.0001	7.07 ± 0.33	16349 ± 819
Maximum X	0.003 ± 0.0001	6.93 ± 0.33	16493 ± 819
Maximum Y	0.001 ± 0.0001	1.75 ± 0.10	6977 ± 380

Table 5.1 Kinematic analysis of head motion associated with blast exposure. (Mean ± SEM; *n* = 20 independent high-speed videos of mouse blast exposure).

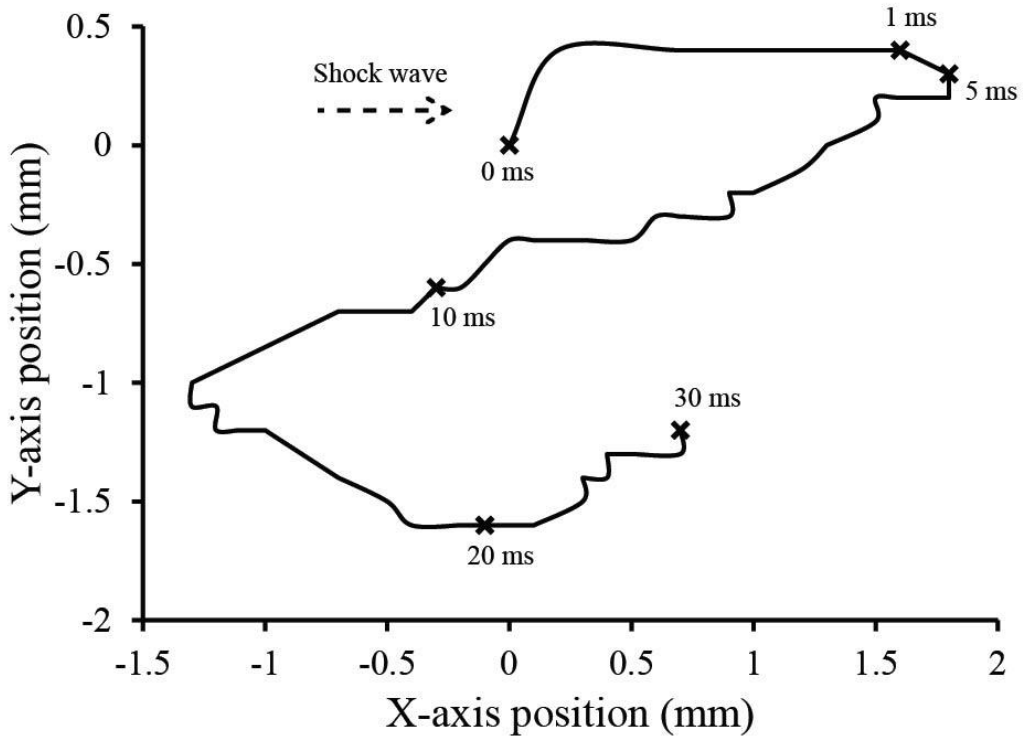

Figure 5.2 Head motion induced by blast exposure for a representative mouse (with head restraint). After blast exposure, the mouse head returned to rest at 31 ms. The direction of the oncoming shock wave is represented by the dashed arrow.

5.3.2 Blast-induced blood-brain barrier opening

In contrast to sham controls, blast resulted in widespread extravasation of NaFl and 3 kDa dextran in the acute period (day 0) after exposure (Figure 5.3A, B). EB was also visible in several injured brain sections in the acute period after exposure, when compared with EB-injected sham animals (Figure 5.3C). However, there was no qualitative indication of extravasation of the 70 or 500 kDa dextrans acutely after injury, except for scattered punctate regions of fluorescence (Figure 5.3D-E). At 1 day after blast exposure, there were no visible differences in extravasation of the different-size dextrans or EB between injured and sham

samples (Figure 5.4A-D), suggesting that the BBB had recovered. Qualitatively as the molecular mass increased, accumulation of dextran in injured samples was less widespread.

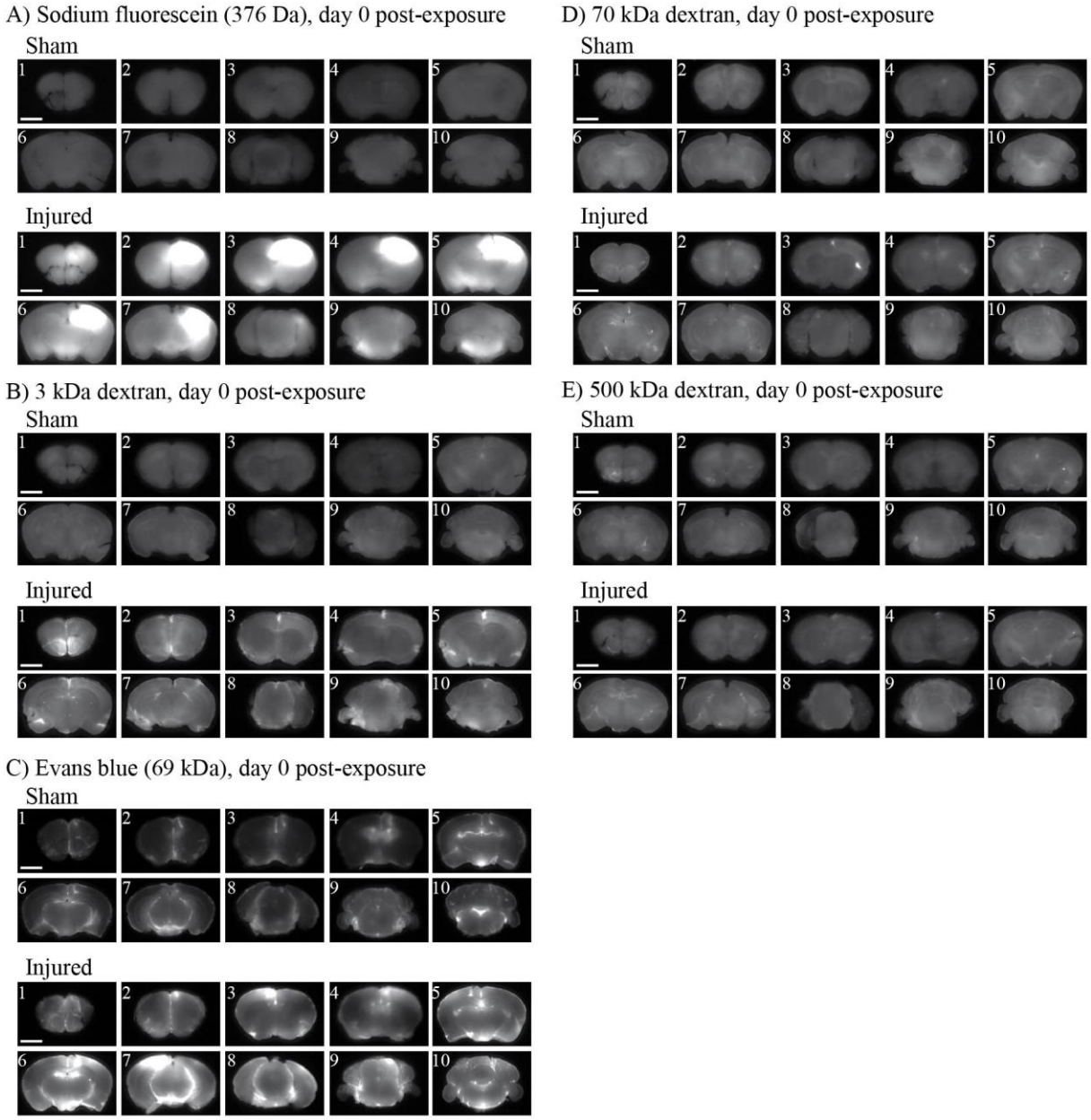

Figure 5.3 Blood-brain barrier opening in the acute post-injury period (day 0). (A) Strong, widespread fluorescence of NaFl throughout the entire blast-injured brain on day 0. (B) Widespread fluorescence of 3 kDa dextran throughout the entire blast-injured brain on day 0. (C) Regions of strong EB fluorescence in several injured brain sections on day 0. (D, E) No qualitative differences in fluorescence of 70 or 500 kDa dextrans between sham and injured brains on day 0. (Scale bar = 3 mm)

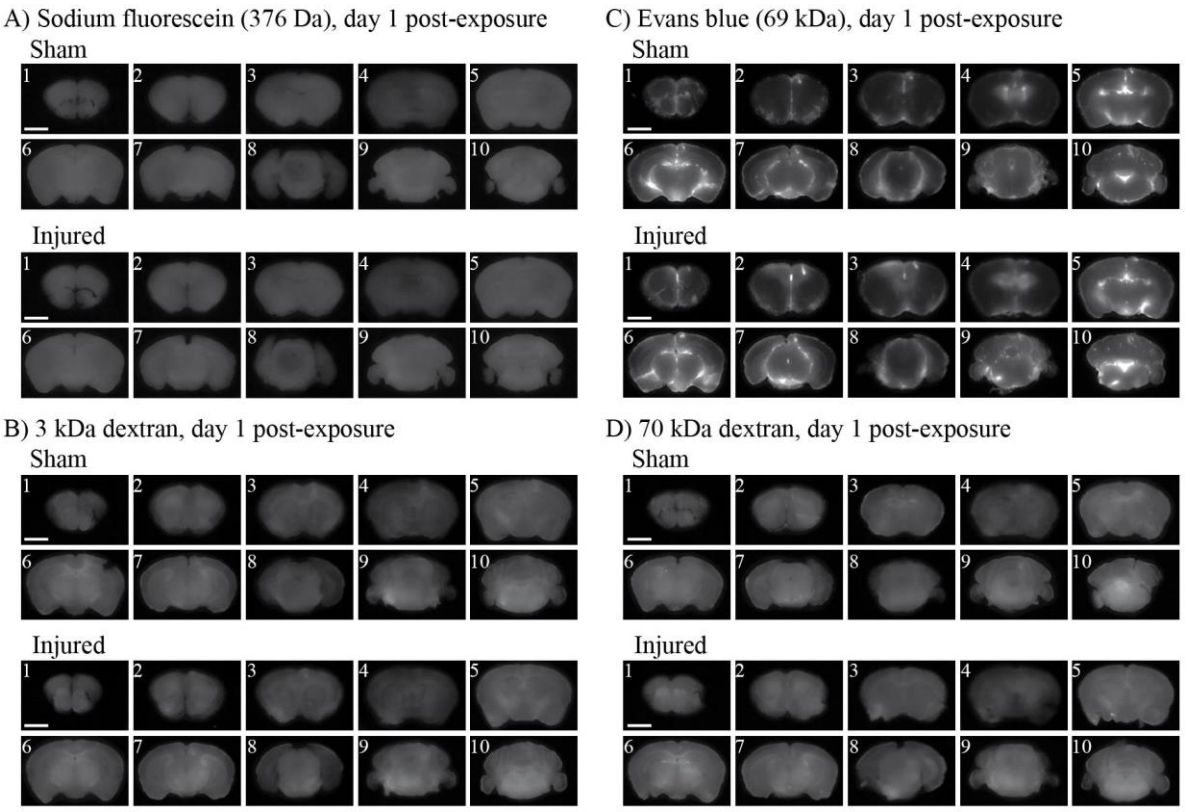

Figure 5.4 Blood-brain barrier opening 1 day post-injury. (A, B, C, D) No qualitative differences in fluorescence of NaFl, 3 or 70 kDa dextrans, or EB on day 1 after injury. (Scale bar = 3 mm)

5.3.3 Quantification of blast-induced blood-brain barrier opening

Quantitative analysis of the mean fluorescence intensity of each brain section confirmed qualitative visual trends. The mean fluorescence intensity of NaFl was significantly increased in the acute period after exposure (day 0) in all injured brain sections (Figure 5.5A). The mean fluorescence intensity of 3 kDa dextran was significantly increased in the acute period after exposure (day 0) in all injured brain sections except in section 10 (S10; $p = 0.061$) (Figure 5.5B). Mean fluorescence intensity of EB was also significantly greater in injured brain sections 3, 7, and 8 (S3, S7, and S8) in the acute period after blast (Figure 5.5C). Fluorescence intensity of 70 or 500 kDa dextrans was not altered in the acute post-injury period (Figure 5.5D-E). At 1 day

after blast exposure, mean fluorescence intensity was unaltered for NaFl and only significantly higher in injured samples in section 4 (S4) for 3 kDa dextran, section 3 (S3) for EB, and section 6 (S6) for 70 kDa dextran (Figure 5.6A-D). The quantitative results support that blast-induced BBB opening permits the influx of molecules less than approximately 70 kDa in the acute post-injury period, with spontaneous recovery of the BBB 1 day after exposure.

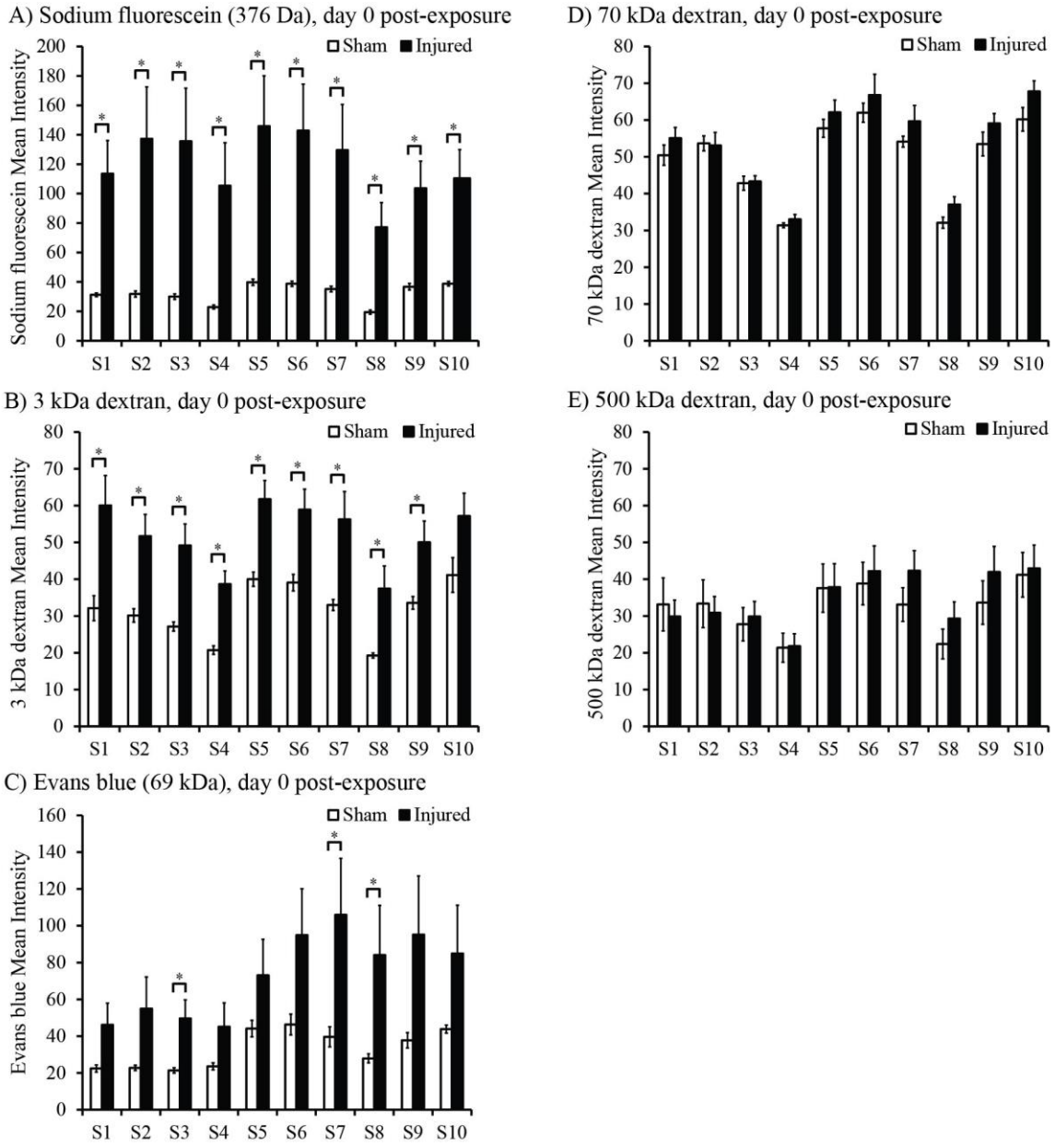

Figure 5.5 Quantification of blood-brain barrier opening in the acute post-injury period (day 0). (A) Mean fluorescence intensity of NaFl significantly increased throughout injured brain sections after blast exposure on day 0 ($n \geq 3$ per exposure condition). (B) Mean fluorescence intensity of 3 kDa dextran significantly increased throughout injured brain sections after blast exposure on day 0 ($n = 7$ per exposure condition). (C) Mean fluorescence intensity of EB significantly increased in several injured brain sections (S3, S7 and S8) after blast exposure on day 0 ($n \geq 6$ per exposure condition). (D, E) No changes in fluorescence of 70 or 500 kDa dextrans after injury on day 0 ($n \geq 5$ per dextran tracer and exposure condition). (* $p < 0.05$; ± SEM)

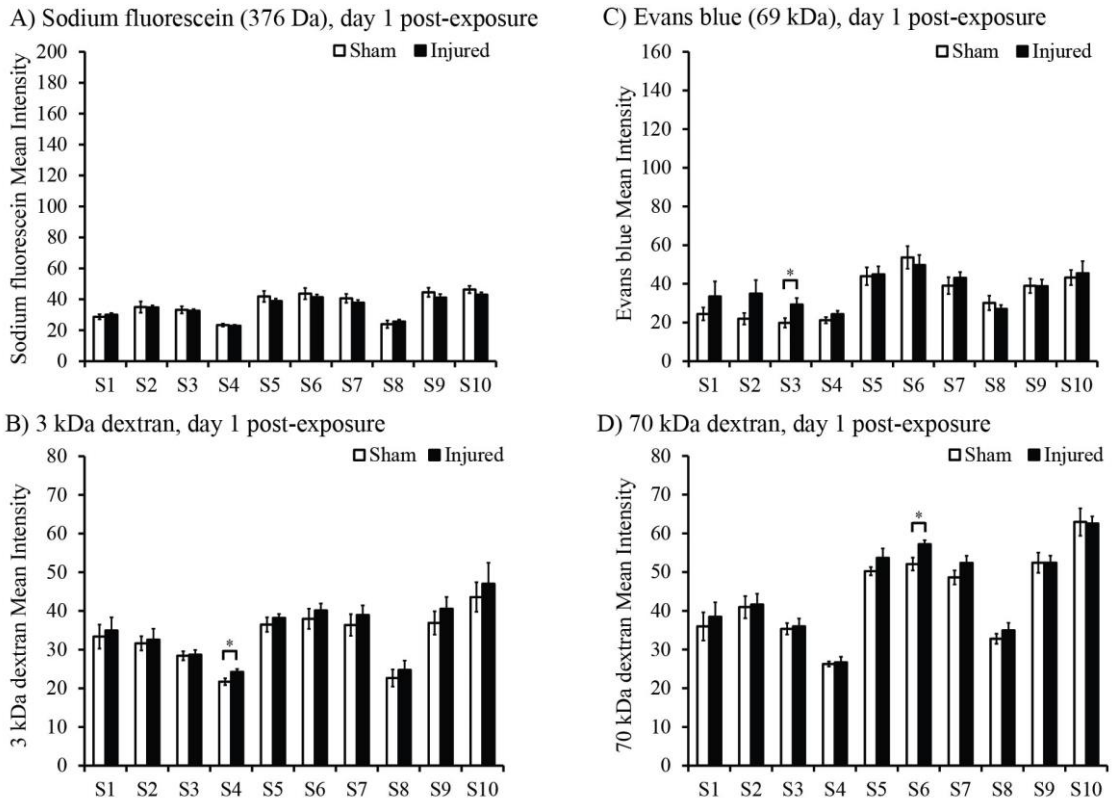

Figure 5.6 Quantification of blood-brain barrier opening 1 day post-injury (day 1). (A, B, C, D) Minimal to no differences in mean fluorescence intensity of NaFl ($n \geq 3$ per exposure condition), 3 and 70 kDa dextrans ($n = 6$ per dextran tracer and exposure condition), and EB ($n = 6$ per exposure condition) on day 1 after blast exposure, strongly supporting the recovery of BBB integrity. (* $p < 0.05$; ± SEM)

5.3.4 Microscopic evaluation of blood-brain barrier damage after blast

In the acute period (day 0) after sham exposure, there were no regions of visibly strong EB fluorescence by high-resolution confocal microscopy in a representative sham sample (section 5; -1.6 mm from Bregma) (Figure 5.7A). By contrast, there was widespread EB fluorescence throughout a corresponding blast-injured brain section that appeared to be strongest in the right motor (MO) and somatosensory cortex (SS), as well as in the left piriform (PIR), entorhinal (ENT), and perirhinal (PERI) cortex (Figure 5.7B). Although specific anatomical regions of fluorescence varied across injured samples, overall BBB breakdown appeared to be

diffuse but strongest in the cerebral cortex, which was consistent with previous findings (Readnower et al. 2010, Garman et al. 2011, Logsdon et al. 2014, Lucke-Wold et al. 2014).

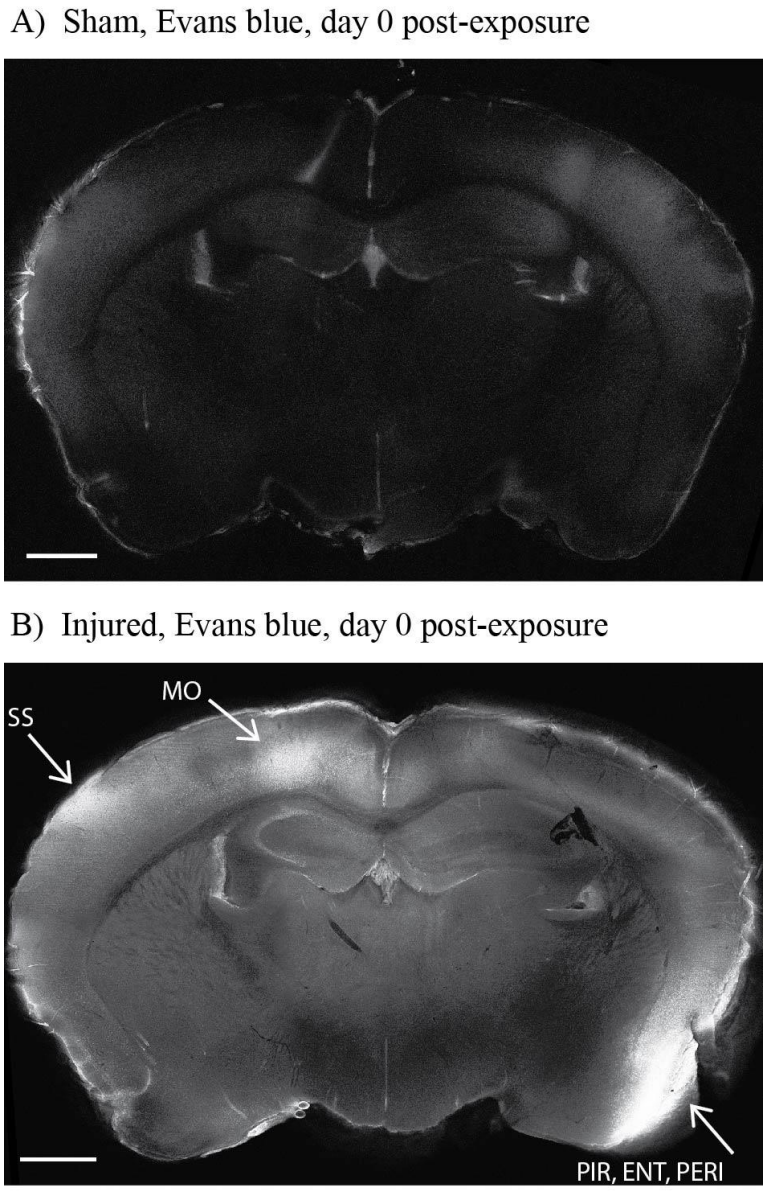

Figure 5.7 Confocal microscopy of Evans blue (EB) fluorescence in the acute period (day 0) after blast exposure. (A) No regions of strong EB fluorescence in sham exposed brain section. (B) Widespread EB fluorescence indicating BBB breakdown in an example injured brain section, with strongest regions of fluorescence in the right motor (MO) and somatosensory (SS) cortex, as well as in the left piriform (PIR), entorhinal (ENT), and perirhinal (PERI) cortex (white arrows). Anatomical regions of BBB damage varied across injured samples, but were generally strongest in the cerebral cortex. (Scale bar = 1 mm)

5.4 Discussion

This study reports a detailed characterization of BBB opening and recovery time course after blast injury using a range of different-sized tracers. We report the recovery of BBB function 1 day after blast exposure in mice, which is in close agreement with a recent *in vivo* bTBI study (Logsdon et al. 2014). In previous reports, acute opening of the BBB after blast, as demonstrated by EB extravasation, persisted for at least 6 hours after injury, with recovery of barrier integrity by 24 hours (Logsdon et al. 2014, Lucke-Wold et al. 2014). This time course of blast-induced BBB dysfunction is also in overall agreement with non-blast models of TBI, in which BBB opening occurs transiently and returns to control levels within hours to a few days (Enters et al. 1992, Tanno et al. 1992, Readnower et al. 2010, Garman et al. 2011, Hue et al. 2013, Hue et al. 2014). Based on findings in our current study, significant differences in mean intensity between sham and injured animals for NaFl, 3 kDa dextran, and EB on day 0 were dramatically reduced by day 1 after injury, providing evidence to support the recovery of BBB integrity 1 day after blast exposure at our loading conditions. The qualitative pattern of dextran fluorescence after blast exposure (Figure 5.3B) was similar to that reported in previous studies of BBB opening induced by focused ultrasound (Choi et al. 2010, Chen and Konofagou 2014). We also recognize that other small tracers and imaging techniques may provide potentially greater sensitivity for detecting small defects in the damaged BBB after TBI, such as gadolinium and magnetic resonance imaging (MRI) (Barzo et al. 1996).

Our data suggest that molecules less than approximately 70 kDa can penetrate the BBB in the acute period after blast injury at conditions tested in our study, but are excluded by 1 day after exposure when the BBB has recovered. However, other studies have reported the extravasation of larger molecules such as IgG (160 kDa) (Tanno et al. 1992) after blast injury

(Readnower et al. 2010, Garman et al. 2011, Skotak et al. 2013, Yeoh et al. 2013). Differences in the apparent pore-size of blast-induced BBB opening between our findings and those of other studies may be attributed to the variety of injury parameters tested (peak overpressure, duration, impulse, head acceleration). It is unclear exactly which biomechanical parameter(s) most strongly contribute to BBB opening *in vivo*, but a number of studies exposed animals to longer overpressure durations (Readnower et al. 2010, Garman et al. 2011, Skotak et al. 2013), others tested similar or greater overpressures (Yeoh et al. 2013), and some may have potentially allowed higher head accelerations without having quantified blast-induced head motion (Chavko et al. 2006, Readnower et al. 2010, Garman et al. 2011). Because IgG is endogenously present in serum, unlike exogenous tracers such as dextran, NaFl, and EB that are rapidly cleared from systemic circulation (Wolman et al. 1981, Vieira and Rajewsky 1988), more IgG may accumulate in the brain for a given defect, thereby improving the limit of detection for BBB breakdown.

Potential disparities in the time course of BBB breakdown that currently exist in the bTBI literature may also be related to variations in the biomechanics of different blast injury models. For example, exposure to primary blast injury (confirming the absence of head motion) at a range of different overpressure levels resulted in widespread IgG staining 24 hours after injury, but was only present in approximately half of all animals tested at a given blast level (Skotak et al. 2013). Focal lesions scattered throughout the brain were also observed by IgG staining after primary blast injury in rats (Yeoh et al. 2013). Another study of primary blast injury reported significant extravasation of EB and NaFl in rats 24 hours after exposure to a shock wave with a 123 kPa overpressure and estimated 4 ms duration (Abdul-Muneer et al. 2013), which was longer than that tested in our study. Other studies suggested that IgG immunoreactivity in the brain was

present 24 hours after blast exposure, and was reduced to control levels by 3 days (Readnower et al. 2010, Garman et al. 2011). However, because head accelerations were typically not measured in these studies, it is difficult to quantify contributions of inertial-driven (i.e. tertiary) injury in addition to blast overpressure (i.e. primary blast) when interpreting BBB breakdown. Although we only tested one exposure level in the current study, we have reported mouse head accelerations and shock wave parameters to more fully describe our blast conditions and enable more direct comparisons with future studies (Table 5.1).

Angular acceleration of the head (without blast exposure) has been postulated to result in widespread pathological and morphological changes to the cerebrovasculature throughout the brain (Maxwell et al. 1992). Controlled angular head accelerations of approximately $1 – 2 \times 10^5$ rad/s^2 resulted in extravasation of blood from vessels throughout the brain as well as subdural and intracerebral hematomas in non-human primates (Adams et al. 1981, Gennarelli et al. 1981, Gennarelli et al. 1982, Maxwell et al. 1992). Rapid rotation of the piglet head with peak angular accelerations of approximately $1 – 1.5 \times 10^5$ rad/s^2 caused subarachnoid bleeding and accumulation of blood in ventricles and the brain parenchyma, without overt BBB disruption as determined by IgG staining (Raghupathi and Margulies 2002). Rotational head acceleration of 2.1×10^5 rad/s^2 in rabbits also resulted in severe subarachnoid hemorrhage, focal intracerebral bleeding, and reactive astrogliosis, potentially causing damage to the BBB (Gutierrez et al. 2001). Rotational head trauma of approximately $3.7 – 10 \times 10^5$ rad/s^2 in rats resulted in damage to blood vessels, subarachnoid hemorrhage, and intraparenchymal lesions (Fijalkowski et al. 2007, Davidsson and Risling 2011), which was further supported in one study by the release of S100B proteins from brain glial cells into the serum (Davidsson and Risling 2011). After blast exposure in mice, Goldstein et al. (2012) reported peak average angular head acceleration of 9.54

x 10^5 rad/s^2, which was associated with microvascular pathology and abnormal BBB ultrastructure (Goldstein et al. 2012). In our current bTBI study, peak angular head acceleration associated with BBB opening was estimated to be 7 x 10^5 rad/s^2 (peak linear acceleration of 16,349 m/s^2) (Table 5.1), within the range of head accelerations reported in non-blast and blast models of TBI.

We have previously demonstrated that restraining head motion, protecting the torso, and modifying the orientation can influence animal survival and neurological deficits after blast exposure (Gullotti et al. 2014). Reduction of head acceleration by using effective head restraint promoted animal survival (Gullotti et al. 2014). In addition, protecting the torso significantly reduced mortality in rats exposed to blast (Long et al. 2009, Svetlov et al. 2010). Others have previously noted the importance of head accelerations on the neurological deficits and pathological consequences of blast injury (Svetlov et al. 2010, Goldstein et al. 2012). Although our careful efforts to restrain the head did reduce overall motion, accelerations remained appreciable (Table 5.1). However, improved mouse survival with the use of head restraint enabled us to study the effects of relatively high blast overpressures when compared with the range tested in related bTBI studies (Readnower et al. 2010, Garman et al. 2011, Abdul-Muneer et al. 2013, Skotak et al. 2013, Yeoh et al. 2013, Logsdon et al. 2014, Lucke-Wold et al. 2014). Our results also highlight a more general challenge in interpreting the effects of blast in the majority of *in vivo* bTBI models, in which inertial contributions of head motion can be minimized but not completely eliminated.

A number of studies describing cerebrovascular compromise after blast injury report the diffuse nature of BBB breakdown. In some cases, damage in general anatomical regions was observed, revealing diffuse staining predominantly in the prefrontal and outer layers of the cortex

(Readnower et al. 2010, Garman et al. 2011, Logsdon et al. 2014, Lucke-Wold et al. 2014), and minimal to no staining in the brainstem and cerebellum (Garman et al. 2011). Consistent with these previous findings, overall BBB breakdown observed in the current study was widespread and diffuse, but generally strongest in the cerebral cortex under microscopic evaluation (Figure 5.7). Others have reported non-region specific focal lesions, determined by IgG staining, that were present throughout the brain and grew larger in size and number after exposure to increasingly more severe primary blast injuries (Yeoh et al. 2013). That particular primary blast study exposed animals to overpressures comparable to or greater than our study, but with much shorter durations on the order of microseconds (Yeoh et al. 2013). Although our findings share general observations of BBB breakdown with previous bTBI studies, there is little current evidence to suggest that specific anatomical brain regions are preferentially susceptible to BBB damage after blast injury.

BBB opening lasting up to 24 hours after blast exposure, as supported by our results, has been associated with neurovascular inflammation, widespread microglial activation, and neuronal degeneration (Readnower et al. 2010, Garman et al. 2011, Abdul-Muneer et al. 2013). These pathological biochemical and cellular processes may cause long-lasting detrimental effects despite apparent BBB recovery occurring as quickly as 1 day after blast. For instance, microglial activation in the hippocampus and substantia nigra have been detected 5-10 days after blast exposure (Readnower et al. 2010) and in the superficial layers of the cerebral and cerebellar cortex for up to 14 days after blast injury in rats (Kaur et al. 1995). Others have hypothesized that free radicals, hydrogen peroxide, and peroxynitrite released from activated microglia contribute to subsequent oxidative damage and neurodegeneration (Readnower et al. 2010). BBB breakdown after traumatic insult has been reported to result in the influx of serum factors

such as albumin, fibrinogen, and thrombin, which together may contribute to microglial activation, oxidative stress, and the release of proinflammatory mediators in the brain (Chodobski et al. 2011, Algattas and Huang 2014, Lozano et al. 2015). Our results of BBB opening hold implications for similar pathological extravasation of blood-borne components that might occur after blast. Ultimately, oxidative injury and neuroinflammation related to blast-induced BBB disruption may be key contributors to prolonged neurological deficits after bTBI. Future work is warranted to determine if BBB opening after blast exposure is a critical initiator to these secondary injury mechanisms, or only worsens ongoing pathological processes.

Although we focused on characterizing the duration and pore-size of BBB opening, future studies will investigate associated secondary injury mechanisms and if the potential infiltration of serum components contributes to longer-term blast-related sequelae. Abdul-Muneer et al. (2013) reported that acute mechanical insult due to shock wave exposure triggered oxidative and nitrosative stress responses involving activation of NADPH oxidase 1 (NOX-1) and inducible nitric oxide synthase (iNOS), matrix metalloproteinases (MMP-2, -3, -9), and water channel aquaporin-4 (AQP4), ultimately exacerbating BBB damage, edema, and neuroinflammation (Abdul-Muneer et al. 2013). These pathological signaling mechanisms may contribute to cognitive and behavioral deficits after blast injury (Chen and Huang 2011, Vandevord et al. 2012, Chen et al. 2013, Logsdon et al. 2014). Despite the fact that BBB breakdown is a transient phenomenon that is repaired within days, barrier compromise may be linked to a number of alternative signaling pathways that can result in long-term pathological effects (Readnower et al. 2010, Hue et al. 2013, Hue et al. 2014, Logsdon et al. 2014). Lucke-Wold et al. (2014) have suggested that blast-induced alterations in the activity of different isozymes of PKC, including PKCα, PKCδ, and PKCε, directly influence cerebrovascular

function (Lucke-Wold et al. 2014). PKCα may regulate localization and function of tight junction proteins ZO-1 and occludin, PKCδ may affect vascular tone, and PKCε may confer neuroprotection after traumatic insult (Lucke-Wold et al. 2014). Blast-induced BBB damage has also been associated with accumulation of intracellular Ca^{2+} due to cellular membrane compromise, triggering endoplasmic reticulum stress, the unfolded protein response, and apoptosis (Arun et al. 2013, Logsdon et al. 2014). Taken together, neuroinflammation, the endoplasmic reticulum stress response, and PKC activity are all important secondary injury mechanisms after blast exposure that may be influenced by concomitant BBB dysfunction (Readnower et al. 2010, Abdul-Muneer et al. 2013, Logsdon et al. 2014, Lucke-Wold et al. 2014).

Some have posited that exposure of the body to blast generates a volumetric blood surge that traverses to the lower-pressure cranial cavity, causing damage to cerebral blood vessels and the BBB (Chen and Huang 2011, Chen et al. 2013, Chen et al. 2013). Our detection of significant BBB breakdown after injury, even after shielding the torso from blast overpressure, strongly supports that the loss of BBB integrity can occur independently of a potential blood-surge originating from the ventral body cavity, in agreement with other studies that protect the torso (Cernak et al. 2011, de Lanerolle et al. 2011, Magnuson et al. 2012, Skotak et al. 2013, Yeoh et al. 2013).

In conclusion, we have determined the time course and pore-size of BBB opening after blast-loading conditions tested in the current study by measuring extravasation of tracers with distinct molecular masses (376 Da – 500 kDa). BBB opening in the acute period after blast injury permitted significant extravasation of molecules less than approximately 70 kDa, followed by recovery of BBB integrity by 1 day post-injury. This study supports the hypothesis that

transient opening of the BBB may permit serum components to infiltrate the brain parenchyma, initiating secondary pathological cascades that can persist long after recovery of the BBB, suggesting that BBB repair may be a therapeutic strategy to pursue in future studies.

6 Summary and discussion

6.1 BBB dysfunction after primary blast exposure *in vitro*

In Chapter 2, we demonstrated that primary blast injury was capable of disrupting the integrity of an *in vitro* model of the BBB (Hue et al. 2013). To test our hypothesis that a potential injury mechanism of bTBI is mediated by damage to the BBB, we subjected an endothelial monolayer representing the BBB to controlled blast-loading conditions at operationally-relevant exposure levels and confirmed barrier disruption by multiple measures. TEER decreased in a dose-dependent manner in the acute post-injury phase, which was most strongly correlated with impulse, rather than the peak overpressure or duration of the blast. Acute alterations in barrier function were further confirmed by increased hydraulic conductivity and solute permeability. Compromised ZO-1 immunostaining was quantified, identifying endothelial tight junctions as a structural basis for BBB breakdown. The TEER of blast-injured cultures recovered over days, showing intrinsic capacity of the BBB for self-repair.

The role of primary blast forces in the neuropathological consequences of bTBI is a complex phenomenon that is not yet fully understood. While previous reports of small animal blast injury models provide insight into the vulnerability of the BBB to blast exposure (Readnower et al. 2010, Garman et al. 2011, Abdul-Muneer et al. 2013, Skotak et al. 2013, Yeoh et al. 2013, Logsdon et al. 2014, Lucke-Wold et al. 2014), differences between the injury parameters used as well as the biomechanical complexity of *in vivo* models make it challenging to separate contributions of inertial loading from the primary blast pressure transient on the brain and BBB. Our study helped to address these shortcomings as our *in vitro* blast injury model provides the capability to isolate the effects of primary blast from secondary or tertiary

(acceleration-driven) phases of blast injury, ultimately leading to better understanding of the biomechanical determinants underlying the development of bTBI in animals and humans.

Our findings are important and exciting as they suggest a possible physical mechanism for the vascular and neuronal pathologies observed after blast exposure. To our knowledge, this study is the first to report impulse-based functional disruption of an *in vitro* BBB model exposed to primary blast injury above a critical threshold, quantify associated effects on BBB permeability and tight junction breakdown, and determine a time-course for spontaneous restoration of barrier integrity. Findings of blast-induced *in vitro* BBB dysfunction reported in this study were also consistent with our subsequent bTBI studies using the same *in vitro* BBB model (Chapters 3 and 4). These results may be important for the development of novel helmet designs and acute therapeutic strategies to mitigate the effects of blast on the BBB.

6.2 BBB disruption after repeated primary blast injury *in vitro*

After demonstrating that exposure to a single blast injury disrupted the integrity of a monolayer of endothelial cells (Chapter 2), we performed a subsequent study to determine if those effects were cumulative (Chapter 3). Repeated primary blast injury caused persistent damage, but not additive disruption, in an *in vitro* BBB model, as described in Chapter 3. We report that two consecutive blasts administered within 24 hours delayed spontaneous recovery of BBB function compared to single blast exposure. With a prolonged inter-injury interval of 72 hours, the effects of multiple injuries on the BBB were found to be independent given sufficient recovery time between injuries. We believe our findings are scientifically important as they suggest a possible physical mechanism for the cerebrovascular pathologies observed after multiple blast exposures. Our study is the first to report sustained damage and delayed recovery

following repeated, pure primary blast injury in an *in vitro* BBB model. Defining the window of vulnerability for damage to the cerebral microvasculature holds important implications for mandatory rest periods to protect service members exposed to an initial blast.

To test our hypothesis that exposure to two consecutive blast injuries would result in exacerbated damage to the BBB, we subjected a brain endothelial monolayer to repeated blast-loading at operationally-relevant exposure levels, and confirmed barrier disruption by multiple measures. However, contrary to our hypothesis, repeated mild or moderate primary blast delivered within 24 or 72 hours compared to a single exposure of the same intensity reduced trans-endothelial electrical resistance (TEER) across a brain endothelial monolayer to the same degree, i.e. there were no additive effects. Permeability of the barrier to different-sized solutes remained unaltered after single and repeated blast, supporting that the effects of repeated blast on BBB integrity were not additive. Single blast exposure significantly reduced immunostaining of ZO-1 and claudin-5 tight junction proteins, consistent with results in Chapter 2, but subsequent exposure did not cause additional damage to tight junctions. Although repeated blast did not further reduce TEER, the second exposure delayed TEER recovery in BBB cultures. Similarly, recovery of hydraulic conductivity through the BBB was delayed by a second exposure. By extending the inter-injury interval to 72 hours, the effects of multiple injuries on the BBB were found to be independent given sufficient recovery time between consecutive exposures.

Augmented brain pathology is considered to be a consequence of repetitive brain injury (blast and non-blast), and our results extend this understanding to repeated blast exposure in an *in vitro* BBB model. It is important to note, however, that our results demonstrated sustained depression in TEER representing persistent injury to the BBB following multiple insults, as opposed to additive damage to the barrier. This outcome underscores and may help resolve

fundamental differences between primary blast injury and inertial- and impact-driven injuries reported in literature.

Effects of blast exposure in the single injury control group of this study (Chapter 3) were in overall agreement with results of the single blast exposure study described in Chapter 2. However, any discrepancies between results of the two studies are likely due to differences in the blast exposure levels tested. For example, TEER of the single injury group recovered 2 days after exposure to a 118 kPa*ms impulse blast (Chapter 3), as compared with TEER recovery 3 days after exposure to a more severe, 186 kPa*ms impulse blast (Chapter 2). In addition, the lack of significant changes in solute permeability or hydraulic conductivity in the single injury group of Chapter 3 was likely influenced by exposure to a lower 118 kPa*ms blast level as well as recovery of the endothelial monolayer at the time of measurement (i.e. 24 hours after exposure). Together, these studies support that BBB breakdown after blast is a transient phenomenon and that initial impairment and later recovery of barrier function may be dependent on the blast injury severity.

6.3 Potentiated BBB recovery with DEX treatment after primary blast

In Chapter 4, we reported that treatment with DEX after primary blast injury promoted faster recovery of an *in vitro* model of the BBB. We used our previously described primary blast injury model to precisely control the biomechanical initiators of injury and measure changes to BBB integrity by methods not possible *in vivo*. We report, for the first time, that treatment with DEX after blast exposure resulted in complete recovery of TEER and hydraulic conductivity 1 day after injury, compared with 3 days for vehicle-treated injured cultures. Administration of

RU486 (mifepristone) inhibited effects of DEX, confirming that accelerated barrier restoration was mediated by glucocorticoid receptor signaling.

We further demonstrated that DEX-induced BBB recovery was accompanied by increased ZO-1 tight junction immunostaining and expression, suggesting that heightened ZO-1 expression was a structural correlate to BBB recovery after blast. Interestingly, augmented ZO-1 protein expression was associated with specific upregulation of the ZO-1α^+ isoform but not ZO-1α^-. This is the first study to provide a mechanistic basis for potentiated recovery of an *in vitro* BBB model with glucocorticoid treatment after blast injury, and our findings hold important implications for development of a potential therapy for restoring BBB function after blast.

Damage to the *in vitro* BBB model due to blast exposure (Chapter 4) was overall consistent with the effects of single blast exposure originally reported in Chapter 2. In particular, TEER and hydraulic conductivity decreased by a similar magnitude in the acute period after exposure to a 186 kPa*ms blast in both studies. Similar changes to the morphology of ZO-1 tight junction protein and the area-percentage of ZO-1 immunostaining were observed in the acute period after blast injury in both studies. In addition, the TEER recovery time course of 3 days was consistent with vehicle-treated injured cultures (Chapter 4) and injured cultures exposed to the same blast exposure level (Chapter 2). These data support that primary blast-induced disruption of the *in vitro* BBB culture is a phenomenon that can be consistently reproduced by generating controlled biomechanical initiators of blast injury (peak overpressure, duration, impulse) using our bTBI model.

Recent reports suggest that factors influencing glucocorticoid effectiveness after traumatic insult, such as blast injury, are numerous and their interactions are complex

(Poungvarin 2004, Roberts et al. 2004, Chen et al. 2010, Campolo et al. 2013, Thal et al. 2013). We believe our findings add significant insight to the literature and hold important experimental and clinical implications for future development of glucocorticoid therapies and for potentially reducing mandatory rest periods for personnel exposed to blast injury.

6.4 Time course and pore-size of BBB opening *in vivo*

Although a number of *in vivo* studies have reported blast-induced BBB disruption by measuring the extravasation of EB or IgG, results from the same studies have also alluded to the inconsistent nature of BBB damage despite efforts to precisely control blast injury parameters (Readnower et al. 2010, Garman et al. 2011, Skotak et al. 2013). For example, one study of primary blast injury observed negligible BBB breakdown in approximately half of injured animals (Skotak et al. 2013). As a result, there has been limited quantitative understanding of the extent of BBB opening and the time course of damage after blast injury. In addition, many studies do not report kinematic parameters of head motion, making it difficult to separate the contributions of primary and tertiary blast-loading.

To help address this controversy, we determined the time course and pore-size of BBB opening after blast injury by measuring extravasation of tracers with distinct molecular masses (376 Da – 500 kDa), as described in Chapter 5. Using an *in vivo* bTBI model, our aim was to estimate the extent of BBB opening and the time course of damage by measuring extravasation of NaFl (376 Da), EB (69 kDa when bound to serum albumin), and dextrans (3 – 500 kDa). Exposure to blast resulted in significant extravasation of NaFl, 3 kDa dextran, and EB in the acute period after injury. However, there was no extravasation of 70 kDa or 500 kDa dextrans in the acute post-injury period, which was consistent with our initial study using our *in vitro* BBB

model (Chapter 2). There was also minimal to no extravasation of NaFl, dextrans, or EB 1 day after exposure in mice. BBB opening in the acute period after blast injury permitted significant extravasation of molecules less than approximately 70 kDa, followed by recovery of BBB integrity by 1 day post-injury. This *in vivo* study is the first to quantify the time course and size of BBB opening after bTBI, further supported by a characterization of kinematic parameters associated with blast-induced head motion. Our findings hold important implications for the duration and size of blood-borne constituents that may infiltrate the brain and initiate damaging secondary pathological cascades after bTBI.

It is surprising that the BBB fully recovered 1 day after injury *in vivo* (Chapter 5), as opposed to 2 – 3 days after injury in the *in vitro* BBB models described in Chapters 2, 3 and 4. However, one possible explanation is that differences in blast severity levels accounts for the differences in BBB recovery time between the *in vitro* and *in vivo* injury models. Mice were exposed to a shock wave with 272 kPa peak overpressure, 0.69 ms duration, and 65 kPa*ms impulse, as opposed to more severe blast levels tested in the *in vitro* single exposure study in Chapter 2 and DEX treatment investigation in Chapter 4 (571 kPa peak overpressure, 1.06 ms duration, and 186 kPa*ms impulse), and the *in vitro* repeated blast exposure study in Chapter 3 (402 kPa peak overpressure, 0.92 ms duration, and 118 kPa*ms impulse). Additionally, the BBB *in vivo* is a complex, multicellular structure that consists not only of brain endothelial cells (i.e. bEnd.3 cells) but also astrocytic end-feet, pericytes, extracellular matrix, and closely associated microglia and neuronal projections (Hawkins and Davis 2005, Shlosberg et al. 2010). It is unclear how blast-induced alterations in signaling activity and associations among these cell types may influence breakdown and subsequent repair mechanisms of the BBB *in vivo*.

6.5 Limitations

There are several limitations associated with our *in vitro* blast injury studies. As described in Chapter 2, there was appreciable loss of cells (12 %) from the Transwell cultures after exposure to the highest level of blast (276 kPa*ms impulse). Although the lower blast levels tested in our study are representative of real-world blast scenarios, the potential detachment of cells would prevent study of the effects of higher levels of primary blast on barrier function. Future studies may optimize the coating of Transwell membranes using components of the basement membrane such as collagen, laminin, or fibronectin in order to enhance endothelial cell attachment to the substrate (Leblond and Inoue 1989, Li et al. 2010). In Chapter 3, we extensively studied the effects of repeated blast at only one exposure level (118 kPa*ms). Although we did not test repeated exposure to a higher blast level, we anticipate that a more severe injury would decrease TEER by a magnitude that would potentially preclude our ability to measure the effect of a subsequent injury (i.e. "floor effect" due to lower operating limit of the measurement device). This limitation may potentially be overcome by culturing brain endothelial cells with factors known to increase baseline TEER (i.e. glucocorticoids or cyclic adenosine monophosphate) (Forster et al. 2006, Patabendige et al. 2013). In addition, the repeated blast injury study of Chapter 3 determined the effects of only 2 consecutive blasts on the BBB. Warfighters can be exposed to as many as 12 explosions per day (Wang et al. 2011), resulting in shorter intervals (< 24 hours) between exposures. Future work is warranted to assess whether the response of the BBB reported in Chapter 3 – delayed recovery but not additive disruption – would still hold true with an additional number of blasts at shorter inter-injury intervals.

Primary cerebromicrovascular endothelial cells more closely resemble the BBB phenotype *in vivo*, as opposed to a cell line (i.e. bEnd.3), due to their ability to form tight monolayers with higher TEER and lower permeability (Gumbleton and Audus 2001, Omidi et al. 2003, Li et al. 2010, Simon et al. 2010). However, their vulnerability to contamination by other neurovascular unit cells, lack of phenotypic stability over multiple passages *in vitro,* and inter- and intra-batch variability between cultures may ultimately reduce experimental sensitivity for identifying injury thresholds (Gumbleton and Audus 2001, Omidi et al. 2003). Given these considerations, we chose to use the bEnd.3 mouse brain microvascular cell line for our *in vitro* BBB studies because of its ability to retain phenotypic stability, preserve physiologic cell architecture, and form a functional paracellular barrier (Gumbleton and Audus 2001, Omidi et al. 2003, Brown et al. 2007, Simon et al. 2010).

Among the *in vitro* studies presented in this thesis, results were generated using an isolated cerebrovascular component, brain endothelial cells, to represent the BBB. *In vivo,* the BBB is a heterogeneous structure consisting of brain capillary endothelial cells, which together with astrocytes, pericytes, microglia, neurons, and the extracellular matrix, make up the entire neurovascular unit (Gumbleton and Audus 2001, Shlosberg et al. 2010). Following mechanical insult (i.e. TBI) to the neurovascular unit, the normal physiological interactions among the various cellular components of this structure are significantly impaired. Such changes can lead to abnormal expression of tight junction proteins, a neuroinflammatory response mediated by astrocytes and microglia, and neuronal dysfunction, among others (Shlosberg et al. 2010). Consistent with this, exposure to primary blast injury in rats resulted in a neuroinflammatory response that encompassed induction of free radical-generating enzymes, oxidative damage, a reduction in tight junction proteins, BBB leakage, upregulation of perivascular matrix

metalloproteinases, and an increase in fluid channel aquaporin-4 expression in astrocytes (Abdul-Muneer et al. 2013). The need to better understand the influence of other cell types of the neurovascular unit on BBB dysfunction after blast injury motivates further study *in vivo*.

Treatment with glucocorticoids was standard clinical practice for patients with head injuries and cerebral edema for over 30 years (Roberts et al. 2004). However, the use of this class of drugs in the clinic remains controversial. Glucocorticoid therapy failed to demonstrate substantial benefit in reducing post-injury sequelae in head-injured patients, stroke patients, and in some animal models of TBI (Poungvarin 2004, Roberts et al. 2004, Chen et al. 2010). Results of the multicenter corticosteroid randomization after significant head injury (CRASH) trial reported that 48 hour infusion of methylprednisolone within 8 hours of head injury increased the risk of mortality in enrolled patients (Roberts et al. 2004). Despite the unpromising results of treatment with methylprednisolone, the exact cause and mechanism of increased mortality associated with the glucocorticoid remain unclear, as multiple complicating factors related to trauma were present (Roberts et al. 2004). Furthermore, unlike head injuries sustained by patients of the CRASH trial, the study described in Chapter 4 investigated effects of DEX treatment in the context of blast-induced TBI, which is a fundamentally different biomechanical injury mechanism that warrants further study of the potential therapeutic benefit of glucocorticoids like DEX.

There are limitations associated with our *in vivo* blast injury model. Although our *in vitro* bTBI experimental setup with sample receiver enables isolation of the effects of primary blast (shock wave) from tertiary blast (inertial loading), our *in vivo* bTBI configuration can reduce blast-induced head motion but not completely eliminate it. As stated in Chapter 5, high-speed video analysis confirmed that head accelerations remained appreciable despite careful

efforts to restrain the head to minimize overall motion. We believe this issue highlights a fundamental challenge in interpreting results from the majority of *in vivo* bTBI studies in the literature, many of which allowed free acceleration and deceleration of the head or implemented restraints to minimize – but not completely eliminate – head motion induced by blast exposure (Readnower et al. 2010, Garman et al. 2011, Logsdon et al. 2014, Lucke-Wold et al. 2014). Nevertheless, a very limited number of studies claim to be able to isolate the effects of primary blast from tertiary loading (verified by high-speed video), and assert that direct interaction with blast overpressure alone is sufficient to cause damage to the BBB *in vivo* (Abdul-Muneer et al. 2013, Skotak et al. 2013, Yeoh et al. 2013). We believe that redesign of our custom mouse holder will help to more effectively immobilize the head, and along with it, better exclude confounding effects of tertiary blast. For instance, future studies may incorporate additional use of Sorbothane to enhance shock absorption and vibration dampening and provide enhanced rigid support for the mouse head and neck to further reduce motion caused by blast exposure.

6.6 Future Directions

Although we reported that exposure to blast caused BBB disruption followed by spontaneous recovery *in vitro* and *in vivo*, future studies may help to achieve greater confidence in the similarities of the two models by exposing them to the same severity of blast exposure. As mentioned above in the Summary and in Chapters 2 and 4, exposure to blast with a 186 kPa*ms impulse resulted in acute disruption of the *in vitro* BBB cultures with recovery 3 days after injury (Hue et al. 2013, Hue et al. 2015). However, exposure to blast with a 65 kPa*ms impulse resulted in acute disruption of the BBB *in vivo*, followed by recovery 1 day after injury. We hypothesize that exposing mice to the higher 186 kPa*ms impulse blast would also result in recovery of the BBB 3 days after injury. Although the 65 kPa*ms impulse blast we previously

tested in mice (Chapter 5) was close to the threshold for lethality using the current experimental configuration, we may be able to improve design of the mouse holder to ensure animal survival at higher exposure levels. As mentioned in the Limitations section, future studies may implement enhanced support for the mouse head and neck to further minimize motion (i.e. to exclude inertial injury) and isolate the effects of primary blast injury. Together, these changes would enable more direct comparisons between primary blast-induced BBB opening in brain endothelial cultures and in mice, helping to resolve any potential disparities between *in vitro* and *in vivo* results and ultimately contribute to a more accurate understanding of the complex phenomenon of BBB dysfunction after bTBI.

A number of epidemiological and experimental studies have suggested that repeated exposure to mild blast overpressure may potentially increase the burden of neurobehavioral, cognitive, and inflammatory outcomes, but together have not conclusively demonstrated exacerbated damage to the brain or BBB following repeated blast exposure (Trudeau et al. 1998, Elder and Cristian 2009, Saljo et al. 2009, Rosenfeld and Ford 2010, Blennow et al. 2011, Saljo et al. 2011, Wang et al. 2011, Ahlers et al. 2012, Elder et al. 2012, Kamnaksh et al. 2012, Kane et al. 2012, Abdul-Muneer et al. 2013). Experimental results described in Chapter 3 demonstrated that repeated primary blast exposure resulted in delayed recovery, but not additive disruption, in an *in vitro* BBB model (Hue et al. 2014). Future *in vivo* studies may expose animals to two blasts with a 24 hour inter-injury interval, each with a 402 kPa peak overpressure, 0.92 ms duration, and 118 kPa*ms impulse, matching exposure conditions tested in our *in vitro* study. We hypothesize that repeated exposure to blast in mice will also result in delayed recovery of the BBB. Along with implementation of the proposed design changes to the mouse holder (mentioned above) to improve animal survival at higher exposure levels, these future

studies would shed valuable insight on the biophysical mechanisms and pathological consequences of multiple blast exposures.

In Chapter 4 we determined that treatment with DEX potentiated recovery of *in vitro* BBB cultures after primary blast; however, further research is necessary to ensure the safety and efficacy of treatment *in vivo.* Previous studies have shown that DEX treatment *in vivo* can be neuroprotective after TBI, especially when administered as part of a combination therapy with other supplements (Campolo et al. 2013, Thal et al. 2013). The use of DEX as part of a combination therapy may help to enhance neuroprotection and minimize unwanted side effects by lowering the required dosage and duration of treatment (Campolo et al. 2013). Generally, the toxicity of glucocorticoids is dependent on the dosage and treatment duration, with higher dosages and longer therapies associated with greater toxicity (Walsh and Avashia 1992). After controlled cortical impact (CCI) in mice, combination treatment with melatonin (10 mg/kg) and DEX (0.025 mg/kg) 1 and 6 hours after injury reduced edema, brain lesion size, apoptosis levels, and oxidative stress (Campolo et al. 2013). Treatment with DEX alone also significantly attenuated infarct size, mitigated motor deficits, and prevented expression of apoptosis proteins (Campolo et al. 2013). Combined treatment with DEX (10 mg/kg) and bortezomib (0.2 mg/kg; a proteasome inhibitor) 30 minutes post-injury prevented proteasomal degradation of the glucocorticoid receptor after TBI, which enhanced the therapeutic benefit of DEX on BBB recovery (Thal et al. 2013). Future *in vivo* work will examine the therapeutic benefit of DEX treatment on BBB recovery using our murine model of blast TBI, possibly in combination with the complementary compounds mentioned above. In addition, we can examine the potent anti-inflammatory and immunosuppressant effects of glucocorticoids, which may contribute to mitigating other pathological effects of blast injury on the brain and BBB. The potential new

insights and mechanistic understanding attained through future *in vivo* studies may stimulate renewed clinical interest in the development of glucocorticoid therapies for TBI and disorders of the CNS.

Also described in Chapter 4, we chose a DEX treatment regimen of 30 minutes post-injury and once per day thereafter primarily to demonstrate potentiated BBB functional recovery with a post-injury administration of DEX. The specific timing of the post-injury treatment was influenced by published *in vivo* studies reporting therapeutic effects with treatment at 30 minutes or 1 hour post-injury (Campolo et al. 2013, Thal et al. 2013). The decision to treat the endothelial cultures once a day after blast injury was informed by other experimental studies suggesting robust effects of DEX with continuous treatment lasting as long as several weeks or months, without adverse effects on culture health (Underwood et al. 1999, Alvarado et al. 2004, Forster et al. 2005). However, because DEX is described as a long-acting glucocorticoid with biological half-life of 36-54 hours and potency greater than other glucocorticoids (Walsh and Avashia 1992), it may be possible that a reduction in the DEX treatment regimen (concentration and duration) would yield similar effects on BBB recovery. Future studies will investigate a therapeutic time window for glucocorticoid delivery to help optimize dosing strategy to rapidly restore BBB integrity while also reducing treatment duration.

The extent and duration of blast-induced BBB opening in mice described in Chapter 5 may be linked to a number of signaling pathways that can result in long-term pathological consequences (Readnower et al. 2010, Hue et al. 2013, Hue et al. 2014, Logsdon et al. 2014), despite the fact that BBB breakdown is a transient phenomenon that is repaired within days. For example, Abdul-Muneer et al. (2013) reported that shock wave exposure was closely linked with oxidative and nitrosative stress responses involving activation of NOX-1, iNOS, MMP-2, -3, and

-9, and AQP4, ultimately exacerbating BBB damage, edema, and neuroinflammation (Abdul-Muneer et al. 2013). Such pathological activity may further contribute to cognitive and behavioral deficits after blast injury (Chen and Huang 2011, Vandevord et al. 2012, Chen et al. 2013, Logsdon et al. 2014). Lucke-Wold et al. (2014) suggested that blast-induced alterations in the activity of different isozymes of PKC, including PKCα, PKCδ, and PKCε, may directly influence cerebrovascular function (Lucke-Wold et al. 2014). BBB compromise after blast has also been associated with accumulation of intracellular Ca^{2+}, triggering endoplasmic reticulum stress, the unfolded protein response, and apoptosis (Arun et al. 2013, Logsdon et al. 2014). However, none of these studies have identified a causative (as opposed to correlational) link between blast-induced BBB dysfunction and neuroinflammation, the endoplasmic reticulum stress response, or PKC activity (Readnower et al. 2010, Abdul-Muneer et al. 2013, Logsdon et al. 2014, Lucke-Wold et al. 2014). To this end, future studies are needed to investigate if BBB opening after blast is a critical initiator of any of these secondary cascades, or if BBB damage only worsens ongoing pathological processes that contribute to longer-term blast-related sequelae.

7 References

Abbott, N. J. and Friedman, A. (2012). "Overview and introduction: the blood-brain barrier in health and disease." Epilepsia **53 Suppl 6**: 1-6.

Abbott, N. J., Patabendige, A. A., Dolman, D. E., Yusof, S. R. and Begley, D. J. (2010). "Structure and function of the blood-brain barrier." Neurobiol Dis **37**(1): 13-25.

Abbott, N. J., Rönnbäck, L. and Hansson, E. (2006). "Astrocyte–endothelial interactions at the blood–brain barrier." Nat Rev Neurosci **7**(1): 41-53.

Abdul-Muneer, P. M., Schuetz, H., Wang, F., Skotak, M., Jones, J., Gorantla, S., Zimmerman, M. C., Chandra, N. and Haorah, J. (2013). "Induction of oxidative and nitrosative damage leads to cerebrovascular inflammation in an animal model of mild traumatic brain injury induced by primary blast." Free Radic Biol Med **60**: 282-291.

Adams, J. H., Graham, D. I. and Gennarelli, T. A. (1981). "Acceleration induced head injury in the monkey. II. Neuropathology." Acta Neuropathol Suppl **7**: 26-28.

Ahlers, S. T., Vasserman-Stokes, E., Shaughness, M. C., Hall, A. A., Shear, D. A., Chavko, M., McCarron, R. M. and Stone, J. R. (2012). "Assessment of the effects of acute and repeated exposure to blast overpressure in rodents: toward a greater understanding of blast and the potential ramifications for injury in humans exposed to blast." Front Neurol **3**: 32.

Algattas, H. and Huang, J. H. (2014). "Traumatic Brain Injury pathophysiology and treatments: early, intermediate, and late phases post-injury." Int J Mol Sci **15**(1): 309-341.

Alvarado, J. A., Betanzos, A., Franse-Carman, L., Chen, J. and Gonzalez-Mariscal, L. (2004). "Endothelia of Schlemm's canal and trabecular meshwork: distinct molecular, functional, and anatomic features." Am J Physiol Cell Physiol **286**(3): C621-634.

Alvarez, J. I., Dodelet-Devillers, A., Kebir, H., Ifergan, I., Fabre, P. J., Terouz, S., Sabbagh, M., Wosik, K., Bourbonniere, L., Bernard, M., van Horssen, J., de Vries, H. E., Charron, F. and Prat, A. (2011). "The Hedgehog pathway promotes blood-brain barrier integrity and CNS immune quiescence." Science **334**(6063): 1727-1731.

Armonda, R. A., Bell, R. S., Vo, A. H., Ling, G., DeGraba, T. J., Crandall, B., Ecklund, J. and Campbell, W. W. (2006). "Wartime Traumatic Cerebral Vasospasm." Neurosurgery **59**(6): 1215-1225.

Arun, P., Abu-Taleb, R., Oguntayo, S., Tanaka, M., Wang, Y., Valiyaveettil, M., Long, J. B., Zhang, Y. and Nambiar, M. P. (2013). "Distinct patterns of expression of traumatic brain injury biomarkers after blast exposure: role of compromised cell membrane integrity." Neurosci Lett **552**: 87-91.

Bain, A. C. and Meaney, D. F. (2000). "Tissue-level thresholds for axonal damage in an experimental model of central nervous system white matter injury." J Biomech Eng **122**(6): 615-622.

Balda, M. S. and Anderson, J. M. (1993). "Two classes of tight junctions are revealed by ZO-1 isoforms." Am J Physiol **264**(4 Pt 1): C918-924.

Barzo, P., Marmarou, A., Fatouros, P., Corwin, F. and Dunbar, J. (1996). "Magnetic resonance imaging-monitored acute blood-brain barrier changes in experimental traumatic brain injury." J Neurosurg **85**(6): 1113-1121.

Bass, C. R., Panzer, M. B., Rafaels, K. A., Wood, G., Shridharani, J. and Capehart, B. (2011). "Brain Injuries from Blast." Ann Biomed Eng **40**(1): 185-202.

Bass, C. R., Rafaels, K. A. and Salzar, R. S. (2008). "Pulmonary injury risk assessment for short-duration blasts." J Trauma **65**(3): 604-615.

Bauman, R. A., Ling, G., Tong, L., Januszkiewicz, A., Agoston, D., Delanerolle, N., Kim, Y., Ritzel, D., Bell, R., Ecklund, J., Armonda, R., Bandak, F. and Parks, S. (2009). "An introductory characterization of a combat-casualty-care relevant swine model of closed head injury resulting from exposure to explosive blast." J Neurotrauma **26**(6): 841-860.

Beaumont, A., Marmarou, A., Hayasaki, K., Barzo, P., Fatouros, P., Corwin, F., Marmarou, C. and Dunbar, J. (2000). "The permissive nature of blood brain barrier (BBB) opening in edema formation following traumatic brain injury." Acta Neurochir Suppl **76**: 125-129.

Belanger, H. G., Vanderploeg, R. D., Curtiss, G. and Warden, D. L. (2007). "Recent neuroimaging techniques in mild traumatic brain injury." J Neuropsychiatry Clin Neurosci **19**(1): 5-20.

Bershad, E., Humphreis, W. and Suarez, J. (2008). "Intracranial Hypertension." Semin Neurol **28**(05): 690-702.

Blecharz, K. G., Haghikia, A., Stasiolek, M., Kruse, N., Drenckhahn, D., Gold, R., Roewer, N., Chan, A. and Forster, C. Y. (2010). "Glucocorticoid effects on endothelial barrier function in the murine brain endothelial cell line cEND incubated with sera from patients with multiple sclerosis." Mult Scler **16**(3): 293-302.

Blennow, K., Jonsson, M., Andreasen, N., Rosengren, L., Wallin, A., Hellstrom, P. A. and Zetterberg, H. (2011). "No neurochemical evidence of brain injury after blast overpressure by repeated explosions or firing heavy weapons." Acta Neurol Scand **123**(4): 245-251.

Blyth, B. J., Farahvar, A., He, H., Nayak, A., Yang, C., Shaw, G. and Bazarian, J. J. (2011). "Elevated Serum Ubiquitin Carboxy-Terminal Hydrolase L1 Is Associated with Abnormal Blood–Brain Barrier Function after Traumatic Brain Injury." J Neurotrauma **28**(12): 2453-2462.

Booth, R. and Kim, H. (2012). "Characterization of a microfluidic in vitro model of the blood-brain barrier (muBBB)." Lab Chip **12**(10): 1784-1792.

Brenner, L. A., Vanderploeg, R. D. and Terrio, H. (2009). "Assessment and diagnosis of mild traumatic brain injury, posttraumatic stress disorder, and other polytrauma conditions: burden of adversity hypothesis." Rehabil Psychol **54**(3): 239-246.

Brethauer, S. A., Chao, A., Chambers, L. W., Green, D. J., Brown, C., Rhee, P. and Bohman, H. R. (2008). "Invasion vs insurgency - US Navy/Marine Corps forward surgical care during Operation Iraqi Freedom." Archives of Surgery **143**(6): 564-569.

Brown, R. C., Morris, A. P. and O'Neil, R. G. (2007). "Tight junction protein expression and barrier properties of immortalized mouse brain microvessel endothelial cells." Brain Res **1130**: 17-30.

Campolo, M., Ahmad, A., Crupi, R., Impellizzeri, D., Morabito, R., Esposito, E. and Cuzzocrea, S. (2013). "Combination therapy with melatonin and dexamethasone in a mouse model of traumatic brain injury." J Endocrinol **217**(3): 291-301.

Cantu, R. C. and Gean, A. D. (2010). "Second-impact syndrome and a small subdural hematoma: an uncommon catastrophic result of repetitive head injury with a characteristic imaging appearance." J Neurotrauma **27**(9): 1557-1564.

Cernak, I., Merkle, A. C., Koliatsos, V. E., Bilik, J. M., Luong, Q. T., Mahota, T. M., Xu, L., Slack, N., Windle, D. and Ahmed, F. A. (2011). "The pathobiology of blast injuries and blast-induced neurotrauma as identified using a new experimental model of injury in mice." Neurobiol Dis **41**(2): 538-551.

Cernak, I. and Noble-Haeusslein, L. J. (2010). "Traumatic brain injury: an overview of pathobiology with emphasis on military populations." J Cereb Blood Flow Metab **30**(2): 255-266.

Chafi, M. S., Karami, G. and Ziejewski, M. (2010). "Biomechanical assessment of brain dynamic responses due to blast pressure waves." Ann Biomed Eng **38**(2): 490-504.

Chavko, M., Prusaczyk, W. K. and McCarron, R. M. (2006). "Lung injury and recovery after exposure to blast overpressure." J Trauma **61**(4): 933-942.

Chen, H. and Konofagou, E. E. (2014). "The size of blood-brain barrier opening induced by focused ultrasound is dictated by the acoustic pressure." J Cereb Blood Flow Metab **34**(7): 1197-1204.

Chen, X., Lin, Y. P., Wang, D. and Zhang, J. N. (2010). "Dexamethasone exacerbates spatial acquisition deficits after traumatic brain injury in rats." Neurol Res **32**(10): 1097-1102.

Chen, Y. and Huang, W. (2011). "Non-impact, blast-induced mild TBI and PTSD: Concepts and caveats." Brain Inj **25**(7-8): 641-650.

Chen, Y. and Huang, W. (2011). "Non-impact, blast-induced mild TBI and PTSD: concepts and caveats." Brain injury **25**(7-8): 641-650.

Chen, Y., Huang, W. and Constantini, S. (2013). "Concepts and strategies for clinical management of blast-induced traumatic brain injury and posttraumatic stress disorder." The Journal of neuropsychiatry and clinical neurosciences **25**(2): 103-110.

Chen, Y., Huang, W. and Constantini, S. (2013). "The Differences between Blast-Induced and Sports-Related Brain Injuries." Frontiers in neurology **4**: 119.

Chen, Y. C., Smith, D. H. and Meaney, D. F. (2009). "In-vitro approaches for studying blast-induced traumatic brain injury." J Neurotrauma **26**(6): 861-876.

Chodobski, A., Zink, B. J. and Szmydynger-Chodobska, J. (2011). "Blood-brain barrier pathophysiology in traumatic brain injury." Transl Stroke Res **2**(4): 492-516.

Choi, J. J., Wang, S., Tung, Y. S., Morrison, B., 3rd and Konofagou, E. E. (2010). "Molecules of various pharmacologically-relevant sizes can cross the ultrasound-induced blood-brain barrier opening in vivo." Ultrasound Med Biol **36**(1): 58-67.

Ciraulo, D. L., Frykberg, E. R., Feliciano, D. V., Knuth, T. E., Richart, C. M., Westmoreland, C. D. and Williams, K. A. (2004). "A Survey Assessment of the Level of Preparedness for Domestic Terrorism and Mass Casualty Incidents among Eastern Association for the Surgery of Trauma Members." The Journal of Trauma: Injury, Infection, and Critical Care **56**(5): 1033-1041.

Coronado, V. G., Xu, L., Basavaraju, S. V., McGuire, L. C., Wald, M. M., Faul, M. D., Guzman, B. R., Hemphill, J. D., Centers for Disease, C. and Prevention (2011). "Surveillance for traumatic brain injury-related deaths--United States, 1997-2007." MMWR Surveill Summ **60**(5): 1-32.

Cucullo, L., Hallene, K., Dini, G., Dal Toso, R. and Janigro, D. (2004). "Glycerophosphoinositol and dexamethasone improve transendothelial electrical resistance in an in vitro study of the blood-brain barrier." Brain Res **997**(2): 147-151.

D.W., H. (2004). "ConWep 2.1.0.8 [Computer Software]." Vicksburg, MS: US Army Engineer Research and Development Center.

Davidsson, J. and Risling, M. (2011). "A new model to produce sagittal plane rotational induced diffuse axonal injuries." Front Neurol **2**: 41.

de Lanerolle, N. C., Bandak, F., Kang, D., Li, A. Y., Du, F., Swauger, P., Parks, S., Ling, G. and Kim, J. H. (2011). "Characteristics of an explosive blast-induced brain injury in an experimental model." J Neuropathol Exp Neurol **70**(11): 1046-1057.

Deli, M. A., Ábrahám, C. S., Kataoka, Y. and Niwa, M. (2005). "Permeability Studies on In Vitro Blood–Brain Barrier Models: Physiology, Pathology, and Pharmacology." Cell Mol Neurobiol **25**(1): 59-127.

Deli, M. A., Descamps, L., Dehouck, M. P., Cecchelli, R., Joo, F., Abraham, C. S. and Torpier, G. (1995). "Exposure of tumor necrosis factor-alpha to luminal membrane of bovine brain capillary endothelial cells cocultured with astrocytes induces a delayed increase of permeability and cytoplasmic stress fiber formation of actin." J Neurosci Res **41**(6): 717-726.

DePalma, R. G., Burris, D. G., Champion, H. R. and Hodgson, M. J. (2005). "Blast injuries." N Engl J Med **352**(13): 1335-1342.

Diringer, M. N. and Zazulia, A. R. (2004). "Osmotic therapy: fact and fiction." Neurocrit Care **1**(2): 219-233.

Effgen, G. B., Hue, C. D., Vogel, E., Panzer, M. B., Meaney, D. F., Bass, C. R. and Morrison, B. (2012). "A Multiscale Approach to Blast Neurotrauma Modeling: Part II: Methodology for Inducing Blast Injury to in vitro Models." Front Neurol **3**.

Eigenmann, D. E., Xue, G., Kim, K. S., Moses, A. V., Hamburger, M. and Oufir, M. (2013). "Comparative study of four immortalized human brain capillary endothelial cell lines, hCMEC/D3, hBMEC, TY10, and BB19, and optimization of culture conditions, for an in vitro blood-brain barrier model for drug permeability studies." Fluids Barriers CNS **10**(1): 33.

Elder, G. A. and Cristian, A. (2009). "Blast-related mild traumatic brain injury: mechanisms of injury and impact on clinical care." Mt Sinai J Med **76**(2): 111-118.

Elder, G. A., Dorr, N. P., De Gasperi, R., Gama Sosa, M. A., Shaughness, M. C., Maudlin-Jeronimo, E., Hall, A. A., McCarron, R. M. and Ahlers, S. T. (2012). "Blast exposure induces post-traumatic stress disorder-related traits in a rat model of mild traumatic brain injury." J Neurotrauma **29**(16): 2564-2575.

Elder, G. A., Gama Sosa, M. A., De Gasperi, R., Stone, J. R., Dickstein, D. L., Haghighi, F., Hof, P. R. and Ahlers, S. T. (2015). "Vascular and inflammatory factors in the pathophysiology of blast-induced brain injury." Front Neurol **6**: 48.

Elliott, M. B., Jallo, J. J., Gaughan, J. P. and Tuma, R. F. (2007). "Effects of Crystalloid-Colloid Solutions on Traumatic Brain Injury." J Neurotrauma **24**(1): 195-202.

Enters, E. K., Pascua, J. R., McDowell, K. P., Kapasi, M. Z., Povlishock, J. T. and Robinson, S. E. (1992). "Blockade of acute hypertensive response does not prevent changes in behavior or in CSF acetylcholine (ACH) content following traumatic brain injury (TBI)." Brain Res **576**(2): 271-276.

Fanning, A. S., Little, B. P., Rahner, C., Utepbergenov, D., Walther, Z. and Anderson, J. M. (2007). "The Unique-5 and -6 Motifs of ZO-1 Regulate Tight Junction Strand Localization and Scaffolding Properties." Mol Biol Cell **18**(3): 721-731.

Fenstermacher, J. (1984). "Volume regulation of the central nervous system." Edema: 383-404.

Fijalkowski, R. J., Stemper, B. D., Pintar, F. A., Yoganandan, N., Crowe, M. J. and Gennarelli, T. A. (2007). "New rat model for diffuse brain injury using coronal plane angular acceleration." J Neurotrauma **24**(8): 1387-1398.

Forster, C., Burek, M., Romero, I. A., Weksler, B., Couraud, P. O. and Drenckhahn, D. (2008). "Differential effects of hydrocortisone and TNFalpha on tight junction proteins in an in vitro model of the human blood-brain barrier." J Physiol **586**(7): 1937-1949.

Forster, C., Silwedel, C., Golenhofen, N., Burek, M., Kietz, S., Mankertz, J. and Drenckhahn, D. (2005). "Occludin as direct target for glucocorticoid-induced improvement of blood-brain barrier properties in a murine in vitro system." J Physiol **565**(Pt 2): 475-486.

Forster, C., Waschke, J., Burek, M., Leers, J. and Drenckhahn, D. (2006). "Glucocorticoid effects on mouse microvascular endothelial barrier permeability are brain specific." J Physiol **573**(Pt 2): 413-425.

Friess, S. H., Ichord, R. N., Ralston, J., Ryall, K., Helfaer, M. A., Smith, C. and Margulies, S. S. (2009). "Repeated traumatic brain injury affects composite cognitive function in piglets." J Neurotrauma **26**(7): 1111-1121.

Fujita, M., Wei, E. P. and Povlishock, J. T. (2012). "Intensity- and interval-specific repetitive traumatic brain injury can evoke both axonal and microvascular damage." J Neurotrauma **29**(12): 2172-2180.

Fukuda, K., Tanno, H., Okimura, Y., Nakamura, M. and Yamaura, A. (1995). "The blood-brain barrier disruption to circulating proteins in the early period after fluid percussion brain injury in rats." J Neurotrauma **12**(3): 315-324.

Gaillard, P. J., Voorwinden, L. H., Nielsen, J. L., Ivanov, A., Atsumi, R., Engman, H., Ringbom, C., de Boer, A. G. and Breimer, D. D. (2001). "Establishment and functional characterization of an in vitro model of the blood-brain barrier, comprising a co-culture of brain capillary endothelial cells and astrocytes." Eur J Pharm Sci **12**(3): 215-222.

Galarneau, M. R., Woodruff, S. I., Dye, J. L., Mohrle, C. R. and Wade, A. L. (2008). "Traumatic brain injury during operation Iraqi freedom: findings from the United States Navy-Marine Corps Combat Trauma Registry." Journal of Neurosurgery **108**(5): 950-957.

Gambihler, S. and Delius, M. (1992). "Transient increase in membrane permeability of L1210 cells upon exposure to lithotripter shock waves in vitro." Naturwissenschaften **79**(7): 328-329.

Garcia, A. N., Vogel, S. M., Komarova, Y. A. and Malik, A. B. (2011). "Permeability of Endothelial Barrier: Cell Culture and In Vivo Models." Methods Mol Biol **763**: 333-354.

Garman, R. H., Jenkins, L. W., Switzer, R. C., Bauman, R. A., Tong, L. C., Swauger, P. V., Parks, S. A., Ritzel, D. V., Dixon, C. E., Clark, R. S. B., Bayır, H., Kagan, V., Jackson, E. K. and Kochanek, P. M. (2011). "Blast Exposure in Rats with Body Shielding Is Characterized Primarily by Diffuse Axonal Injury." J Neurotrauma **28**(6): 947-959.

Gennarelli, T. A., Adams, J. H. and Graham, D. I. (1981). "Acceleration induced head injury in the monkey.I. The model, its mechanical and physiological correlates." Acta Neuropathol Suppl **7**: 23-25.

Gennarelli, T. A., Thibault, L. E., Adams, J. H., Graham, D. I., Thompson, C. J. and Marcincin, R. P. (1982). "Diffuse axonal injury and traumatic coma in the primate." Ann Neurol **12**(6): 564-574.

Glushakova, O. Y., Johnson, D. and Hayes, R. L. (2014). "Delayed increases in microvascular pathology after experimental traumatic brain injury are associated with prolonged inflammation, blood-brain barrier disruption, and progressive white matter damage." J Neurotrauma **31**(13): 1180-1193.

Goldstein, L. E., Fisher, A. M., Tagge, C. A., Zhang, X. L., Velisek, L., Sullivan, J. A., Upreti, C., Kracht, J. M., Ericsson, M., Wojnarowicz, M. W., Goletiani, C. J., Maglakelidze, G. M., Casey, N., Moncaster, J. A., Minaeva, O., Moir, R. D., Nowinski, C. J., Stern, R. A., Cantu, R. C., Geiling, J., Blusztajn, J. K., Wolozin, B. L., Ikezu, T., Stein, T. D., Budson, A. E., Kowall, N. W., Chargin, D., Sharon, A., Saman, S., Hall, G. F., Moss, W. C., Cleveland, R. O., Tanzi, R. E., Stanton, P. K. and McKee, A. C. (2012). "Chronic traumatic encephalopathy in blast-exposed military veterans and a blast neurotrauma mouse model." Sci Transl Med **4**(134): 134ra160.

Greish, K. (2007). "Enhanced permeability and retention of macromolecular drugs in solid tumors: a royal gate for targeted anticancer nanomedicines." J Drug Target **15**(7-8): 457-464.

Grossetete, M., Phelps, J., Arko, L., Yonas, H. and Rosenberg, G. A. (2009). "Elevation of Matrix Metalloproteinases 3 and 9 in Cerebrospinal Fluid and Blood in Patients with Severe Traumatic Brain Injury." Neurosurgery **65**(4): 702-708.

Gullotti, D. M., Beamer, M., Panzer, M. B., Chen, Y. C., Patel, T. P., Yu, A., Jaumard, N., Winkelstein, B., Bass, C. R., Morrison, B. and Meaney, D. F. (2014). "Significant head accelerations can influence immediate neurological impairments in a murine model of blast-induced traumatic brain injury." J Biomech Eng **136**(9): 091004.

Gumbleton, M. and Audus, K. L. (2001). "Progress and limitations in the use of in vitro cell cultures to serve as a permeability screen for the blood-brain barrier." J Pharm Sci **90**(11): 1681-1698.

Gutierrez, E., Huang, Y., Haglid, K., Bao, F., Hansson, H. A., Hamberger, A. and Viano, D. (2001). "A new model for diffuse brain injury by rotational acceleration: I model, gross appearance, and astrocytosis." J Neurotrauma **18**(3): 247-257.

Hamm, S., Dehouck, B., Kraus, J., Wolburg-Buchholz, K., Wolburg, H., Risau, W., Cecchelli, R., Engelhardt, B. and Dehouck, M. P. (2004). "Astrocyte mediated modulation of blood-brain barrier permeability does not correlate with a loss of tight junction proteins from the cellular contacts." Cell Tissue Res **315**(2): 157-166.

Hawkins, B. T. and Davis, T. P. (2005). "The blood-brain barrier/neurovascular unit in health and disease." Pharmacol Rev **57**(2): 173-185.

Hawkins, C. P., Munro, P. M., MacKenzie, F., Kesselring, J., Tofts, P. S., du Boulay, E. P., Landon, D. N. and McDonald, W. I. (1990). "Duration and selectivity of blood-brain barrier breakdown in chronic relapsing experimental allergic encephalomyelitis studied by gadolinium-DTPA and protein markers." Brain **113 (Pt 2)**: 365-378.

Hayashi, T., Kaneko, Y., Yu, S., Bae, E., Stahl, C. E., Kawase, T., van Loveren, H., Sanberg, P. R. and Borlongan, C. V. (2009). "Quantitative analyses of matrix metalloproteinase activity after traumatic brain injury in adult rats." Brain Res **1280**: 172-177.

Hicks, R. R., Fertig, S. J., Desrocher, R. E., Koroshetz, W. J. and Pancrazio, J. J. (2010). "Neurological Effects of Blast Injury." J Trauma **68**(5): 1257-1263.

Higashida, T., Kreipke, C. W., Rafols, J. A., Peng, C., Schafer, S., Schafer, P., Ding, J. Y., Dornbos, D., 3rd, Li, X., Guthikonda, M., Rossi, N. F. and Ding, Y. (2011). "The role of hypoxia-inducible factor-1alpha, aquaporin-4, and matrix metalloproteinase-9 in blood-brain barrier disruption and brain edema after traumatic brain injury." J Neurosurg **114**(1): 92-101.

Hoge, C. W., McGurk, D., Thomas, J. L., Cox, A. L., Engel, C. C. and Castro, C. A. (2008). "Mild traumatic brain injury in U.S. Soldiers returning from Iraq." N Engl J Med **358**(5): 453-463.

Huber, J. D., Egleton, R. D. and Davis, T. P. (2001). "Molecular physiology and pathophysiology of tight junctions in the blood-brain barrier." Trends Neurosci **24**(12): 719-725.

Hue, C. D., Cao, S., Dale Bass, C. R., Meaney, D. F. and Morrison, B., 3rd (2014). "Repeated primary blast injury causes delayed recovery, but not additive disruption, in an in vitro blood-brain barrier model." J Neurotrauma **31**(10): 951-960.

Hue, C. D., Cao, S., Haider, S. F., Vo, K. V., Effgen, G. B., Vogel, E., 3rd, Panzer, M. B., Bass, C. R., Meaney, D. F. and Morrison, B., 3rd (2013). "Blood-brain barrier dysfunction after primary blast injury in vitro." J Neurotrauma **30**(19): 1652-1663.

Hue, C. D., Cho, F. S., Cao, S., Dale Bass, C. R., Meaney, D. F. and Morrison Iii, B. (2015). "Dexamethasone potentiates in vitro blood-brain barrier recovery after primary blast injury by glucocorticoid receptor-mediated upregulation of ZO-1 tight junction protein." J Cereb Blood Flow Metab.

Kaal, E. C. and Vecht, C. J. (2004). "The management of brain edema in brain tumors." Curr Opin Oncol **16**(6): 593-600.

Kamnaksh, A., Kovesdi, E., Kwon, S. K., Wingo, D., Ahmed, F., Grunberg, N. E., Long, J. and Agoston, D. V. (2011). "Factors Affecting Blast Traumatic Brain Injury." J Neurotrauma **28**(10): 2145-2153.

Kamnaksh, A., Kwon, S. K., Kovesdi, E., Ahmed, F., Barry, E. S., Grunberg, N. E., Long, J. and Agoston, D. (2012). "Neurobehavioral, cellular, and molecular consequences of single and multiple mild blast exposure." Electrophoresis **33**(24): 3680-3692.

Kane, M. J., Angoa-Perez, M., Briggs, D. I., Viano, D. C., Kreipke, C. W. and Kuhn, D. M. (2012). "A mouse model of human repetitive mild traumatic brain injury." J Neurosci Methods **203**(1): 41-49.

Kaur, C., Singh, J., Lim, M. K., Ng, B. L., Yap, E. P. and Ling, E. A. (1995). "The response of neurons and microglia to blast injury in the rat brain." Neuropathol Appl Neurobiol **21**(5): 369-377.

Kimberly, R. P. (1991). "Mechanisms of action, dosage schedules, and side effects of steroid therapy." Curr Opin Rheumatol **3**(3): 373-379.

Kirchhoff, C., Stegmaier, J., Bogner, V., Buhmann, S., Mussack, T., Kreimeier, U., Mutschler, W. and Biberthaler, P. (2006). "Intrathecal and systemic concentration of NT-proBNP in patients with severe traumatic brain injury." J Neurotrauma **23**(6): 943-949.

Klatzo, I. (1987). "Pathophysiological aspects of brain edema." Acta Neuropathol **72**(3): 236-239.

Kniesel, U. and Wolburg, H. (2000). "Tight junctions of the blood-brain barrier." Cell Mol Neurobiol **20**(1): 57-76.

Kodama, T., Hamblin, M. R. and Doukas, A. G. (2000). "Cytoplasmic molecular delivery with shock waves: importance of impulse." Biophys J **79**(4): 1821-1832.

Korn, A., Golan, H., Melamed, I., Pascual-Marqui, R. and Friedman, A. (2005). "Focal cortical dysfunction and blood-brain barrier disruption in patients with Postconcussion syndrome." J Clin Neurophysiol **22**(1): 1-9.

Kuehn, R., Simard, P. F., Driscoll, I., Keledjian, K., Ivanova, S., Tosun, C., Williams, A., Bochicchio, G., Gerzanich, V. and Simard, J. M. (2011). "Rodent model of direct cranial blast injury." J Neurotrauma **28**(10): 2155-2169.

Lai, C.-H., Kuo, K.-H. and Leo, J. M. (2005). "Critical role of actin in modulating BBB permeability." Brain Res Rev **50**(1): 7-13.

Lamprecht, M. R. and Morrison, B., 3rd (2014). "GPR30 activation is neither necessary nor sufficient for acute neuroprotection by 17beta-estradiol after an ischemic injury in organotypic hippocampal slice cultures." Brain Res **1563**: 131-137.

Landis, D. M. (1994). "The early reactions of non-neuronal cells to brain injury." Annu Rev Neurosci **17**: 133-151.

Langlois, J. A., Kegler, S. R., Butler, J. A., Gotsch, K. E., Johnson, R. L., Reichard, A. A., Webb, K. W., Coronado, V. G., Selassie, A. W. and Thurman, D. J. (2003). "Traumatic

brain injury-related hospital discharges. Results from a 14-state surveillance system, 1997." MMWR Surveill Summ **52**(4): 1-20.

Langlois, J. A., Rutland-Brown, W. and Wald, M. M. (2006). "The epidemiology and impact of traumatic brain injury: a brief overview." J Head Trauma Rehabil **21**(5): 375-378.

Larsson, H. B., Stubgaard, M., Frederiksen, J. L., Jensen, M., Henriksen, O. and Paulson, O. B. (1990). "Quantitation of blood-brain barrier defect by magnetic resonance imaging and gadolinium-DTPA in patients with multiple sclerosis and brain tumors." Magn Reson Med **16**(1): 117-131.

Leblond, C. P. and Inoue, S. (1989). "Structure, composition, and assembly of basement membrane." Am J Anat **185**(4): 367-390.

Li, G., Simon, M. J., Cancel, L. M., Shi, Z.-D., Ji, X., Tarbell, J. M., Morrison, B. and Fu, B. M. (2010). "Permeability of Endothelial and Astrocyte Cocultures: In Vitro Blood–Brain Barrier Models for Drug Delivery Studies." Ann Biomed Eng **38**(8): 2499-2511.

Liebner, S., Corada, M., Bangsow, T., Babbage, J., Taddei, A., Czupalla, C. J., Reis, M., Felici, A., Wolburg, H., Fruttiger, M., Taketo, M. M., von Melchner, H., Plate, K. H., Gerhardt, H. and Dejana, E. (2008). "Wnt/beta-catenin signaling controls development of the blood-brain barrier." J Cell Biol **183**(3): 409-417.

Ling, G., Bandak, F., Armonda, R., Grant, G. and Ecklund, J. (2009). "Explosive blast neurotrauma." J Neurotrauma **26**(6): 815-825.

Liu, H. M. and Sturner, W. Q. (1988). "Extravasation of plasma proteins in brain trauma." Forensic Sci Int **38**(3-4): 285-295.

Loane, D. J. and Faden, A. I. (2010). "Neuroprotection for traumatic brain injury: translational challenges and emerging therapeutic strategies." Trends Pharmacol Sci **31**(12): 596-604.

Logsdon, A. F., Turner, R. C., Lucke-Wold, B. P., Robson, M. J., Naser, Z. J., Smith, K. E., Matsumoto, R. R., Huber, J. D. and Rosen, C. L. (2014). "Altering endoplasmic reticulum stress in a model of blast-induced traumatic brain injury controls cellular fate and ameliorates neuropsychiatric symptoms." Front Cell Neurosci **8**: 421.

Long, J. B., Bentley, T. L., Wessner, K. A., Cerone, C., Sweeney, S. and Bauman, R. A. (2009). "Blast overpressure in rats: recreating a battlefield injury in the laboratory." J Neurotrauma **26**(6): 827-840.

Longhi, L., Saatman, K. E., Fujimoto, S., Raghupathi, R., Meaney, D. F., Davis, J., McMillan, B. S. A., Conte, V., Laurer, H. L., Stein, S., Stocchetti, N. and McIntosh, T. K. (2005). "Temporal window of vulnerability to repetitive experimental concussive brain injury." Neurosurgery **56**(2): 364-374; discussion 364-374.

Lozano, D., Gonzales-Portillo, G. S., Acosta, S., de la Pena, I., Tajiri, N., Kaneko, Y. and Borlongan, C. V. (2015). "Neuroinflammatory responses to traumatic brain injury:

etiology, clinical consequences, and therapeutic opportunities." Neuropsychiatr Dis Treat **11**: 97-106.

Lucke-Wold, B. P., Logsdon, A. F., Smith, K. E., Turner, R. C., Alkon, D. L., Tan, Z., Naser, Z. J., Knotts, C. M., Huber, J. D. and Rosen, C. L. (2014). "Bryostatin-1 Restores Blood Brain Barrier Integrity following Blast-Induced Traumatic Brain Injury." Mol Neurobiol.

Mac Donald, C. L., Johnson, A. M., Cooper, D., Nelson, E. C., Werner, N. J., Shimony, J. S., Snyder, A. Z., Raichle, M. E., Witherow, J. R., Fang, R., Flaherty, S. F. and Brody, D. L. (2011). "Detection of blast-related traumatic brain injury in U.S. military personnel." N Engl J Med **364**(22): 2091-2100.

Madara, J. L. (1998). "Regulation of the movement of solutes across tight junctions." Annu Rev Physiol **60**: 143-159.

Magnuson, J., Leonessa, F. and Ling, G. S. (2012). "Neuropathology of explosive blast traumatic brain injury." Curr Neurol Neurosci Rep **12**(5): 570-579.

Masel, B. E. and DeWitt, D. S. (2010). "Traumatic brain injury: a disease process, not an event." J Neurotrauma **27**(8): 1529-1540.

Maxwell, W. L., Whitfield, P. C., Suzen, B., Graham, D. I., Adams, J. H., Watt, C. and Gennarelli, T. A. (1992). "The cerebrovascular response to experimental lateral head acceleration." Acta Neuropathol **84**(3): 289-296.

Miller, D. H., Thompson, A. J., Morrissey, S. P., MacManus, D. G., Moore, S. G., Kendall, B. E., Moseley, I. F. and McDonald, W. I. (1992). "High dose steroids in acute relapses of multiple sclerosis: MRI evidence for a possible mechanism of therapeutic effect." J Neurol Neurosurg Psychiatry **55**(6): 450-453.

Mizee, M. R., Wooldrik, D., Lakeman, K. A. M., van het Hof, B., Drexhage, J. A. R., Geerts, D., Bugiani, M., Aronica, E., Mebius, R. E., Prat, A., de Vries, H. E. and Reijerkerk, A. (2013). "Retinoic Acid Induces Blood-Brain Barrier Development." Journal of Neuroscience **33**(4): 1660-1671.

Morganti-Kossmann, M. C., Hans, V. H., Lenzlinger, P. M., Dubs, R., Ludwig, E., Trentz, O. and Kossmann, T. (1999). "TGF-beta is elevated in the CSF of patients with severe traumatic brain injuries and parallels blood-brain barrier function." J Neurotrauma **16**(7): 617-628.

Mori, T., Wang, X., Aoki, T. and Lo, E. H. (2002). "Downregulation of matrix metalloproteinase-9 and attenuation of edema via inhibition of ERK mitogen activated protein kinase in traumatic brain injury." J Neurotrauma **19**(11): 1411-1419.

Morrison, B., 3rd, Cater, H. L., Wang, C. C., Thomas, F. C., Hung, C. T., Ateshian, G. A. and Sundstrom, L. E. (2003). "A tissue level tolerance criterion for living brain developed with an in vitro model of traumatic mechanical loading." Stapp Car Crash J **47**: 93-105.

Morrison, B., 3rd, Elkin, B. S., Dolle, J. P. and Yarmush, M. L. (2011). "In vitro models of traumatic brain injury." Annu Rev Biomed Eng **13**: 91-126.

Naik, P. and Cucullo, L. (2012). "In vitro blood-brain barrier models: current and perspective technologies." J Pharm Sci **101**(4): 1337-1354.

Nakagawa, A., Manley, G. T., Gean, A. D., Ohtani, K., Armonda, R., Tsukamoto, A., Yamamoto, H., Takayama, K. and Tominaga, T. (2011). "Mechanisms of primary blast-induced traumatic brain injury: insights from shock-wave research." J Neurotrauma **28**(6): 1101-1119.

Nelson, T. J., Clark, T., Stedje-Larsen, E. T., Lewis, C. T., Grueskin, J. M., Echols, E. L., Wall, D. B., Felger, E. A. and Bohman, H. R. (2008). "Close proximity blast injury patterns from improvised explosive devices in Iraq: a report of 18 cases." J Trauma **65**(1): 212-217.

Ohno, K., Pettigrew, K. D. and Rapoport, S. I. (1978). "Lower limits of cerebrovascular permeability to nonelectrolytes in the conscious rat." Am J Physiol **235**(3): H299-307.

Olson, J. E., Banks, M., Dimlich, R. V. and Evers, J. (1997). "Blood-brain barrier water permeability and brain osmolyte content during edema development." Acad Emerg Med **4**(7): 662-673.

Omidi, Y., Campbell, L., Barar, J., Connell, D., Akhtar, S. and Gumbleton, M. (2003). "Evaluation of the immortalised mouse brain capillary endothelial cell line, b.End3, as an in vitro blood–brain barrier model for drug uptake and transport studies." Brain Res **990**(1-2): 95-112.

Owens, B. D., Kragh, J. F., Jr., Wenke, J. C., Macaitis, J., Wade, C. E. and Holcomb, J. B. (2008). "Combat wounds in operation Iraqi Freedom and operation Enduring Freedom." J Trauma **64**(2): 295-299.

Panzer, M. B., Bass, C. R., Rafaels, K. A., Shridharani, J. and Capehart, B. P. (2012). "Primary blast survival and injury risk assessment for repeated blast exposures." J Trauma Acute Care Surg **72**(2): 454-466.

Panzer, M. B., Matthews, K. A., Yu, A. W., Morrison, B., 3rd, Meaney, D. F. and Bass, C. R. (2012). "A Multiscale Approach to Blast Neurotrauma Modeling: Part I - Development of Novel Test Devices for in vivo and in vitro Blast Injury Models." Front Neurol **3**: 46.

Panzer, M. B., Myers, B. S., Capehart, B. P. and Bass, C. R. (2012). "Development of a finite element model for blast brain injury and the effects of CSF cavitation." Ann Biomed Eng **40**(7): 1530-1544.

Pardridge, W. M. (1999). "Blood-brain barrier biology and methodology." J Neurovirol **5**(6): 556-569.

Pardridge, W. M. (2007). "Blood-brain barrier delivery." Drug Discov Today **12**(1-2): 54-61.

Patabendige, A., Skinner, R. A., Morgan, L. and Abbott, N. J. (2013). "A detailed method for preparation of a functional and flexible blood-brain barrier model using porcine brain endothelial cells." Brain Res **1521**: 16-30.

Patel, T. P., Gullotti, D. M., Hernandez, P., O'Brien, W. T., Capehart, B. P., Morrison, B., 3rd, Bass, C., Eberwine, J. E., Abel, T. and Meaney, D. F. (2014). "An open-source toolbox for automated phenotyping of mice in behavioral tasks." Front Behav Neurosci **8**: 349.

Peskind, E. R., Petrie, E. C., Cross, D. J., Pagulayan, K., McCraw, K., Hoff, D., Hart, K., Yu, C. E., Raskind, M. A., Cook, D. G. and Minoshima, S. (2011). "Cerebrocerebellar hypometabolism associated with repetitive blast exposure mild traumatic brain injury in 12 Iraq war Veterans with persistent post-concussive symptoms." Neuroimage **54 Suppl 1**: S76-82.

Poungvarin, N. (2004). "Steroids have no role in stroke therapy." Stroke **35**(1): 229-230.

Prins, M. L., Alexander, D., Giza, C. C. and Hovda, D. A. (2013). "Repeated mild traumatic brain injury: mechanisms of cerebral vulnerability." J Neurotrauma **30**(1): 30-38.

Raghupathi, R. and Margulies, S. S. (2002). "Traumatic axonal injury after closed head injury in the neonatal pig." J Neurotrauma **19**(7): 843-853.

Readnower, R. D., Chavko, M., Adeeb, S., Conroy, M. D., Pauly, J. R., McCarron, R. M. and Sullivan, P. G. (2010). "Increase in blood-brain barrier permeability, oxidative stress, and activated microglia in a rat model of blast-induced traumatic brain injury." J Neurosci Res **88**(16): 3530-3539.

Rhen, T. and Cidlowski, J. A. (2005). "Antiinflammatory action of glucocorticoids--new mechanisms for old drugs." N Engl J Med **353**(16): 1711-1723.

Risau, W. and Wolburg, H. (1990). "Development of the blood-brain barrier." Trends Neurosci **13**(5): 174-178.

Roberts, I., Yates, D., Sandercock, P., Farrell, B., Wasserberg, J., Lomas, G., Cottingham, R., Svoboda, P., Brayley, N., Mazairac, G., Laloe, V., Munoz-Sanchez, A., Arango, M., Hartzenberg, B., Khamis, H., Yutthakasemsunt, S., Komolafe, E., Olldashi, F., Yadav, Y., Murillo-Cabezas, F., Shakur, H., Edwards, P. and collaborators, C. t. (2004). "Effect of intravenous corticosteroids on death within 14 days in 10008 adults with clinically significant head injury (MRC CRASH trial): randomised placebo-controlled trial." Lancet **364**(9442): 1321-1328.

Romero, I. A., Radewicz, K., Jubin, E., Michel, C. C., Greenwood, J., Couraud, P. O. and Adamson, P. (2003). "Changes in cytoskeletal and tight junctional proteins correlate with decreased permeability induced by dexamethasone in cultured rat brain endothelial cells." Neurosci Lett **344**(2): 112-116.

Rosenfeld, J. V. and Ford, N. L. (2010). "Bomb blast, mild traumatic brain injury and psychiatric morbidity: a review." Injury **41**(5): 437-443.

Sahler, C. S. and Greenwald, B. D. (2012). "Traumatic brain injury in sports: a review." Rehabil Res Pract **2012**: 659652.

Saljo, A., Arrhen, F., Bolouri, H., Mayorga, M. and Hamberger, A. (2008). "Neuropathology and pressure in the pig brain resulting from low-impulse noise exposure." J Neurotrauma **25**(12): 1397-1406.

Saljo, A., Mayorga, M., Bolouri, H., Svensson, B. and Hamberger, A. (2011). "Mechanisms and pathophysiology of the low-level blast brain injury in animal models." Neuroimage **54 Suppl 1**: S83-88.

Saljo, A., Svensson, B., Mayorga, M., Hamberger, A. and Bolouri, H. (2009). "Low-level blasts raise intracranial pressure and impair cognitive function in rats." J Neurotrauma **26**(8): 1345-1352.

Schacke, H., Docke, W. D. and Asadullah, K. (2002). "Mechanisms involved in the side effects of glucocorticoids." Pharmacol Ther **96**(1): 23-43.

Schneiderman, A. I., Braver, E. R. and Kang, H. K. (2008). "Understanding sequelae of injury mechanisms and mild traumatic brain injury incurred during the conflicts in Iraq and Afghanistan: persistent postconcussive symptoms and posttraumatic stress disorder." Am J Epidemiol **167**(12): 1446-1452.

Shapira, Y., Setton, D., Artru, A. A. and Shohami, E. (1993). "Blood-brain barrier permeability, cerebral edema, and neurologic function after closed head injury in rats." Anesth Analg **77**(1): 141-148.

Sheth, B., Fesenko, I., Collins, J. E., Moran, B., Wild, A. E., Anderson, J. M. and Fleming, T. P. (1997). "Tight junction assembly during mouse blastocyst formation is regulated by late expression of ZO-1 alpha+ isoform." Development **124**(10): 2027-2037.

Shetty, A. K., Mishra, V., Kodali, M. and Hattiangady, B. (2014). "Blood brain barrier dysfunction and delayed neurological deficits in mild traumatic brain injury induced by blast shock waves." Front Cell Neurosci **8**: 232.

Shitaka, Y., Tran, H. T., Bennett, R. E., Sanchez, L., Levy, M. A., Dikranian, K. and Brody, D. L. (2011). "Repetitive closed-skull traumatic brain injury in mice causes persistent multifocal axonal injury and microglial reactivity." J Neuropathol Exp Neurol **70**(7): 551-567.

Shlosberg, D., Benifla, M., Kaufer, D. and Friedman, A. (2010). "Blood–brain barrier breakdown as a therapeutic target in traumatic brain injury." Nat Rev Neurol **6**(7): 393-403.

Sill, H. W., Chang, Y. S., Artman, J. R., Frangos, J. A., Hollis, T. M. and Tarbell, J. M. (1995). "Shear stress increases hydraulic conductivity of cultured endothelial monolayers." Am J Physiol **268**(2 Pt 2): H535-543.

Simard, J. M., Yurovsky, V., Tsymbalyuk, N., Melnichenko, L., Ivanova, S. and Gerzanich, V. (2008). "Protective Effect of Delayed Treatment With Low-Dose Glibenclamide in Three Models of Ischemic Stroke * Supplemental Methods." Stroke **40**(2): 604-609.

Simon, M. J., Kang, W. H., Gao, S., Banta, S. and Morrison, B. (2010). "TAT Is Not Capable of Transcellular Delivery Across an Intact Endothelial Monolayer In Vitro." Ann Biomed Eng **39**(1): 394-401.

Singer, K. L., Stevenson, B. R., Woo, P. L. and Firestone, G. L. (1994). "Relationship of serine/threonine phosphorylation/dephosphorylation signaling to glucocorticoid regulation of tight junction permeability and ZO-1 distribution in nontransformed mammary epithelial cells." J Biol Chem **269**(23): 16108-16115.

Skotak, M., Wang, F., Alai, A., Holmberg, A., Harris, S., Switzer, R. C. and Chandra, N. (2013). "Rat injury model under controlled field-relevant primary blast conditions: acute response to a wide range of peak overpressures." J Neurotrauma **30**(13): 1147-1160.

Sonden, A., Svensson, B., Roman, N., Brismar, B., Palmblad, J. and Kjellstrom, B. T. (2002). "Mechanisms of shock wave induced endothelial cell injury." Lasers Surg Med **31**(4): 233-241.

Sonden, A., Svensson, B., Roman, N., Ostmark, H., Brismar, B., Palmblad, J. and Kjellstrom, B. T. (2000). "Laser-induced shock wave endothelial cell injury." Lasers Surg Med **26**(4): 364-375.

Suneson, A., Hansson, H. A. and Seeman, T. (1990). "Pressure wave injuries to the nervous system caused by high-energy missile extremity impact: Part II. Distant effects on the central nervous system--a light and electron microscopic study on pigs." J Trauma **30**(3): 295-306.

Svetlov, S. I., Prima, V., Kirk, D. R., Gutierrez, H., Curley, K. C., Hayes, R. L. and Wang, K. K. (2010). "Morphologic and biochemical characterization of brain injury in a model of controlled blast overpressure exposure." J Trauma **69**(4): 795-804.

Svetlov, S. I., Prima, V., Kirk, D. R., Gutierrez, H., Curley, K. C., Hayes, R. L. and Wang, K. K. W. (2010). "Morphologic and Biochemical Characterization of Brain Injury in a Model of Controlled Blast Overpressure Exposure." J Trauma **69**(4): 795-804.

Taber, K. H., Warden, D. L. and Hurley, R. A. (2006). "Blast-related traumatic brain injury: what is known?" J Neuropsychiatry Clin Neurosci **18**(2): 141-145.

Tanno, H., Nockels, R. P., Pitts, L. H. and Noble, L. J. (1992). "Breakdown of the blood-brain barrier after fluid percussion brain injury in the rat: Part 2: Effect of hypoxia on permeability to plasma proteins." J Neurotrauma **9**(4): 335-347.

Tanno, H., Nockels, R. P., Pitts, L. H. and Noble, L. J. (1992). "Breakdown of the blood-brain barrier after fluid percussive brain injury in the rat. Part 1: Distribution and time course of protein extravasation." J Neurotrauma **9**(1): 21-32.

Taylor, P. A. and Ford, C. C. (2009). "Simulation of blast-induced early-time intracranial wave physics leading to traumatic brain injury." J Biomech Eng **131**(6): 061007.

Thal, S. C., Schaible, E. V., Neuhaus, W., Scheffer, D., Brandstetter, M., Engelhard, K., Wunder, C. and Forster, C. Y. (2013). "Inhibition of proteasomal glucocorticoid receptor degradation restores dexamethasone-mediated stabilization of the blood-brain barrier after traumatic brain injury." Crit Care Med **41**(5): 1305-1315.

Thurman, D. J., Alverson, C., Dunn, K. A., Guerrero, J. and Sniezek, J. E. (1999). "Traumatic brain injury in the United States: A public health perspective." J Head Trauma Rehabil **14**(6): 602-615.

Tofts, P. S. and Kermode, A. G. (1991). "Measurement of the blood-brain barrier permeability and leakage space using dynamic MR imaging. 1. Fundamental concepts." Magn Reson Med **17**(2): 357-367.

Tomkins, O., Shelef, I., Kaizerman, I., Eliushin, A., Afawi, Z., Misk, A., Gidon, M., Cohen, A., Zumsteg, D. and Friedman, A. (2008). "Blood-brain barrier disruption in post-traumatic epilepsy." J Neurol Neurosurg Psychiatry **79**(7): 774-777.

Tompkins, P., Tesiram, Y., Lerner, M., Gonzalez, L. P., Lightfoot, S., Rabb, C. H. and Brackett, D. J. (2013). "Brain injury: neuro-inflammation, cognitive deficit, and magnetic resonance imaging in a model of blast induced traumatic brain injury." J Neurotrauma **30**(22): 1888-1897.

Trudeau, D. L., Anderson, J., Hansen, L. M., Shagalov, D. N., Schmoller, J., Nugent, S. and Barton, S. (1998). "Findings of mild traumatic brain injury in combat veterans with PTSD and a history of blast concussion." J Neuropsychiatry Clin Neurosci **10**(3): 308-313.

Underwood, J. L., Murphy, C. G., Chen, J., Franse-Carman, L., Wood, I., Epstein, D. L. and Alvarado, J. A. (1999). "Glucocorticoids regulate transendothelial fluid flow resistance and formation of intercellular junctions." Am J Physiol **277**(2 Pt 1): C330-342.

Unterberg, A., Stover, J., Kress, B. and Kiening, K. (2004). "Edema and brain trauma." Neuroscience **129**(4): 1019-1027.

Vagnozzi, R., Signoretti, S., Tavazzi, B., Floris, R., Ludovici, A., Marziali, S., Tarascio, G., Amorini, A. M., Di Pietro, V., Delfini, R. and Lazzarino, G. (2008). "Temporal window of metabolic brain vulnerability to concussion: a pilot 1H-magnetic resonance spectroscopic study in concussed athletes--part III." Neurosurgery **62**(6): 1286-1295; discussion 1295-1286.

Vajtr, D., Benada, O., Kukacka, J., Prusa, R., Houstava, L., Toupalik, P. and Kizek, R. (2009). "Correlation of ultrastructural changes of endothelial cells and astrocytes occurring during blood brain barrier damage after traumatic brain injury with biochemical markers of BBB leakage and inflammatory response." Physiol Res **58**(2): 263-268.

Valiyaveettil, M., Alamneh, Y., Wang, Y., Arun, P., Oguntayo, S., Wei, Y., Long, J. B. and Nambiar, M. P. (2013). "Contribution of systemic factors in the pathophysiology of repeated blast-induced neurotrauma." Neurosci Lett **539**: 1-6.

van Asperen, J., Mayer, U., van Tellingen, O. and Beijnen, J. H. (1997). "The functional role of P-glycoprotein in the blood-brain barrier." J Pharm Sci **86**(8): 881-884.

Vandevord, P. J., Bolander, R., Sajja, V. S., Hay, K. and Bir, C. A. (2012). "Mild neurotrauma indicates a range-specific pressure response to low level shock wave exposure." Ann Biomed Eng **40**(1): 227-236.

Victorino, G. P., Newton, C. R. and Curran, B. (2003). "The Impact of Albumin on Hydraulic Permeability: Comparison of Isotonic and Hypertonic Solutions." Shock **20**(2): 171-175.

Vieira, P. and Rajewsky, K. (1988). "The half-lives of serum immunoglobulins in adult mice." Eur J Immunol **18**(2): 313-316.

Vilalta, A., Sahuquillo, J., Rosell, A., Poca, M. A., Riveiro, M. and Montaner, J. (2008). "Moderate and severe traumatic brain injury induce early overexpression of systemic and brain gelatinases." Intensive Care Med **34**(8): 1384-1392.

Wade, A. L., Dye, J. L., Mohrle, C. R. and Galarneau, M. R. (2007). "Head, face, and neck injuries during Operation Iraqi Freedom II: results from the US Navy-Marine Corps Combat Trauma Registry." J Trauma **63**(4): 836-840.

Walsh, D. and Avashia, J. (1992). "Glucocorticoids in clinical oncology." Cleve Clin J Med **59**(5): 505-515.

Wang, Y., Wei, Y., Oguntayo, S., Wilkins, W., Arun, P., Valiyaveettil, M., Song, J., Long, J. B. and Nambiar, M. P. (2011). "Tightly coupled repetitive blast-induced traumatic brain injury: development and characterization in mice." J Neurotrauma **28**(10): 2171-2183.

Warden, D. (2006). "Military TBI during the Iraq and Afghanistan wars." J Head Trauma Rehabil **21**(5): 398-402.

Willis, C. L., Nolan, C. C., Reith, S. N., Lister, T., Prior, M. J. W., Guerin, C. J., Mavroudis, G. and Ray, D. E. (2004). "Focal astrocyte loss is followed by microvascular damage, with subsequent repair of the blood-brain barrier in the apparent absence of direct astrocytic contact." Glia **45**(4): 325-337.

Willott, E., Balda, M. S., Heintzelman, M., Jameson, B. and Anderson, J. M. (1992). "Localization and differential expression of two isoforms of the tight junction protein ZO-1." Am J Physiol **262**(5 Pt 1): C1119-1124.

Wojcik, B. E., Stein, C. R., Bagg, K., Humphrey, R. J. and Orosco, J. (2010). "Traumatic Brain Injury Hospitalizations of US Army Soldiers Deployed to Afghanistan and Iraq." American Journal of Preventive Medicine **38**(1): S108-S116.

Wolburg, H. and Lippoldt, A. (2002). "Tight junctions of the blood-brain barrier: development, composition and regulation." Vascul Pharmacol **38**(6): 323-337.

Wolman, M., Klatzo, I., Chui, E., Wilmes, F., Nishimoto, K., Fujiwara, K. and Spatz, M. (1981). "Evaluation of the dye-protein tracers in pathophysiology of the blood-brain barrier." Acta Neuropathol **54**(1): 55-61.

Wu, J., Pajoohesh-Ganji, A., Stoica, B. A., Dinizo, M., Guanciale, K. and Faden, A. I. (2012). "Delayed expression of cell cycle proteins contributes to astroglial scar formation and chronic inflammation after rat spinal cord contusion." J Neuroinflammation **9**: 169.

Yen, L. F., Wei, V. C., Kuo, E. Y. and Lai, T. W. (2013). "Distinct patterns of cerebral extravasation by Evans blue and sodium fluorescein in rats." PLoS One **8**(7): e68595.

Yeoh, S., Bell, E. D. and Monson, K. L. (2013). "Distribution of Blood-Brain Barrier Disruption in Primary Blast Injury." Ann Biomed Eng.

Yuan, W., Li, G., Zeng, M. and Fu, B. M. (2010). "Modulation of the blood–brain barrier permeability by plasma glycoprotein orosomucoid." Microvascular research **80**(1): 148-157.

Zhuo, Y. H., He, Y., Leung, K. W., Hou, F., Li, Y. Q., Chai, F. and Ge, J. (2010). "Dexamethasone disrupts intercellular junction formation and cytoskeleton organization in human trabecular meshwork cells." Mol Vis **16**: 61-71.

Zouris, J. M., Walker, J., Dye, J. and Galarneau, M. (2006). "Wounding patterns for US marines and sailors during Operation Iraqi Freedom, major combat phase." Military Medicine **171**(3): 246-252.

8 Appendix A: Publications

8.1 Journal manuscripts

Hue, C.D., Cho, F.S., Cao, S., Nicholls, R.E., Vogel, E.W., 3rd, Sibindi, C., Arancio, O., Bass, C.R., Meaney, D.F., Morrison, B., 3rd. (Under Review). Time course and size of blood-brain barrier opening in a mouse model of blast-induced traumatic brain injury.

Hue, C.D., Cho, F.S., Cao, S., Bass, C.R., Meaney, D.F., Morrison, B., 3rd. (2015). Dexamethasone potentiates in vitro blood-brain barrier recovery after primary blast injury by glucocorticoid receptor-mediated upregulation of ZO-1 tight junction protein. J Cereb Blood Flow Metab. Epub ahead of print.

- Featured in: Columbia Engineering, Neuroscience News, Science Daily

Effgen, G.B., Vogel, E.W., 3rd, Lynch, K.A., Lobel, A., **Hue, C.D.**, Meaney, D.F., Bass, C.R., Morrison, B., 3rd. (2014). Isolated primary blast alters neuronal function with minimal cell death in organotypic hippocampal slice cultures. J Neurotrauma 31, 1202-1210.

Hue, C.D., Cao, S., Bass, C.R., Meaney, D.F., Morrison, B., 3rd. (2014). Repeated primary blast injury causes delayed recovery, but not additive disruption, in an in vitro blood-brain barrier model. J Neurotrauma 31, 951-960.

Hue, C.D., Cao, S., Haider, S.F., Vo, K.V., Effgen, G.B., Vogel, E., 3rd, Panzer, M.B., Bass, C.R., Meaney, D.F., Morrison, B., 3rd. (2013). Blood-brain barrier dysfunction after primary blast injury in vitro. J Neurotrauma 30, 1652-1663.

- Cover feature: October 1, 2013 issue

Effgen, G.B., **Hue, C.D.**, Vogel, E., 3rd, Panzer, M.B., Meaney, D.F., Bass, C.R., Morrison, B., 3rd. (2012). A Multiscale Approach to Blast Neurotrauma Modeling: Part II: Methodology for Inducing Blast Injury to in vitro Models. Front Neurol 3, 23.

Gao, S., Simon, M.J., **Hue, C.D.**, Morrison, B., 3rd, Banta, S. (2011). An unusual cell penetrating peptide identified using a plasmid display-based functional selection platform. ACS Chem Biol 6(5), 484-491.

8.2 Conference proceedings

Hue, C.D., Cao, S., Bass, C.R., Meaney, D.F., Morrison, B., 3rd. (2013). Interval-specific, blood-brain barrier disruption in vitro after repetitive primary blast injury. International Research Council on Biomechanics of Injury, Gothenburg, Sweden.

Hue, C.D., Vo, K.V., Effgen, G.B., Vogel III, E., Panzer, M.B., Bass, C.R., Meaney, D.F., Morrison, B., 3rd. (2012). Integrity disruption of an in vitro blood-brain barrier model following exposure to blast overpressure. International Research Council on Biomechanics of Injury, Dublin, Ireland.

- Winner of 2012 Murray Mackay Young Researcher Award

8.3 Abstracts

Hue, C.D., Cao, S., Bass, C.R., Meaney, D.F., Morrison, B., 3rd. (2014). Dexamethasone potentiates recovery of the blood-brain barrier after primary blast injury in vitro. National Neurotrauma Society, San Francisco, CA.

- Winner of 2014 Travel Grant Award

Hue, C.D., Cao, S., Bass, C.R., Meaney, D.F., Morrison, B., 3rd. (2013). Window of heightened vulnerability to repetitive primary blast injury in an in vitro blood-brain barrier model. National Neurotrauma Society, Nashville, TN.

Haider, S.F., **Hue, C.D.**, Bass, C.R., Meaney, D.F., and Morrison, B., 3rd. (2012). Increased solute permeability of an in vitro blood-brain barrier model exposed to blast overpressure. Annual Biomedical Research Conference for Minority Students, San Jose, CA.

- Oral Presentation Award in Engineering, Mathematics and Physics (Haider, S.F.)

Hue, C.D., Vo, K.V., Panzer, M.B., Bass, C.R., Meaney, D.F., Morrison, B., 3rd. (2012). Blast-induced disruption of an in vitro blood-brain barrier model. National Neurotrauma Society, Phoenix, AZ.

Hue, C.D., Panzer, M.B., Bass, C.R., Meaney, D.F., Morrison, B., 3rd. (2011). Incident blast overpressure induces disruption of brain endothelial monolayer integrity. Biomedical Engineering Society Annual Meeting, Hartford, CT.

Hue, C.D., Panzer, M.B., Bass, C.R., Meaney, D.F., Morrison, B., 3rd. (2011). Blast overpressure induces disruption of brain endothelial monolayer integrity. National Neurotrauma Society, Ft. Lauderdale, FL.

- Winner of 2011 Travel Grant Award